Paleoneurology of the Proboscidea (Mammalia, Afrotheria): Insights from Their Brain Endocast and Labyrinth

Julien Benoit, George Lyras, Arnaud Schmitt, Mpilo Nxumalo, Rodolphe Tabuce, Teodor Obada, Vladislav Mararsecul, Paul Manger

CHAPTER 15 PROBOSCIDEA

PALEONEUROLOGY OF THE PROBOSCIDEA (MAMMALIA, AFROTHERIA): INSIGHTS FROM THEIR BRAIN ENDOCAST AND LABYRINTH

Julien Benoit[1], George Lyras[2], Arnaud Schmitt[3], Mpilo Nxumalo[1], Rodolphe Tabuce[4], Teodor Obada[5], Vladislav Mararsecul[6], and Paul Manger[7]

[1]Evolutionary Studies Institute (ESI), University of the Witwatersrand, Braamfontein, 2050, Johannesburg, South Africa

[2]Faculty of Geology and Geoenvironment, National and Kapodistrian University of Athens, Greece

[3]Museum National d'Histoire Naturelle, Paris, France

[4]Institut des Sciences de l'Évolution (UM, CNRS, IRD, EPHE), Université Montpellier, France

[5]Institute of Zoology, Republic of Moldova, National Museum of Ethnography and Natural History of Moldova, Chişinău, Moldova

[6]Institute of Zoology, Republic of Moldova

[7]School of Anatomical Sciences, University of the Witwatersrand, 7 York Road, Parktown, 2193, Johannesburg, South Africa

Abstract:

The elephant brain is famous for its higher than average encephalization quotient, memory capacities, large cerebellum, large facial and trigeminal nerves, and the extensive repertoire of complex behaviors and social interactions it produces, the last of which being supported by infrasonic communication. The evolutionary history of Proboscidea is amongst the best-documented among mammals but knowledge of the group's paleoneurological history remains comparatively fragmentary. Here, we summarize and build upon more than 150 years of research on the evolution of the proboscidean nervous system. We find that the morphology of the endocranial cast and bony labyrinth of the basal-most proboscideans is consistent with the generalized plesiomorphic conditions for placental mammals (e.g. linearly organized brain parts, low encephalization quotient, presence of a secondary common crus), whereas their conditions become essentially elephant-like in the Elephantimorpha around the Oligocene. This suggests that a higher encephalization quotient and adaptations to low-frequency hearing (e.g. loss of the secondary bony lamina) evolved in parallel with the formation and evolution of a trunk, adaptation to a drier environment, and a higher body mass. We hypothesize that these structures co-evolved as a response to the changing climate in the Oligocene.

Keywords: Elephants, Endocranial cast, climate change, infraorbital foramen, proboscis, infrasound

15.1 HISTORICAL REVIEW AND CURRENT DATA ON THE VARIATIONS OF THE ENDOCRANIAL CAST ACROSS PROBOSCIDEAN PHYLOGENY

15.1 Introduction

Extant elephants are known for displaying a wide array of complex behaviors, equalling, if not surpassing, that of many primates, including such features as a detailed long-term memory storage and retrieval, behavioral adaptability, self-awareness, mourning of the dead, sophisticated problem-solving abilities, and the ability to modify their environment and to manufacture tools with their trunk (see Cozzi et al. 2001; Shoshani et al. 2006; Hart et al. 2008 for reviews). In addition, they are the shortest sleepers of all mammals studied to date (Gravett et al. 2017). As such, studying the brain of elephants to understand how it produces the array of complex behavioral repertoires observed has a long-standing fascination.

In the past two decades, many detailed studies have been conducted on various aspects of the neuroanatomy of extant elephants (e.g., Cozzi et al. 2001; Kupsky et al. 2001; Shoshani et al. 2006; Hart et al. 2008; Manger et al. 2009, 2010, 2012; Hakeem et al. 2009; Pettigrew et al. 2010; Bianchi et al. 2011; Jacobs et al. 2011; Ngwenya et al. 2011; Maseko et al. 2012, 2013a, 2013b; Herculano-Houzel et al. 2014; Stoeger and Manger 2014; Patzke et al. 2014; Kharlamova et al. 2015, 2016; Limacher-Burrell et al. 2018). Unfortunately, the paucity of extant proboscidean species, the three species belonging to the sole extant family Elephantidae, limits comparative neuroanatomical analyses related to variations in behavioral repertoires (Byrne and Bates 2007). The paleoneurology of extinct species, although limited to the study of the shape and size of the endocranial casts, in part compensates for this lack of extant diversity, as almost 200 extinct species of proboscideans are known across the Cenozoic fossil record (Shoshani and Tassy 2005; Sanders et al. 2010; Shauer 2010). Earlier studies describing endocranial casts of proboscideans have been based on the rather rare

natural casts of the braincase (e.g., Simionescu and Morosan 1937; Bever et al. 2008), on artificial casts of the braincase made with the least fragile fossil skulls (e.g., Andrews 1906; Dechaseaux 1958; Jerison 1973), or on sections of fossil skulls (e.g., Warren 1855; Boule and Thevenin 1920) (Fig. 15.1). Unfortunately, the former two types of material are quite uncommon because the extensive sinuses that comprise the majority of the volume of the proboscidean skull make it almost impossible for the *tabula interna* to withstand the natural or artificial processes that generate an endocranial cast. Sectioning fossil skulls, being destructive, has never been routinely performed. Recently, micro-computed tomography X-ray (CT-scan) has become common in paleontology laboratories, and palaeoneurological studies can now be conducted more easily and without risk of damage to the fossils (Benoit et al. 2013b). Nevertheless, the cost of a CT scan and the large size and weight of most fossil proboscidean skulls remain two major obstacles to the study of proboscidean palaeoneurology.

Here we aim to provide a comprehensive review of published data on the endocranial anatomy of extinct proboscideans, summarizing the research undertaken over the past two hundred years aimed at increasing our knowledge of proboscidean brain evolution, bringing the number of species for which data are available from three (Shoshani et al. 2006) to twenty species (Table 15.1; the classification and phylogeny of fossil species follows Sanders et al. (2010), Shauer (2010), and Fisher (2018)). This chapter highlights some major aspects of the paleoneurological history of the proboscidean endocranial cast, i.e. endocranial capacity, endocast morphology, and cortical gyrification.

Akin to humans, elephants are large-brained terrestrial mammals that originated in Africa and dispersed out of the African continent to populate most major landmasses, making them one of the best analogs to humans for tracing the evolution of brain size and behavioral complexity (Roca and O'Brien 2005; Goodman et al. 2009; Jebb and Hiller 2018). For

example, paedomorphic scaling of brain size occurring during the evolution of insular dwarfing in elephants has stimulated the debate on whether *Homo floresiensis* should be considered a dwarf human species or a pathological case (Weber et al. 2005; Weston and Lister 2009). In addition, proboscidean brain size increased under an herbivorous diet, which also offers a unique opportunity to test whether an enlarged brain requires high-quality food to evolve (Finlay et al. 2001). Understanding how the elephantine brain evolved during the Cenozoic, therefore, has implications beyond proboscidean palaeoneurology alone as it may directly echo our own origin and evolution.

(Insert Fig. 15.1 and Table 15.1)

Institutional abbreviations

AMNH: American Museum of Natural History, New York, USA; AMPG: Museum of Palaeontology and Geology, National and Kapodistrian University of Athens, Athens, Greece; LACM: Natural History Museum of Los Angeles County; MCFFM: Academy of Sciences of Moldova, Institute of Zoology; MNHN: Muséum national d'Histoire Naturelle, Paris, France; NHM-UK: Natural History Museum, London, UK; MGG: Museo Geologico e Paleontologico G.G. Gemmellaro, Palermo, Italy. NMNHS: National Museum of Natural History of Sofia; SMNS: Stuttgart Museum für Naturkunde; UM: Université de Montpellier, France.

15.2 EVOLUTION OF ENDOCRANIAL CAPACITY

15.2.1 The tools to study the evolution of brain size in extinct proboscideans

To estimate the mass or volume of the brain in a fossil proboscidean is a difficult task, primarily because the endocranial volume comprises the volume of the brain and that of meninges that encapsulate it (Manger et al. 2009). Discrepancies surround the estimation of

brain volume based on differing concepts of the meningeal thickness in proboscideans. For example, (Osborn 1931, 1936, 1942) estimated that the meninges could represent as much as 20% of the endocranial capacity in recent species. This is consistent with the observations made by Kharlamova et al. (2016, 2021) in the juvenile mammoth Yuka, in which the *dura mater* occupied 18.56% of the endocranial volume. In contrast, the dura mater was proposed to constitute only 11% of the total mass of the tissue filling the endocranial space in extant elephants according to Shoshani et al. (2006). Benoit (2015) and Kharlamova et al. (2016) independently proposed a systematic method to estimate meningeal thickness in extinct proboscidean species. It is based on a regression using data on brain and endocast volume primarily from Rohrs and Ebinger (2001). The equation proposed by Benoit (2015) is the most commonly used (Lyras 2018; Benoit et al. 2019), as it includes more data. The derived regression is:

Brain volume = 0.8877 x endocast volume – 2.9408

The resulting estimates of meningeal volume indicate that the meninges occupy, on average, 14% of the endocranial space in proboscideans (Benoit 2015). Historically, the specific gravity of endocranial tissues in proboscideans was considered to be the same as that of water (e.g., Jerison 1973; but see Lyras 2018). Accordingly, these authors consider that brain mass is essentially equal to the calculated brain volume. More recently, brain tissue has been considered to be denser than water, with a specific gravity of 1.036 (Stephan et al. 1970; Palombo and Giovinazzo 2005; Benoit 2015; Benoit et al. 2019; Kharlamova et al. 2016), which is the approach taken herein (Table 15.1). In this case, brain mass equals 1.036 times brain volume; however, this assumption has been criticized by Lyras (2018) who argues that the specific gravity of the brain has been found to range from 1.027 to 1.100 $g.cm^3$.

The resulting brain mass can be compared using the encephalization quotient (EQ) (Jerison 1973), a ratio between the observed brain mass (or volume) of an animal and the

expected brain mass (or volume) of an animal of the same body mass (these expected values are calculated using a regression of known brain mass to body mass data across mammalian species). Mammals with a brain larger than expected have an EQ above 1, whereas mammals with a brain smaller than expected have a value below 1. Many methods of calculating EQs exist, but those of Jerison (1973) and Manger (2006) have been the most commonly used to compare encephalization across proboscideans (Jerison 1973; Palombo and Giovinazzo 2005; Shoshani et al. 2006; Benoit et al. 2013b, 2019; Benoit 2015; Lyras 2018). They are expressed as follow:

Jerison's EQ = (Brain mass)/(0.12*Body mass$^{2/3}$)

Manger's EQ = (Brain mass)/(0.0535*Body mass$^{0.7294}$)

Manger's EQ is similar to, but preferred over Eisenberg's EQ (Eisenberg 1981) as it includes more species to calculate the regression, and excludes outliers such as primates and cetaceans (Manger 2006).

15.2.2 Patterns of encephalization evolution in proboscideans

The brains of extant elephants are the largest in absolute size amongst terrestrial animals (Shoshani et al. 2006; Manger et al. 2013; Herculano-Houzel et al. 2014). On average, the EQs of extant elephants range between 1 and 2, with an average of 1.88 for Jerison's EQ (Shoshani et al. 2006) and 1.51 for Manger's EQ (Benoit et al. 2019). Though not markedly different from that of an animal of similar body mass (Manger et al. 2013), modern proboscideans usually have a larger brain than predicted (Jerison 1973; Shoshani et al. 2006; Benoit et al. 2013b; Benoit 2015; Benoit et al. 2019). This implies that both absolute and relative brain size increased sometime during the phylogenetic history of elephants, and thus effort has been made to understand the causal factors and evolutionary timing of the

enlarged brain in proboscideans (Jerison 1973; Shoshani et al. 2006; Benoit et al. 2013b; Benoit 2015; Jebb and Hiller 2018; Benoit et al. 2019).

The geologically earliest endocranial cast of a proboscidean belongs to the 'plesielephantiform' *Moeritherium lyonsi* and dates from the late Eocene (~40-35Ma) of the Fayum (Egypt; Andrews 1906; Jerison 1973; Fig. 15.1). Its endocast volume was estimated as 240 cm^3 by Jerison (1973) using the water displacement method for determining endocast volume on the cast of the braincase made by Andrews (1906). Jerison's and Manger's EQs of *Moeritherium* provide an estimate of 0.2 (Table 15.1), an EQ that is an order of magnitude smaller than the EQ of extant elephants. Similar low EQ values have also been reported in the hyracoid *Seggeurius* and the sirenian *Prorastomus* (Table 15.1), two early Eocene Paenungulata, and the closest relatives of proboscideans (Benoit et al. 2013b, 2016). As a consequence, Jerison (1973), Benoit et al. (2013b), Manger et al. (2013), and Benoit (2015) hypothesized that a small relative and absolute brain size is the primitive condition for Proboscidea. This has since been supported by Benoit et al. (2019), who used ancestral character state reconstruction based on maximum likelihood to reconstruct that the last common ancestor of Proboscidea most likely had a Manger's EQ of 0.24 (Fig. 15.2). The relatively small size of the brain cavity compared to the skull in *Phosphatherium* and *Numidotherium*, two basal 'plesielephantiforms' from the Early Eocene of North Africa (-56 to -48Ma) depicted by Gheerbrant et al. (2005) and Benoit et al. (2013b: appendix B), also support this conclusion (Fig. 15.2a). Unfortunately, the endocast of *Moeritherium* remains the only complete one currently known for a 'plesielephantiform'.

All other fossil proboscidean endocasts described, and for which endocranial capacity has been estimated, belong to the Elephantiformes (Table 15.1). The basal-most elephantiform, and only non-elephantimorph elephantiform taxon for which the endocranial capacity has been estimated is *Palaeomastodon beadnelli*, from the Oligocene of Egypt

(Benoit et al. 2019). As early as 1917, Larger (1917: p.397) reported a personal communication from Andrews who hypothesized that *Palaeomastodon* and *Moeritherium* would have shared a similar brain size, roughly equivalent to that of a tapir (about 200 g according to Pérez-Barbería and Gordon 2005). Given that *Palaeomastodon* is the basal-most Elephantiformes (Gheerbrant and Tassy 2009; Fisher 2018), and that the Elephantimorpha have long been known for having high EQ values (Jerison 1973), this would imply that the endocranial volume likely did not increase prior to the origin of the Elephantimorpha (or, less parsimoniously, convergently in the Mammutida and Elephantoidea). The endocranial capacity of *Palaeomastodon* was measured for the first time by Benoit et al. (2019) using double graphic integration on a drawing of the reconstructed endocast, a method for which the accuracy has been validated by Radinsky (1977, p.48). The *Palaeomastodon* brain has a volume of approximately 771 cm^3, which is almost four times as large as that of *Moeritherium*, but since the estimated body mass of *Palaeomastodon* is three times larger than *Moeritherium*, the resulting EQs are quite similar (about 0.3, Table 15.1). Accordingly, the ancestral Manger's EQ for the Elephantiformes clade is 0.31 (Benoit et al. 2019), which is similar to that seen in basal proboscideans and other Eocene paenungulates (Table 15.1). Encephalization was thus relatively stable, and brain mass seems to have co-varied tightly with body mass, in Palaeogene proboscideans, as hypothesized by Manger et al. (2013), although the endocast of some noticeably large-bodied non-elephantimorph taxa such as the deinotheriids and *Barytherium* still need to be studied in detail to confirm this trend (Benoit et al. 2019). In this respect, the exposed braincase of a specimen of *Deinotherium bosazi* from the National Museums of Kenya (KNM-ER 1087) measuring about 14 cm across, and that shows no sign of expanded temporal lobes would support this prediction (J.B. Pers. Obs.).

The Elephantimorpha most likely originated during the late Oligocene (~28-24Ma) according to both molecular dating techniques (Rohland et al. 2007; Palkopoulou et al. 2018)

and the fossil record (Gheerbrant and Tassy 2009; Sanders et al. 2010; Shauer 2010); however, no data on endocranial volume is known for elephantimorphs prior to the late Miocene (Benoit 2015; Benoit et al. 2019). Benoit (2015) was the first to hypothesize that the EQ increased beyond the value of 1 in the Elephantimorpha, although crucial supportive data for elephantiforms was missing. Building upon Benoit's (2015) work, Benoit et al. (2019) showed that the relative brain size (calculated using Manger's EQ) doubled in the last common ancestor of Elephantimorpha compared to the primitive paenungulate-like condition, reaching a value of 0.73 (Fig. 15.2).

This value is close to that reconstructed for the last common ancestor of the Mammutida by Benoit et al. (2019), which is 0.64 (Fig. 15.2). The Mammutida include the largest species in the dataset, *Zygolophodon borsoni*, from the Pliocene of Moldova, for which body mass is estimated to 16 tons (Larramendi 2015). The endocranial size of *Zygolophodon* was acquired through digitization of an artificial endocast using photogrammetry (Benoit et al. 2019). It is noteworthy that despite its large body mass, both Jerison's and Manger's EQs of *Zygolophodon* (0.62 and 0.50 respectively) are only about 30% lower than the EQs of the two Pleistocene *Mammut americanum*, which have body masses about half of that of *Zygolophodon* (Table 15.1). This illustrates that the evolution of encephalization in proboscideans is strongly tied to phylogeny, even compared to the effect of body mass (Benoit et al. 2019).

The other major clade of the Elephantimorpha is the Elephantoidea (Fig. 15.2). Benoit et al. (2019) additionally found that another steep increase in relative brain size occurred in the more derived Elephantoidea, for which the Manger's EQ of the last common ancestor was reconstructed as equalling 1.09 (Fig. 15.2). Jerison's and Manger's EQs appear to stabilize at this phylogenetic level, as the EQ values of the basal-most elephantoid, the late Miocene

Stegodon insignis (1.85 and 1.69 respectively) are comparable to those in later, more derived, Elephantidae (on average 1.75 and 1.58 respectively) (Benoit et al. 2019).

(Insert Fig. 15.2)

15.2.3 The effect of insular dwarfism on brain size

A pervasive pattern exhibited across island mammals worldwide is the general trend for gigantism in smaller-bodied species and dwarfism in larger-bodied species, a trend coined 'the Island Rule' by Van Valen (1973) and subsequent authors. A major factor in evolution under insular conditions is the ecological release from mammalian competitors and predators resulting in dwarfism in insular representatives of large-bodied taxa (Lomolino et al. 2012, 2013). Elephants provide some of the most spectacular cases of body size decrease under insular conditions. For example, the Middle Pleistocene elephant *Palaeoloxodon falconeri* from Spinagallo Cave (Sicily) evolved a body mass reduction to just 2% of the size (body mass) of its mainland ancestor *P. antiquus* (Lomolino et al. 2012, 2013). More than 20 extinct species of dwarf proboscidians are known from 17 islands worldwide (Herridge and Lister 2012; van der Geer et al. 2016). Nevertheless, available data for their brain is limited to just three *Palaeoloxodon* species: *P.*aff. *mnaidriensis* (late Middle Pleistocene of Sicily), *P. tiliensis* (Late Pleistocene of Tilos) and *P. falconeri* (early Middle Pleistocene of Sicily) (Accordi and Palombo 1971; Benoit 2015; Larramendi 2015; Larramendi and Palombo 2015; Lyras 2018; Benoit et al. 2019) (Fig. 15.3). Of these, a detailed description of the endocranial morphology has been published only for *P. falconeri* (Accordi and Palombo 1971).

(Insert Fig. 15.3)

A major challenge in estimating the relative brain size of insular proboscideans is to accurately predict their body size relative to that of their direct mainland ancestor. This applies especially to *P. falconeri*, the smallest of all insular elephants, given the magnitude of its dwarfing. As a result, the EQ estimates of *P. falconeri* range from 3.75 (Lyras 2018), 3.94 (Larramendi and Palombo 2015), 4.30 (Palombo and Giovinazzo 2005), 5.22 (Benoit et al. 2019), up to even 7.08 (Benoit 2015). This wide range is due to differences that exist in the literature between individual estimates of the body masses of dwarf elephants in general. The body mass of insular *Palaeoloxodon* species has been estimated using skeletal scaling relationships (Roth 1990; Palombo and Giovinazzo 2005; Lomolino et al. 2012, 2013; van der Geer et al. 2014, 2016) or volumetric reconstructions (Larramendi and Palombo 2015; Romano et al. 2019). Prediction regressions are hampered by two main issues: (1) many dwarf elephants, such as those of Sicily and Tilos, were considerably smaller than the smallest mature individuals of the extant species; and (2) the small-sized living relatives of elephants have significantly different body proportions compared to the island forms. Roth (1990) developed prediction equations after examining the relationship between lengths of long limb bones and body masses in 33 mammalian species ranging from mice to African elephants. Thus, in the absence of small-sized living relatives with similar physical proportions, she used a reference dataset of «all» mammals. Using the length of long limb bones Roth (1990) estimated the body mass of *P. falconeri* to 60-90 kg. Christiansen (2004) and Palombo and Giovinazzo (2005) restricted their datasets to elephants only. Palombo and Giovinazzo (2005) used regressions that predict body mass from pad circumferences and shoulder height. Their calculations for *P. falconeri* range between 51.1 kg and 141.1 kg. Christiansen (2004) on the other hand developed prediction equations using the skeletal measurements from seven Asian elephant individuals of known body mass and thus restricted his dataset to elephants only. His equations were used by Lomolino et al. (2013), who estimated the body mass of *P. falconeri*

to be 189 kg, of *P. tiliensis* to be 727 kg, and that of *P.* aff. *mnaidriensis* to be 1380 kg. Instead of using individual bones, Larramendi and Palombo (2015) and Romano et al. (2019) used composite skeletal mounts and applied volumetric approaches. Their estimates for the body mass of *P. falconeri* range from 150 to 304.5 kg.

Using the mass estimations of Lomolino et al. (2013) the Manger EQ rises from 1.14 in *P. antiquus* to 2.45-2.48 in *P.* aff. *mnaidriensis,* 2.76 in *P. tiliensis*, and 4.42 in *P. falconeri* (Table 15.1). Although the brain of insular dwarfs is larger than predicted for a mammal of their size, their brain is smaller than what is predicted by the allometric trend of continental Elephantidae (Lyras 2018). Furthermore, their brains are smaller than what the static and late ontogenetic allometries of modern elephants predict (Fig. 15.4). This is particularly evident for the smallest Sicilian dwarf, *P. falconeri.*

Different values of EQ arise when alternative body mass estimations are taken into consideration, but in all cases, there is a progressive increase of EQ with reduced body mass (Fig. 15.4). It appears that the larger the difference in body mass between the insular and its mainland ancestral species, the more their EQ differs.

The brains of the dwarf elephants of Sicily and Tilos are not simply scaled-down models of their mainland relative, *P. antiquus*. Their cerebellum is relatively smaller; there is a relative reduction of the temporal lobes; the frontal lobe is more massive; the olfactory bulbs are placed more caudally (Fig. 15.3). These changes seem to be gradual and are most pronounced in *P. falconeri*, the smallest species. Some of these changes might be related to 'packaging' problems. In insular dwarfs, the brain is contained in a much smaller space than in the continental forms. The relatively massive frontal lobe of *P. falconeri* could thus be just the result of tighter packing. A similar phenomenon has been observed in some small-sized dog breeds, which also have massive and downward rotated frontal lobes (Seiferle 1966; Radinsky 1973). The position of the olfactory bulbs is related to changes in the position of the

respiratory axis. In *P. falconeri,* the skull's center of gravity is shifted anteriorly (van der Geer et al. 2018). This has an impact on the orientation of the respiratory axis, which is more horizontal in *P. falconeri* than in *P. antiquus* (Palombo and Giovinazzo 2005). The reduction of the temporal lobes could be the result of a spatial constraint in the postnatal development of the lobe. The relative size of the temporal lobe of modern elephants increases during ontogenetic development (Shoshani et al. 2006). The temporal lobes of *P. falconeri* resemble those of juvenile *P. tiliensis*. Although the two species are not phylogenetically related, this resemblance is in line with previous suggestions that the relatively large brain of *P. falconeri* (for an average mammal of that size) is the result of heterochrony (Palombo and Giovinazzo 2005). An alternative explanation is that the small temporal lobes of *P. falconeri* are the result of allometric scaling. The morphology of the skull in insular elephants is, to a significant extent, a function of size (van der Geer et al. 2018). Therefore, the morphology of the brain in dwarf elephants could be the result of their smaller size.

(Insert Fig. 15.4)

15.2.4 Why did Elephantimorpha evolve an enlarged brain?

Many hypotheses have been proposed in the literature to account for the origin and evolution of the absolutely and relatively larger brains in elephants, and these can be divided into four categories.

The first category is composed of hypotheses that aimed to find a correlation between brain size and a given life-history trait. Many life-history traits correlate with brain size in mammals, such as longevity, sexual maturation, body mass, or metabolic rate (Jerison 1973; Martin 1981; Hofman 1993; González-Lagos et al. 2010; Weisbecker and Goswami 2011; DeCasien et al. 2018). According to Manger et al. (2013), brain size in proboscideans scales

almost normally with their body mass (except for *P. falconeri*), which implies that a large brain would have co-evolved with large body size since the Paleogene in proboscideans. This is only partly supported by the study of Benoit et al. (2019), who found a significant correlation between brain and body mass variations in proboscideans, but also found that brain size increased faster than body size in the last common ancestors of Elephantimorpha and Elephantoidea, resulting in two pulses of increase in both absolute and relative brain size. Pérez-Barbería and Gordon (2005) also pointed out a positive correlation between large brain mass and gestation length in paenungulates, artiodactyls, and perissodactyls, an interesting point given that elephants have the longest gestation period of all mammals (two years) (Shoshani and Tassy 1996), but yet impossible to address due to deficiencies in the fossil record.

The second category of hypotheses proposed to explain brain enlargement in proboscideans are those related to the 'social brain' hypothesis. Pérez-Barbería and Gordon (2005), and Shultz and Dunbar (2006) suggested that life in herds and group size are highly correlated with brain enlargement in paenungulates, artiodactyls, and perissodactyls. In support of this hypothesis, they argue that gregariousness would represent a gain of fitness primarily because it provides defence against predators. The corollary is an increase in social complexity that positively selects for larger brains in order to manage social interactions that require rapid and elaborate responses (Pérez-Barbería and Gordon 2005; Shultz and Dunbar 2006). Indeed, elephants share tight social bonds (Hart et al. 2008) and gregariousness is documented in the fossil record of Elephantimorpha (presumably in *Stegotetrabelodon*) as early as the Late Miocene, by footprints indicating that a family of 13 individuals (which is about the average for extant elephants) lived as a herd (Bibi et al. 2012). Elephants are known for possessing long-term social memory that involves: (i) chemical memory (e.g. recognition of other individuals using chemosensory characteristics of their urine), which is proposed to

correlate to the enlargement of the hippocampus (Hakeem et al. 2005; Hart et al. 2008; Shultz and Dunbar 2006; but see Kupsky et al. 2001; Patzke et al. 2014 who demonstrated that the hippocampus of elephants is not enlarged beyond what one would expect for a five-kilogram mammalian brain); and (ii) acoustic memory (it has been reported that elephants can discriminate the calls of more than hundred individuals [Hart et al. 2008]), which could also be linked to the seemingly large, but unverified, size of their temporal lobe (Shoshani et al. 2006).

The third category of hypotheses are the adaptationist hypotheses. They are based on the fact that brain tissue is metabolically expensive, and natural selection usually does not maintain such costly tissue without any adaptive functions (Shultz and Dunbar 2006). Accordingly, Jerison (1973: p8-9) has formulated his principle of proper mass: "the mass of neural tissue controlling a particular function is appropriate to the amount of information processing involved in performing the function. This implies that in comparisons among species the importance of a function in the life of each species will be reflected by the absolute amount of neural tissue for that function in each species." This principle has been applied to elephants by Shoshani et al. (2006) who associated their brain size with proposed extensive memory capacities and intelligence, such as the capacity to use tools, the ability to 'think' and consciousness. The fitness benefit of long-term memory has been emphasized by many authors as it is thought to help matriarchs to recall the location of water holes during dry seasons (Hart et al. 2008; Benoit et al. 2019). Lister (2013) also proposed that behavioral accommodation has preceded morphological adaptation to a grazing diet (i.e. increase in teeth hypsodonty and lamellar number) in proboscideans during the late Miocene (~7 Ma). It seems, however, unlikely that this triggered an increase in brain size since: (i) no pulse of absolute or relative brain enlargement is documented in late Miocene proboscideans (Benoit

et al. 2019); and (ii) because Pérez-Barbería and Gordon (2005) found no indisputable correlation between diet and brain size in paenungulates, artiodactyls, and perissodactyls.

Finally, it has been hypothesized that absolute and relative brain enlargement in proboscideans may reflect an increase in intelligence and/or behavioral flexibility to cope with some major environmental, climatic and biogeographic changes that occurred in Africa between the end of the Oligocene and the beginning of the Miocene (Benoit 2015; Benoit et al. 2019). Benoit et al. (2019) noted two pulses of relative increase in brain size that roughly coincide with increased aridity, rapid temperature changes, and megafauna dispersal events in and out of Africa. According to Kappelman et al. (2003), competition with the continuous influx of artiodactyls and perissodactyls from Asia since the Late Eocene perhaps contributed to the fragmentation of proboscidean populations and increased the selective pressure on proboscideans, which then underwent a period of rapid adaptive radiation. Whether the arrival of these newcomers influenced the evolution of the cognitive capacities of endemic fauna still remains to be tested quantitatively as this hypothesis relies heavily on the apparent coincidence of variations in relative brain size and environmental changes pointed out by Benoit et al. (2019).

15.3 EVOLUTION OF BRAIN MORPHOLOGY

15.3.1 Neuroanatomy of modern elephants

The extant elephants possess the largest terrestrial brains coupled with the largest terrestrial bodies. Despite these large brains, until recently very little was known about the structure, and through inference, functional capacities of the elephant brain. A 2001 review of the neuroanatomical data available for the elephant brain (Cozzi et al. 2001) demonstrated that only 52 scientific papers had been published that were specifically dedicated to structural

aspects of the elephant brain, and that 20 of these were written in the 19th century. It was concluded by Cozzi et al. (2001, p.255) that the lack of interest in the elephant brain is: "…probably due to the feeling that no 'front line' discovery can be derived from these studies…", and a lack of interest in support for such studies from funding agencies. Since the publication of this review, a number of detailed studies of the elephant brain have been published (e.g., Kupsky et al. 2001; Shoshani et al. 2006; Manger et al. 2009, 2010, 2012; Hakeem et al. 2009; Pettigrew et al. 2010; Ngwenya et al. 2011; Maseko et al. 2011, 2012, 2013a,b; Herculano-Houzel et al. 2014; Stoeger and Manger 2014; Patzke et al. 2014; Limacher-Burrell et al. 2018), the majority on the brain of the African elephant (Manger et al. 2009), with these studies providing a great deal more information regarding the structure and potential functional capacities of the elephant central nervous system. Rather than provide an exhaustive review of this work, here we examine five central themes of elephant neuroanatomy, and their associated proposed behavioral parallels, that are of most interest in terms of understanding the extant elephants, and contextualizing studies of the evolution of the proboscidean brain. The five aspects of interest to be discussed here include: (1) the cerebral cortex, due to the reported behavioral complexity and flexibility of extant elephants (Hart et al. 2008); (2) the hippocampal formation, due to the near-mythical status assigned to the memory of elephants (Patzke et al. 2014); (3) the olfactory system, due to the large olfactory sensory range of the elephants (Ngwenya et al. 2011; Niimura et al. 2014); (4) the cerebellum, due to its potential association with control of the trunk (Maseko et al. 2012, 2013a); and (5) the production and reception of infrasound, due to the central involvement of the somatosensory, auditory and motor systems in this aspect of elephant communication (Maseko et al. 2013b; Stoeger and Manger 2014). Many of these features potentially brought about changes in the shape and size of the proboscidean brain throughout their evolutionary

history, and therefore are important to our interpretation of fossil proboscidean endocasts and what the variations observed may indicate regarding the evolution of brain and behavior.

The cerebral cortex is an important structure because this is where the most complex processing of neural information occurs. Although debunked, for many years it was believed that brains with cerebral cortices that were more highly fissured and folded (gyrencephalic) reflected greater cognitive capacities of the species in which these features were present. The cerebral cortex of the extant elephant appears, at a superficial glance to be highly gyrencephalic, but when measured systematically and compared to other mammals, while clearly having many gyri and sulci, the elephant brain is no more gyrencephalic than one would expect for a mammal brain weighing five kilograms (Manger et al. 2012). A similar conclusion can be reached regarding the cerebral cortex of the extinct woolly mammoth (Kharlamova et al. 2015, 2016). The cerebral cortex of the African elephant has a mass that approaches 3 kg (including both grey and white matter, 1.4 kg of grey matter alone), and contains approximately 5.59×10^9 neurons, approximately 1/3 of the neurons found in the human cerebral cortex, and less than the approximately 9×10^9 cortical neurons observed in the cerebral cortex of great apes (Herculano-Houzel et al. 2014). Thus, despite having a cerebral cortical mass far greater than apes, including humans, the number of neurons is far lower. However, there is evidence of regional variation in cortical structure and neuronal density (Herculano-Houzel et al. 2014), and evidence for the presence of very large, complexly organized neurons that rival the most complex neurons observed in the cerebral cortex of humans (Jacobs et al. 2011, 2016a). Thus, there are mixed lines of evidence regarding the level of complexity of information processing in the elephant cerebral cortex, some that hint at high levels of complexity, and some that hint at lower levels of complexity. It is only with further study that greater certainty regarding the level of complexity of the cerebral cortex of the elephant can be attained and how this may relate to their observable

behaviors. In addition, it must be noted that the surface of the cerebral cortex is covered by thick meninges, in places being up to 15 mm thick (Shoshani et al. 2006; Manger et al. 2009), which effectively obscures the impression of the pattern of gyri sulci on the inner surface of the cortical mantle, making it very difficult to infer structural or regional variation of the cerebral cortex over proboscidean evolutionary history through the examination of fossil endocasts. It is only through the examination of large-scale structural units of the cortex, such as cortical lobes, that any hints regarding the evolutionary history of the elephant cerebral cortex can be gleaned. In this sense, the temporal (see below), occipital and frontal lobes are the most salient features of the elephant cerebral hemisphere for palaeoneurological analysis.

The apparently extraordinary capacities of the elephant memory system are a feature of their behavior that has been dramatically exaggerated by the field of evolutionary psychology, leading to misrepresentations of the size and complexity of the hippocampal formation (the central structure that functions to form and recall memories) in the extant elephants (Hakeem et al. 2005). Indeed, when placed in an appropriate context, the elephant hippocampal formation, having a volume of 10.84 cm^3, is very close to the size that one would expect for a mammal with an approximately five-kilogram brain (Patzke et al. 2014, 2015). The general structure of the hippocampal formation of the elephant is quite similar to that observed in other mammals, with one exception – the molecular layer of the dentate gyrus appears to have double the number of sublamina observed in other mammalian species (Patzke et al. 2014), although the effect this may have on the formation and recall of memories is unclear. At present it is best to be pragmatic about elephant memory capacities, assuming that the quality, quantity, and clarity of memories stored within the elephant brain parallel the needs of a long-lived terrestrial mammal. In this sense, “enlargement” of the hippocampal formation, putatively leading to an enlargement of the temporal lobe in which it is found, is an unlikely scenario leading to variations in the shape and size of the fossil proboscidean endocast and

can be excluded from palaeoneurological analyses as a factor in the evolution of the shape of the brain in fossil proboscideans.

The olfactory bulbs of the extant elephant are large in size, with a combined mass of almost 42 g, and 908.37 million neurons (Herculano-Houzel et al. 2014). Within the olfactory bulbs of the elephant, the typically mammalian layered organization is observed, although the glomerular layer expresses a honey-combed appearance compared to the mono-layered appearance observed in other mammals (Ngwenya et al. 2011). This large size and complexity of the glomerular layer are clearly associated with the presence of up to 2000 active olfactory receptor genes in the elephants (Niimura et al. 2014). These observations indicate that the sense of smell is a crucial aspect of the life history of the elephant. While there is a distinct and functional vomeronasal organ in the elephant (Johnson and Rasmussen, 2002), interestingly, the accessory olfactory bulb, part of the pathway that processes information acquired through the vomeronasal organ for the odorous detection of pheromones, is absent in the elephant olfactory bulb (Ngwenya et al. 2011), as are the more central nuclei of the brain that are known to process accessory olfactory odorant information (Limacher-Burrell et al. 2018). This would indicate that pheromones are not detected as odorants by the elephants, but rather as tactile sensations (presumably *via* the trigeminal nerve), which may be of great importance in understanding the effects of pheromones on elephant behavior (Limacher-Burrell et al. 2018). Despite these microstructural intricacies, it is clear that the large size and anteroventral location of the elephant olfactory bulbs create important skeletal markers in the study of fossil endocasts and the evolution of behavioral repertoires associated with olfaction in the proboscideans.

The cerebellum of the elephant, with a volume of approximately 925 ml, is relatively the largest cerebellum of all mammals studied to date (Maseko et al. 2012). The African elephant cerebellum is composed of 250.71 x 10^9 neurons (Herculano-Houzel et al. 2014),

and these neurons are far more complex, in terms of dendritic length and branching complexity, than observed in other mammalian species (Maseko et al. 2013a). As the cerebellum functions to control the force, extent, and duration of muscular contractions, this large volume and enormous population of complex neurons appear to be related to the control of the intricate musculature of the trunk and perhaps the production of the varied elephantine vocalizations. In this sense, understanding when in proboscidean evolutionary history the cerebellum obtained its large proportions is likely to provide circumstantial evidence regarding the evolution of the trunk and vocal communication systems in this lineage.

The last aspect of the extant elephant brain, and possibly that most amenable to elucidation through the examination of the fossil endocasts, involves the production and reception of infrasonic and other vocalizations. Indeed, for both the production and reception of vocalizations by the elephants there are numerous specific neural specializations (Maseko et al. 2013a; Stoeger and Manger 2014), but the majority of these specializations are unlikely to be reflected in fossil endocasts. It is well-known that across mammals the temporal lobe is involved in the processing of the auditory sense, and it is reasonable to assume that the temporal lobe of the elephant plays a similar role. It is also known that the temporal lobe of the elephant appears to be expanded, thus creating a very specific signature that can be readily observed in the fossil endocasts. It would be reasonable to assume, given the specializations of the auditory system, especially in the dorsal thalamus where a unique nucleus ideally situated to process infrasonic sound is found within the medial geniculate body (Maseko et al. 2013b), that the expansion of the temporal lobe of the elephant was driven by the need for greater cortical processing of auditory information (Shoshani et al. 2006). This expanded temporal lobe may be responsible for the extraction of the semantic content of elephant vocalizations and the integration of seismic and air-borne infrasonic vocalizations for the localization of the source of infrasound (Maseko et al. 2013a; Stoeger and Manger 2014).

Given this potentially vital role of the cerebral cortex forming the temporal lobe, the expansion of the temporal lobe in the evolutionary history of the proboscideans is likely to be an important marker of the timing when the auditory sense became very prominent, likely reflecting the evolution of the production, reception, and use of infrasonic vocalizations.

This survey of the extant elephant brain, while mostly derived from studies of the African elephant brain, has indicated that the evolution of morphological and behaviorally important aspects of the elephant brain that may be elucidated through the study of fossils include: (1) The lobes of the cerebral hemisphere, most specifically the temporal lobe, but also the frontal and occipital lobes; (2) the olfactory bulbs; (3) and the cerebellum. This survey also indicates that inferences regarding the patterns of sulci and gyri of the cerebral cortex and the relationship between the expansion of the temporal lobe and the hippocampal formation are not likely to contribute to changes in the shape of the endocast during proboscidean evolution. Using this more focused approach we re-evaluate the evolution of the proboscidean endocast.

15.3.2 Morphology of the endocranial cast in stem proboscideans

The endocast of modern elephants reflects their highly derived neuroanatomy. It is characterized by: (i) its rostrally prominent and flexed frontal lobe; (ii) its laterally and ventrally protruding temporal lobe; (iii) the unclearly defined occipital lobe; and (iv) its large cerebellum (Fig. 15.2i). In stem proboscideans, the endocast was very different. In *Moeritherium*, the endocranial cast has been investigated by numerous authors (primarily Andrews (1906) and Jerison (1973), but see Edinger (1975) for a complete list of workers). Unlike in modern elephants, the brain is rather linearly arranged as the olfactory bulbs are completely exposed dorsally (Fig. 15.1). A linearly arranged endocast is a primitive feature for proboscideans as it is also found in basal paenungulates such as early sirenians and

hyracoids (Benoit et al. 2013b). The dorsal surface of the hemispheres is however slightly more rounded and protruding dorsally in *Moeritherium* than in other Paleogene paenungulates (Benoit et al. 2013b) (Fig. 15.1), which foreshadows the flexed condition of the hemisphere in more derived species. The cerebellum is dorsally exposed in *Moeritherium* and contributes to about one-third of the dorsal and lateral surface of the endocast, which suggests that it was already enlarged as in modern proboscideans (Fig. 15.1). There are no visible dorsal delineating features of the occipital lobe in *Moeritherium*, though this cortical region might be obscured by the presence of the superior sagittal sinus (Fig. 15.1). The neopallium is smooth as in all Tethytheria (Benoit et al. 2013b). The temporal lobes appear large, but do not protrude laterally and ventrally to the extent that they do in the Elephantimorpha (Fig. 15.1). Friant (1951, 1954) noted that the lengthened and rather primitive aspect of the endocast of *Moeritherium* appears reminiscent to that of the brain of a twelve-month-old fetus of *Loxodonta africana*.

Comparative anatomy, isotopic analyses, ancestral molecular sequence reconstruction, and other data of various types have given substantial support to the hypothesis that *Moeritherium* was a semi-aquatic mammal (e.g. Osborn 1936; Clementz et al. 2008; Liu et al. 2008; Mirceta et al. 2013). Noticeably, adaptation to a semi-aquatic life history is known to dramatically affect brain function and morphology as it increases corticalization and decreases the size of olfactory bulbs (primarily because the sense of smell is less efficient underwater) (Bauchot and Stephan 1968; Pirlot and Kamiya 1985). This brings into question whether the endocranial morphology of *Moeritherium* is truly representative of the typical stem proboscidean condition, or if it autapomorphically reflects its adaptation to a semiaquatic lifestyle. In this respect, Matsumoto and Andrews (1923) noted that the endocast of *Moeritherium* looks like that of a terrestrial mammal as its volume is comparatively small (as stated above, its EQs reflect the primitive condition for Paenungulata, Table 15.1) and its

olfactory bulbs are large and pedunculated. These features are in sharp contrast with what would be expected from a brain affected by adaptation to a semi-aquatic environment, which indicates that the endocast of *Moeritherium* is a reliable estimate of the primitive condition in Proboscidea. To test this assertion, more work will have to be done on other "plesielephantiform" taxa. Unfortunately, as stated above, *Moeritherium* is the only specimen sufficiently documented to date. In *Phosphatherium*, one of the basal-most proboscideans, the exposed braincase has not been studied in detail. The brain cavity is described as globular and two times smaller than the rostrum of the skull (~50 mm in length) (Gheerbrant et al. 2005). The cerebral cavity in *Numidotherium*, as illustrated by Benoit et al. (2013c), is too badly crushed to give any reliable indication of endocast morphology.

15.3.3 Morphology of the endocranial cast in Elephantiformes

15.3.3.1 Evolution of the temporal lobe

Descriptions of the evolution of the temporal lobe in fossil proboscideans are scarce. In Elephantimorpha, a deep pseudosylvian sulcus marks the anterior limit of the temporal lobe, which protrudes laterally and appears almost vertical in lateral view (Fig. 15.1d-p) (Elliot Smith 1902). This gives the temporal lobe of Elephantimorpha a hypertrophied appearance in dorsal view (Fig. 15.1d-p), even compared to that of Primates (Shoshani et al. 2006).

The temporal lobe in the basal elephantiform *Palaeomastodon beadnelli* (as reconstructed in Benoit et al. [2019], based on the exposed braincase of specimen NHM-UK PV M 8464), does not protrude laterally to the same extent as in more derived Elephantimorpha. This condition is similar to that observed in *Moeritherium* (and seemingly *Deinotherium* and *Phosphatherium*), and the temporal lobe is similarly ill-defined in other

basal paenungulates such as sirenians, embrithopods, and hyracoids (Andrews 1906; Edinger 1960; Benoit et al. 2013b). These observations indicate that an unspecialized temporal lobe is most likely the plesiomorphic condition for proboscideans (Benoit et al. 2013b).

The temporal lobe is especially prominent in the largest taxa for which complete endocasts are known, *Zygolophodon borsoni* (16-ton body mass) and *Mammuthus meridionalis* (11-ton body mass) (Fig. 15.1; Benoit et al. 2019). In contrast, the endocast of the dwarf *P. falconeri* appears globular with rather blunt, weakly demarcated temporal lobes (Accordi and Palombo 1971; Palombo and Giovinazzo 2005). These observations indicate that the dimensions of the temporal lobe may vary in concert with body and/or brain size rather than to a particular function, which would be consistent with the appearance of an enlarged temporal lobe in Elephantimorpha. In *Choerolophodon* and *Gomphotherium*, the shape of the temporal lobe and the whole cerebral hemisphere seems to slightly differ from that in other Elephantimorpha according to Gervais (1872) and Schlesinger (1922), but these authors have also emphasized the poor state of preservation of their specimens.

The temporal lobe is involved in the processing of auditory stimuli, which is noteworthy given that the auditory capabilities of proboscideans and their acoustic environment have dramatically changed in elephantimorphs (Shoshani 1998; Shoshani et al. 2006; Benoit et al. 2013b; but see section 15.3.1). In elephants, social communications are transmitted by infrasonic vocalizations (15-25 Hz) and foot-stomping to produce seismic waves (10-40 Hz) (Langbauer 2000; O'Connell-Rodwell 2007a). The necessity to maintain communication and recognition within and between herds may have placed a major selective pressure leading to temporal lobe enlargement in elephantimorphs (Benoit 2015; Benoit et al. 2019). Bolstering this possibility is the fossil evidence that suggests that the morphological adaptations to produce infrasonic vocalization (inferred from muscle scars on fossil hyoid bones of mammoths, mammutids, and gomphotheres) and to perceive infrasonic calls (wide

interaural distance, enlarged middle ear ossicles, absence of a secondary bony lamina on the bony labyrinth) were both present in the last common ancestor of the Elephantimorpha (Meng et al. 1997; Shoshani 1998; Shoshani et al. 2001; Shoshani and Tassy 2005; Benoit et al. 2013b; see section 15.2.3).

15.3.3.2 Frontal lobes and olfactory bulbs

According to Edinger (1960), proboscideans retain the 'ancestral sausage shape' of the frontal lobe encountered in their close relatives the extinct tethytheres *Arsinoitherium*, desmostylians, extant and extinct sirenians (Andrews 1906; Edinger 1975) and Mesozoic mammals (Edinger 1964; Kielan-Jaworowska 1986). Nevertheless, the frontal lobe of elephants does not appear so primitive according to Maccagno (1962), Shoshani et al. (2006), and Bever et al. (2008) who argue that the evolution of the proboscidean frontal lobe is characterized by a progressive ventral bending of its anterior-most part that ultimately results in the covering of the olfactory bulbs in dorsal view (Fig. 15.2). A similar pattern of ventral bending and flexion of the frontal lobe is observed during ontogeny in extant elephants (Friant 1957; van der Merwe et al. 1995). On the one hand, a ventral flexion of the frontal lobe leading to the covering of the olfactory bulbs in dorsal view is present in most Elephantidae (Fig. 15.2), the most extreme example being observed in the dwarf elephant of Sicily, in which the olfactory bulbs are oriented ventrally (Accordi and Palombo 1971) (Fig. 15.3). *Stegodon insignis* (Stegodontiidae, the sister group to the Elephantidae) from the Miocene of the Himalayas displays a morphology similar to that of extant elephantids, with short and large olfactory bulbs completely covered by the flexed frontal lobe (Fig. 15.1). Some noticeable exceptions among elephantids are worth mentioning. The specimen of *Paleoloxodon antiquus* depicted by Osborn (1931, 1942) displays a small dorsal exposure of olfactory bulbs anteriorly, whereas in specimen MPUR sn1 from Pian dell'Olmo the olfactory

bulbs are not exposed at all in dorsal view (Maccagno 1962; Accordi and Palombo 1971; Palombo and Giovinazzo 2005). The endocast of an Asian elephant depicted by Elliot Smith (1902: figs. 175, 177), also appears to have the olfactory bulbs exposed dorsally, whereas that shown by Dechaseaux (1958: fig. 4) does not (Fig. 15.1n). Finally, the olfactory bulbs are partially visible in the dorsal view of the endocast of *Mammuthus meridionalis* (Dechaseaux 1958), but not in *M. columbii* (Bever et al. 2008) and *M. primigenius* (Simionescu and Morosan 1937) (Fig. 15.1i, k, m).

On the other hand, the olfactory bulbs are indisputably exposed in the dorsal view of the *Moeritherium* endocast (Jerison 1973; Shoshani et al. 2006; Bever et al. 2008) (Fig. 15.1). These observations would concur with Maccagno (1962), Shoshani et al. (2006) and Bever et al. (2008), that the frontal lobe increasingly flexes from basal to derived proboscideans, but the condition and polarity of this character in basal elephantiforms are far from clear. In *Palaeomastodon*, the olfactory bulbs were not clearly reconstructed (Benoit et al. 2019, SI 1) (Fig. 15.2c). Among the Mammutida, the anterior tips of the olfactory bulbs are partially visible in dorsal view in *Zygolophodon borsoni* (Benoit et al. 2019, SI 1), but there is much debate about their appearance in *Mammut americanum*. According to Jerison (1973), Shoshani et al. (2006) and Bever et al. (2008) the olfactory bulbs should be readily apparent in the dorsal view of the endocast in *M. americanum*, but Warren (1855: plate 17), Marsh (1873: fig. 74), Andrews (1906: fig. 42), and Edinger (1960: fig. 2d), depicted specimens in which the olfactory bulbs are not visible in dorsal view (Fig. 15.2d, e, b). Our own observations of specimen PV OR 40977 indicate that its olfactory bulbs are only partially visible when examining the specimen from the dorsal aspect. The extent to which the olfactory bulbs lie below the frontal lobe is also unclear among “mastodonts”. According to Gervais (1872), the endocast of a juvenile *Gomphotherium angustidens* from Sansan (France) has large and anteriorly protruding olfactory bulbs. Two other gomphotheres, *Cuvieronius* and

Stegomastodon, also possess a rather non-flexed brain cavity at the level of the frontal lobe (Boule and Thevenin 1920) (Fig. 15.2h). In contrast, the olfactory bulbs in *Choerolophodon pentelici* are oriented ventrally (Fig. 15.2g), though the frontal lobe does not appear significantly flexed (Schlesinger 1922).

It is important to note that the uncertainty surrounding the polarity of this character in basal elephantiformes and the discrepancies between previous observations might be due to differences in the orientation of the braincase/endocast. A braincase/endocast tilted upward anteriorly is more likely to expose the olfactory bulbs, as in the *Cuvieronius* and *Stegomastodon* specimens described in Boule and Thevenin (1920) (Fig. 15.2h). As a consequence, the state of exposure of the olfactory bulbs in dorsal views of the endocasts may have been affected by the orientation of the specimens depicted by the original authors (a parameter that cannot be controlled) instead of the actual state of this character. Even though this does not invalidate that a ventral flexion of the frontal lobe occurred during proboscidean evolution, further observations are necessary to better understand when and how this phenomenon occurred.

15.3.3.3 The cerebellum and evolution of the trunk

The cerebellum is readily visible in dorsal views of the endocranial cast in all extant and extinct proboscideans, but the occipital lobe is ill-defined (Fig. 15.1). This greatly differs from the condition seen in humans, in which the occipital lobe is well developed and overlies the cerebellum in dorsal view (Jerison 1973; Holloway 2013; Beaudet et al. 2019). In this regard, Shoshani et al. (2006) indicated that as the occipital lobe is the center of vision, vision is not an elaborated sense in elephants (but see Pettigrew et al. 2010; Maseko et al., 2013). The cerebellum of extant elephants is proportionately and absolutely the largest of all mammals examined to date (Maseko et al. 2012). The large size of the cerebellum likely plays

an important role in the coordination of pharyngeal muscles for vocalizations and complex motions of the proboscis (Shoshani et al. 2006; Maseko et al. 2012). The proboscis alone represents 150,000 muscle bundles capable of lifting 350 kg, whereas its finger-like tips can achieve extremely delicate actions such as shelling peanuts or making tools (Shoshani 1998). As a consequence, it has been proposed that cerebellum size would have co-evolved with the development of the proboscis (Maseko et al. 2012).

Although a rich fossil record chronicles the evolutionary history of Proboscidea, the evolution of their most defining feature, the trunk (or proboscis) is not well documented as soft tissues do not readily preserve (Shoshani 1998). Historically, authors made use of osteological correlates to estimate the presence and dimensions of the proboscis such as the size of the infraorbital foramen (for the infraorbital ramus of the maxillary branch of the trigeminal nerve), retraction of the osseous naris, and length of the mandibular symphysis and other osteological proxies (Osborn 1936, 1942; Wall 1980; Witmer et al. 1999; Knoll et al. 2006; Muchlinski 2008, 2010; Crumpton and Thompson 2013; Nabavizadeh 2015; Nabavizadeh and Reidenberg 2019).

The trigeminal nerve is one of the largest nerves in proboscideans as it is responsible for mostly providing tactile sensation to the face, narial area, trunk, and dentition of the upper (V1, V2) and lower jaws (V3), as well as carrying out some motor functions to the lower jaw (Boas 1908; Shoshani 1982; Rodella et al. 2012; Higashiyama and Kuratani 2014; Nabavizadeh and Reidenberg 2019). The infraorbital ramus of the maxillary branch (V2) of the trigeminal nerve innervates the follicles of the sensory hairs and skin of the elephant trunk (Osborn 1936, 1942; Wall 1980; Witmer et al. 1999; Knoll et al. 2006; Muchlinski 2008, 2010; Crumpton and Thompson 2013; Nabavizadeh 2015; Nabavizadeh and Reidenberg 2019). It passes through a bony tunnel through the maxilla called the infraorbital canal, which opens caudally within the orbit (maxillary foramen) and rostrally on the lateral aspect of the

maxilla (infraorbital foramen) (Muchlinski 2008; Crumpton and Thompson 2013; Benoit et al. 2019). The dimensions of the infraorbital foramen are directly correlated to the number of nerve fibers passing through the infraorbital canal in mammals (Muchlinski 2008, 2010). As the proboscis developed during proboscidean evolution, it is thus inferred that the size of the infraorbital foramen on fossilized skulls would reflect the increasing innervation of the "growing" trunk (Andrews 1904; Osborn 1936, 1942). To the best of our knowledge, no quantitative approach to tracing the evolution of the dimensions of the proboscidean infraorbital foramen has been undertaken, and only qualitative accounts are available.

It is noteworthy that even the basal-most "Plesielephantiformes", such as *Eritherium*, *Phosphatherium,* and *Numidotherium* (Mahboubi et al. 1984; Gheerbrant et al. 2005; Gheerbrant 2009; Gheerbrant et al. 2012), already present with a relatively large infraorbital foramen, surrounded by a deep infraorbital fossa (or canine fossa) for the attachment of a presumably well-developed *levator alae nasi* muscle (Boas 1908; Shoshani 1982). This strongly suggests that a mobile and prehensile upper lip was already present in the basal-most proboscideans and is likely a plesiomorphic feature of the Tethytheria (Gheerbrant et al. 2005) (Fig. 15.5). Deinotheriidae and Elephantiformes, including the basal elephantiform *Palaeomastodon*, possess a very large infraorbital foramen, comparable to that of modern elephants (Andrews 1904; Osborn 1936, 1942; Sanders et al. 2010), although some variations exist and remain to be fully explored, like in *Gomphotherium angustidens*, which exhibits a condition where the infraorbital canal is divided into a small dorsal foramen and a relatively larger ventral one (Tassy 2013). In general, the infraorbital canal is long and runs horizontally in basal "plesielephantiforms", but becomes relatively short and more obliquely oriented in deinotherids and elephantiforms as the rostrum shortens and the external nares are retracted (Andrews 1904; Osborn 1936, 1942; Sanders et al. 2010) (Fig. 15.5).

The proboscis, molars, and tusks weigh altogether hundreds of kilograms (Shoshani and Eisenberg 1982; Larramendi 2015) contributing 5 to 10% of the total body mass in modern elephants. The proboscideans skull, therefore developed a highly pneumatized skull and deep insertions for the nuchal ligaments to compensate for the cranial extra weight (Andrews 1904; Osborn 1936, 1942; van der Merwe et al. 1995; Shoshani and Tassy 1996; Sanders et al. 2010). *Eritherium*, *Phosphatherium,* and *Moeritherium* show little signs of cranial pneumatization, whereas *Numidotherium* and *Barytherium* do (Mahboubi et al. 1984; Delmer 2005; Gheerbrant et al. 2005; Gheerbrant 2009; Gheerbrant and Tassy 2009; Gheerbrant et al. 2012; Benoit et al. 2013c), which makes it difficult to point out the exact origin of a pneumatized skull among "plesielephantiforms". It is nevertheless likely that *Moeritherium* secondarily lost its cranial pneumaticity as an adaptation to a semi-aquatic lifestyle (Matsumoto and Andrews 1923; Tassy 1981). The deinotherids, *Palaeomastodon*, and more derived elephantiformes all share the presence of cranial pneumaticity and deep nuchal fossae for ligamentous attachment (Andrews 1904; Osborn 1936, 1942; Shoshani and Tassy 1996; Sanders et al. 2010).

Due to the evolution of the proboscis, the proboscidean skull changed in overall gross morphology to accommodate attachments of the heavy labial and nasal musculature needed to operate the massive trunk, i.e. the nares became increasingly large and retracted, the snout shortened and the premaxilla became wider (Andrews 1904; Osborn 1936, 1942; Shoshani 1998; Gheerbrant and Tassy 2009). The earliest proboscidean to display an enlarged narial opening is *Numidotherium koholense*, whereas the first hints of narial retraction appear with *Barytherium* and *Moeritherium* (Andrews 1906; Mahboubi et al. 1984; Delmer 2005; Sanders et al. 2010). These anatomical changes are consistent with a gradual increase in size of the pre-existing mobile upper lip. Among early proboscideans, the deinotheriid *Deinotherium* achieved some of the widest premaxilla and largest nasal opening (Andrews 1921; Harris

1973; Sanders et al. 2010), although as it retains a relatively long and flexible neck and limbs, and shallow facial muscle attachments, it is traditionally reconstructed with a wide but short tapir-like trunk (Markov and Spassov 2001; Larramendi 2015).

Andrews (1904) and subsequent authors (e.g., Nabavizadeh 2015; Nabavizadeh and Reidenberg 2019) hypothesized that the onset of a very long mandibular symphysis in basal elephantiforms (i.e. *Palaeomastodon*, Mammutida, Gomphotheriinae, Choerolophodontinae, Amebelodontinae and other "gomphotheres") and deinotherids accompanied the evolution of the proboscis. The proboscis would occlude with the symphysis to enhance trophic activities and food processing, and as such the growth of the trunk would parallel the lengthening of the symphysis throughout phylogeny (Nabavizadeh 2015). This initial lengthening is coupled with the formation of tusk-like upper and shovel-shaped lower incisors (Andrews 1904; Noubhani et al. 2008; Nabavizadeh 2015). The maximum length of the mandibular symphysis is reached in Choerolophodontinae, and Amebelodontinae indicating that a trunk comparable to that in modern elephants was present as early as the middle Miocene, and is followed by the convergent, secondary reduction of the symphysis in the late Miocene and Pliocene in the Mammutida and Stegodontidae (modern elephant ancestors) while the proboscis remained stable (Andrews 1904; Osborn 1936, 1942; Van der Made 2010; Tassy 2013; Nabavizadeh 2015) (Fig. 15.5). The convergent loss of lower tusks may be correlated to the decrease of global temperature and humidity in the upper Miocene and Pliocene as the presence of four tusks would enhance heat loss (Mothé et al. 2016).

Based on the retraction of the narial opening, length of the mandibular symphysis, enlargement of the infraorbital foramen, and other cranial adaptations, it is most likely that basal "plesielephantiforms" had a prehensile upper lip (Fig. 15.5). The facial and narial musculature eventually evolved into a large and mobile proboscis in the last common ancestor

of the Deinotheriidae and Elephantiformes in the late Eocene (Andrews 1904; Osborn 1936, 1942; Nabavizadeh 2015).

The presence of a prehensile upper lip would account for the relatively large cerebellum of *Moeritherium* which makes up about one-third of the total length of the endocast in dorsal view (Fig. 15.1). The endocasts of all known Elephantiformes display an enlarged cerebellum comparable to that in modern elephants (Benoit 2015; Benoit et al. 2019) (Fig. 15.2). In the rare occasion when it is preserved and depicted, the cast of the trigeminal nerve is correspondingly large on the endocranial cast of elephantiforms (Andrews 1906; Dechaseaux 1958; Palombo and Giovinazzo 2005; Shoshani et al. 2006). Though the cerebellar morphology of deinotherids is unknown, the size of the *foramen rotundum* indicates that the trigeminal nerve was relatively large (Andrews 1921; Harris 1973).

(Insert Fig. 15.5)

15.3.3.4 Cortical sulcation and gyrification

One of the most striking features of the elephantine brain surface anatomy is the extent to which the cerebral cortex is fissured and folded, termed gyrencephaly (Cozzi et al. 2001; Shoshani et al. 2006). It has been shown that, broadly across mammalian species, the larger the brain (in absolute size), the more gyrencephalic the cerebral cortex (Manger et al. 2012). It should be noted that the extent of gyrencephaly of the elephant brain is what would be considered typical for a mammal with a brain mass of five kilograms (Manger et al. 2012). Nevertheless, the endocranial cast of proboscideans, including fossils, is surprisingly lissencephalic (smooth; Figs. 15.1-3; Andrews 1906; Simionescu and Morosan 1937; Dechaseaux 1958; Palombo and Giovinazzo 2005; Benoit et al. 2013b). This is likely due to the thickness of the meninges (which comprise meningeal vessels, the pia mater, the

arachnoid, and the dura mater) that encapsulate the brain and obfuscate the cortical gyral and sulcal patterns (Osborn 1931; Dechaseaux 1962; Manger et al. 2009). The functional significance of this thick layer of meninges and meningeal vessels in elephants include mechanical protection, blood supply and drainage, thermoregulation (through a possible rete mirabile formed by meningeal arteries), a housing of stem cells in case of injury, and as a 'vascular hydraulic skeleton' through blood pressure (Shoshani et al. 2006; Bruner et al. 2011; Decimo et al. 2012). The thickness of meninges in extant elephants ranges between five and fifteen millimeters, depending on the location sampled (Shoshani et al. 2006; Manger et al. 2009), and this thickness obscures the cortical sulci on the endocranial cast (Figs. 15.1-3). Meningeal thickness co-varies with brain size (Edinger 1948; Benoit 2015; Kharlamova et al. 2016) and as such, a smooth endocast is often found in mammals with large absolute brain size, such as humans, cetaceans, proboscideans, ground sloths, *Arsinoitherium*, *Elasmotherium*, and *Paraceratherium* (Andrews 1906; Granger et al. 1936; Dechaseaux 1958; Milne-Edwards 1868; Gervais 1872; Jerison 1973). It may be hypothesized that the smaller brained proboscideans (e.g. *Phosphatherium* and *Eritherium*) (Gheerbrant et al. 2005; Gheerbrant 2009) may have had a visibly gyrencephalic endocast, although a visibly lissencephalic condition appears to be the most likely primitive condition (Benoit et al. 2013b). The endocast of *Moeritherium lyonsi* is lissencephalic (Jerison 1973). The Sirenia, which are the closest living relatives of elephants (Poulakakis and Stamatakis 2010; Kuntner et al. 2011) have, since the early Eocene, been observed to have visibly lissencephalic endocasts (Ronald et al. 1978; O'Shea and Reep 1990; Furusawa 2004; Benoit et al. 2013b; Orihuela et al. 2019). The brains and endocasts of the extant Sirenia are also lissencephalic for the most part (O'Shea and Reep 1990). A visibly lissencephalic endocast is also found in *Arsinoitheirum* and *Desmostylus* (Andrews 1906; Edinger 1963, 1975), two extinct representatives of the orders Embrithopoda and Desmostylia respectively, which also belong

to the Tethytheria along with the sirenians and the proboscideans (Novacek and Wyss 1987; Seiffert 2007a; Asher 2007). As such, addressing the precise evolution of the gyral and sulcal pattern in extinct proboscideans is not tenable, except in the case of the well-preserved frozen brain tissue in *Mammuthus primigenius* (Kharlamova et al. 2016).

For more than 150 years, biologists and palaeobiologists have investigated the cranial cavity of frozen woolly mammoths from Siberia in order to study the soft brain tissue of this extinct species. As early as 1846 and 1904, Gleboff (1846) and Salensky (1904) respectively investigated the fleshy brain of *Mammuthus primigenius*, but they did not find anything more than a heavily decayed substance in place of the brain. Nonetheless, they could distinguish a distinct dura mater. Gleboff even depicted some identifiable neural cells that remained intact (Gleboff 1846:111-119, plate VII). About one hundred years later, Kreps et al. (1979, 1981) recorded the presence of a large variety of lipids in the brain of various specimens of *Mammuthus primigenius* and again later, Vereschagin (1981, 1999) and Maschenko et al. (2013) provided the first descriptions of partly preserved neural tissues from a variety of frozen calves. Fisher et al. (2014) briefly described the first endocast of a well-preserved *Mammuthus primigenius* neonate, although endocasts of adult specimens had been known for a long time already (Simionescu and Morosan 1937; Kubacska 1944). Lastly, a very well-preserved brain of a juvenile *M. primigenius* has been thoroughly described (Kharlamova et al. 2015, 2016). The analysis of this approximately ten-year-old specimen, nicknamed Yuka, shows that the overall external morphology of the brain, including the sulcal pattern, is quite comparable to that of extant elephants. As in extant elephants, the whole brain surface is densely sulcated, the temporal lobe is disproportionally large and laterally expanded, the cerebellum is large, with a narrow vermis, and is widely exposed dorsally. This represents the first time that the anatomy of the *true* brain of an extinct species is described (Kharlamova et al. 2015, 2016).

15.4 EVOLUTION OF THE BONY LABYRINTH, HEARING, AND BALANCE

15.4.1 Historical review

The first detailed study of the ear region and bony labyrinth of an elephant dates back to 300 years ago (Blair 1710a, b, 1717). A hundred years later, the labyrinth of an elephant was described again by Fick (1844) and Hyrtl (1845). These early studies were completed by Watson (1874), Buck (1888, 1890), Richards (1890), and Eales (1926) who described several aspects of soft tissue anatomy, osteology, and ontogeny of the ear region and petrosal of the African and Asian elephants.

The study by Claudius (1865) of the bony labyrinth of *Deinotherium giganteum* was the first known attempt to describe the bony labyrinth of an extinct member of the Proboscidea (Fig. 15.6c). Apart from this, the bony labyrinth of extinct proboscideans has only been investigated in recent years. A natural endocast of the cochlear canal of *Moeritherium* from the Eocene of Libya was briefly described by Tassy (1981) (Fig. 15.6b). A more complete study of a natural cast of the cochlear canal of *Numidotherium* from El Kohol (Algeria) (Fig. 15.6a) suggested that they were not adapted to low-frequency hearing (Court 1992), which was later confirmed by the CT-assisted study and digital reconstruction of a more complete bony labyrinth of *N. koholense* (Benoit et al. 2013c). The petrosal of *Moeritherium* was described in detail for the first time by Court (1994) as displaying an undivided perilymphatic foramen which demonstrated that this genus was more derived than *Numidotherium*. In 2013, Tassy provided the first detailed description of the petrosal of *Gomphotherium angustidens*. The development and increasing use of CT-scanning techniques paved the way for further study of extinct proboscideans, starting with the dwarf elephant *Palaeoloxodon tiliensis* (Provatidis et al. 2011), although these authors did not focus their study on the ear region. The first thorough CT study and 3D reconstruction of the bony

labyrinth of an extinct proboscidean were performed by Ekdale (2011) on an isolated petrosal (presumably *Mammuthus* or *Mammut*) from Texas (Fig. 15.6d). The bony labyrinths of *Numidotherium* and *Arsinoitherium* studied by Benoit et al. (2013c) later evidenced the convergent evolution of low-frequency hearing in elephantiforms and embrithopods. Further studies of the basal "plesielephantiforms" *Eritherium* and *Phosphatherium* later refined the understanding of early proboscidean labyrinthine evolution (Schmitt and Gheerbrant 2016).

As is evident from this historical review, only a handful of proboscidean bony labyrinths has been described and published. The main objective of this work is thus to provide the first comprehensive description of morphological variations and evolution of the bony labyrinth in modern elephants, including *Elephas maximus*, *Loxodonta cyclotis*, and *L. africana* and 14 genera of extinct proboscideans (*Eritherium azzouzorum*, *Phosphatherium escuilliei*, *Numidotherium koholense*, *Moeritherium lyonsi*, *M. cf. lyonsi*, *M. trigodon*, *Prodeinotherium bavaricum*, *Deinotherium giganteum*, *Mammut americanum*, *Gomphotherium angustidens*, *Cuvieronius* sp., *Stegomastodon* sp., *Platybelodon grangeri*, *Anancus arvernensis*, *Stegodon orientalis*, and *Palaeoloxodon antiquus*) using published data, CT scanning, manual segmentation, 3D reconstructions, and measurements (see details in the Online Supplementary Material). This increases the number of proboscidean taxa for which the bony labyrinth is documented from six (including Ekdale's (2011) unidentified elephantimorph and Claudius' (1865) *Deinotherium*) to seventeen. The petrosal and bony labyrinth of *Palaeoloxodon tiliensis* were described too recently to be considered here, but their morphology is almost identical to that of modern elephants (Liakopoulou et al., 2021).

(insert Fig. 15.6)

15.4.2 Bony labyrinth anatomy of extant elephants

The petrosal and bony labyrinth of modern elephants show no clear distinctive features between genera or species (Tables 15.2 and 15.3). In general, the semicircular canals

of extant elephants appear stocky and thick compared to other mammals (Fig. 15.6e-i). They are flattened in cross-section, a feature previously observed in *Arsinoitherium* (Benoit et al. 2013c). In general, the semicircular canals appear flatter in *Loxodonta*. The average semicircular canals thickness ratio tends to be higher in *Elephas* than in *Loxodonta*, but this character strongly varies intraspecifically (see Table 15.2). The angles between semicircular canals show great variability but usually, the most acute angle is between the anterior and lateral semicircular canals, whereas the most obtuse angle is between the posterior and lateral canals (Table 15.2). The ampullae of the canals are poorly defined, as the distinction between a canal and the swelling of the corresponding ampulla is poorly marked, unlike in most mammals (Fig. 15.6e-i). In both genera, the anterior semicircular canal is oval in anterior view (Fig. 15.6g) and the posterior one is circular in posterior view (Fig. 15.6h). Compared to other mammals, the lateral canal appears shorter and smaller than the two vertical canals (Fig. 15.6i). Unlike the vertical canals, the shape of the lateral semicircular canal in dorsal view varies greatly, from oval to almost circular between specimens of the same species. The lateral canal is also the one that shows the most variation in deviation from planarity (Fig. 15.6j), whereas the anterior and posterior canals do not undulate. The average values of the radii of curvature are similar between *Elephas* and *Loxodonta* (respectively 5.4 mm and 5.7 mm for the anterior canal, 5.2 mm and 5.3 mm for the posterior canal and 3.6 mm and 3.5 mm for the lateral canal on average). In general, the radii in *Elephas* are less variable than in *Loxodonta* (Table 15.2). In both genera, the anterior canal is consistently larger than the posterior one in terms of radii of curvature and length (Table 15.2). The dorsal apex of the anterior canal projects higher than that of the posterior canal (Fig. 15.6e, j). The point of entry of the lateral canal into the vestibule is located low and close to the posterior ampulla, but there is usually no secondary common crus (Fig. 15.6e, j), except a short one in two specimens of *Elephas* (MNHN.AC.ZM.1904-273 and 2008-81) and one of *Loxodonta*

(MNHN.AC.ZM.2008-71). The crus commune is usually stocky in elephants but may appear slightly more elongated and slender in some specimens of *Loxodonta*. Many specimens exhibit bumps and ridges on their crus commune (Fig. 15.6g, h, l) that seem to occur randomly. They may represent ossification scars or grooves that contained blood vessels in life (although this last hypothesis seems unlikely as specimen CEB150009 shows no blood vessels preserved in this area). Similar ridges are also present in some extinct proboscideans and *Arsinoitherium* (Benoit et al. 2013c).

The stapedial ratio varies greatly in elephants from a rather rounded *fenestra vestibuli* (1.53) to a rather oval one (1.83). This is consistent with the extreme values that Ekdale (2011) found in a large sample of Pleistocene elephantimorphs (1.4 to 2.1). On the cochlear canal, the secondary bony lamina (*lamina secundaria*) is absent in both genera (Fig. 15.6g, h). This is interpreted as an adaptation to low-frequency hearing since the absence of a secondary bony lamina widens the basilar membrane, making it less stiff and therefore more sensitive to low frequencies (Court 1992; Ketten 1992; Meng et al. 1997). Elephants are known to have the lowest low-frequency hearing limit of all extant terrestrial mammals (17Hz at 60dB in *Elephas*, Manoussaki et al. 2008), which aligns well with the infrasound they can produce by both vocalization (20Hz) and foot-drumming (10 to 40Hz) (Payne et al. 1986; Poole et al. 1988, 2005; O'Connell-Rodwell et al. 2001, 2007; Günther et al. 2004; O'Connell-Rodwell 2007b; Nair et al. 2009; Stoeger et al. 2011; Stoeger and Manger 2014). The radii ratio of the cochlear canal (the quotient between the radius of the basal turn over that of the apical turn) is between 5.35 and 8.85, which is consistent with low-frequency hearing (Manoussaki et al. 2008). The average relative volume of the cochlear canal is the same between *Elephas* and *Loxodonta* (respectively 47.7% and 47.0%). Viewed in profile, the cochlear canal appears planispiral (Fig 15.6g) and both genera share the same mean aspect ratios (0.39). The aspect ratio of the cochlear canal varies within species but remains between 0.30 and 0.45 (Table

15.3).

The number of turns of the cochlea is not a constant feature in extant elephants as it varies from less than two to almost three full turns (Table 15.3; Fig. 15.6F, j, k); it varies less in *Elephas* than in *Loxodonta* (Table 15.3). Noticeably, specimen MNHN.ZM.AC.2008-71 displays the smallest number of turns in the right ear (1.625 turns, 585°), but two turns (720°) in the left ear (Table 15.3). In contrast, the relative volume of the cochlear canal seems to be quite conservative in extant elephants as it varies mostly around 50% of the total volume of the bony labyrinth (except in specimens MNHN.ZM.AC.1956-194 and MNHN.ZM.AC.1957-465, in which it is 39.5% and 43.4% respectively, Table 15.3).

(insert Tables 15.2 and 15.3)

15.4.3 Evolution of the ear region and bony labyrinth in Proboscidea

To reconstruct the evolutionary history of the bony labyrinth in Proboscidea, we mapped ear region characters on a phylogenetic tree of proboscideans (Fig. 15.7). The consensus tree used to map the characters is a synthesis of Tassy (1994), Shoshani and Tassy (1996), Shoshani (1998), and Fisher (2018). The character matrix, originally designed for phylogenetic analysis at the scale of the superorder Afrotheria (Schmitt 2016), includes 12 petrosal characters and 20 bony labyrinth characters (Online Supplementary Material).

15.4.3.1. Basal proboscideans

The ear region morphotype of extant elephants was not acquired at the evolutionary root of the Proboscidea clade, but gradually during the evolutionary history of the Proboscidea (Fig. 15.7). Compared to modern proboscideans, *Eritherium* and *Phosphatherium* display a primitively slender and unspecialized vestibular morphology common to basal Paenungulata (Gheerbrant et al. 2014; Benoit et al. 2013a, 2016; Schmitt and Gheerbrant

2016), i.e. the outline of their semicircular canals form a circle, their cross-section is round, the lateral semicircular canal is long, the anterior semicircular canal does not project dorsally, the ampullae are well defined, the *crus commune* is slender (Table 15.4), and a secondary common crus (*crus commune secundaria*) is present (Figs. 15.8-15.12). The secondary common crus is short in *Eritherium*, but is longer in *Phosphatherium, Numidotherium,* and is likely present and short in *Moeritherium* (Figs. 15.8-12). The presence of a secondary common crus is generally considered plesiomorphic for Eutheria (Ekdale 2013) and Afrotheria (Benoit et al. 2013a, 2015). However, a secondary common crus is absent and the lateral canal enters the posterior ampulla in the oldest and basal-most paenungulate *Ocepeia daouiensis* (Gheerbrant et al. 2014) and the basal hyracoid *Seggeurius* (Benoit et al. 2016) (a condition also found in *Mammut*, *Palaeoloxodon*, *Platybelodon* and some specimens of *Loxodonta* among more derived proboscideans, Figs. 15.8-12), which makes the polarity of this character uncertain for paenungulates. Since a secondary common crus is consistently present in the basal-most proboscideans as well as in basal sirenians (Benoit et al. 2013a), it appears reasonable to consider its presence plesiomorphic for Proboscidea.

Eritherium exhibits the most slender semicircular canals (thickness ratio of 1.08, Table 15.5), whereas the canals in *Phosphatherium* and *Numidotherium* are slightly thicker (thickness ratio of 2.24 and 2.16 respectively), but still relatively more slender than in *Prodeinotherium* (thickness ratio of 2.82) and the Elephantimorpha (thickness ratio around or 3.00 and up to 4.86). It appears that the semicircular canals of proboscideans were primitively thin and became progressively thicker during their evolutionary history. This is supported by comparisons with *Ocepeia* (Gheerbrant et al. 2014), the early sirenians *Prorastomus* and that from Chambi (Benoit et al. 2013a), the basal hyracoid *Seggeurius* (Benoit et al. 2016) and the basal embrithopod *Stylolophus* (Gheerbrant et al. in press), which all exhibit slender semicircular canals. Additionally, *Eritherium*, *Phosphatherium,* and *Numidotherium* display

well-defined and bulbous ampullae, which contrasts with the poorly defined ampullae of more derived proboscideans (Figs. 15.8-12). The condition in *Moeritherium* is unclear from the CT scan (Figs. 15.8-12d), but judging from Tassy's (1981) figure, the ampullae appear poorly defined, as in more derived proboscideans (Fig. 15.7). In basal paenungulates such as *Ocepeia* (Gheerbrant et al. 2014), *Seggeurius* (Benoit et al. 2016), *Prorastomus* and the sirenian from Chambi (Benoit et al. 2013a), and *Arsinoitherium* (Benoit et al. 2013c), the ampullae are well defined too, which indicates that the condition in *Eritherium*, *Phosphatherium,* and *Numidotherium* is plesiomorphic.

(Insert Fig. 15.7)

The *fenestra cochleae* and cochlear aqueduct are separated in *Eritherium*, as in *Phosphatherium,* and *Numidotherium* (Figs. 15.8, 15.10). On the cochlear canal, there is a well-defined secondary bony lamina that expands on the ¾ turn of the cochlear canal in *Eritherium* and the ½ turn in *Phosphatherim* (Figs. 15.10, 15.11a, b). The cochlear canal makes two full turns in *Eritherium* (Table 15.4; not preserved in *Phosphatherium*). The basal turn of the cochlear canal is especially thick in *Phosphatherium* (Fig. 15.10b), resulting in a high cochlear volume (69% of the bony labyrinth volume). This is similar to *Ocepeia*, in which the cochlear canal represents about two-thirds of the total volume of the bony labyrinth (Table 15.4). In contrast, *Eritherium* and every other proboscidean have a vestibular canal contributing about 50% of the labyrinthine volume or less (Table 15.4), which suggests that the condition in *Phosphatherium* might be autapomorphic. An apical lacuna for the modiolus is present in most "plesielephantiformes", except *Deinotherium* (Claudius 1865) and one specimen of *Numidotherium* (Court 1992) (Fig. 15.9). This character may be considered plesiomorphic for proboscideans given its presence in *Ocepeia* (Gheerbrant et al. 2014); however, it is very variable in modern elephants, which prevents any definitive conclusion.

The cochlear aspect ratio is remarkably low in *Eritherium* (0.35, Table 15.4), which

indicates a rather flat cochlea. A cochlear canal with a high aspect ratio (>0.6, character 26) seems to be plesiomorphic for Paenungulata. The "condylarthran" *Ocepeia*, and the basal sirenian from Chambi both have a rather high aspect ratio (0.72 and 0.67 respectively) (Benoit et al. 2013a; Gheerbrant et al. 2014). In contrast, the aspect ratio is consistently low (always inferior to 0.6) in all studied proboscideans preserving a complete cochlear canal (Table 15.4). A rather flat cochlear canal may thus constitute a synapomorphy of the Proboscidea; however, it should be noted that the basal hyracoid *Seggeurius* (Benoit et al. 2016) and the basal sirenian *Prorastomus* (Benoit et al. 2013a) both have low cochlear aspect ratios (0.48 and 0.34 respectively). This casts some doubts about the polarity of this character and, in addition to the plesiomorphic aspect of the bony labyrinth of *Eritherium*, suggests that the origin of proboscideans may not have been accompanied by any unambiguous inner ear synapomorphies (Fig. 15.7).

While *Eritherium* exhibits a generalized morphology similar to more basal Paenungulata, *Phosphatherium* already displays a few proboscidean features: in the unnamed node C (Fig. 15.7) the *crista falciformis* becomes thinner and deeply embedded in the external auditory meatus (character 9) as in *Numidotherium* and more derived taxa (node D) (Court 1994; Benoit et al. 2013c), and the subarcuate fossa (character 1) becomes less deep before becoming shallow or absent at node E (Fig. 15.7). This last character change may seem surprising, as a shallow subarcuate fossa has long been recognized as a derived feature shared by Paenungulata (Novacek and Wyss 1986). Nevertheless, recent findings of a deep subarcuate fossa in *Eritherium* and the basal paenungulate *Ocepeia* (Gheerbrant et al. 2014; Schmitt and Gheerbrant 2016), and that of a moderately deep one in the hyracoid *Seggeurius*, the basal sirenian from Chambi and *Phosphatherium* (Gheerbrant et al. 2005; Benoit et al. 2013c, 2016) now makes the presence of a rather deep subarcuate fossa the plesiomorphic condition at the root of the Proboscidea clade without ambiguity.

In *Numidotherium* and more derived species (Clade D), the subarcuate fossa is lost (character 1) and the posterior semicircular canal defines a more oval space (character 18, although this character is quite variable). The petrosal of *Numidotherium* is unique as its *pars cochlearis* is excavated by a transpromontory sulcus (Court and Jaeger 1991; Benoit et al. 2013c) for the internal carotid artery (Klaauw 1931; Wible 1986). A transpromontorial (or lateral) course of the internal carotid artery is considered primitive for Placentalia (Wible 1986), whereas the derived condition (a medial or perbullar course) is documented or reconstructed based on the absence of a transpromontory sulcus in every other extant and extinct proboscidean, sirenian and hyracoid currently known, including *Eritherium* and *Phosphatherium* (Blair 1717; Klaauw 1931; Wible 1986; Fischer 1990, 1992; Court 1990, 1994; Court and Jaeger 1991; Gheerbrant et al. 2005; Ekdale 2011; Benoit et al. 2013a, 2015, 2016; Tassy 2013). *Ocepeia* and *Numidotherium* are the only known paenungulates in which a transpromontory sulcus is present (Court and Jaeger 1991; Benoit et al. 2013c; Gheerbrant et al. 2014), suggesting that this feature is not homologous in the two taxa and better interpreted as a homoplasy.

In *Moeritherium* and more derived proboscideans (node E) the anterior semicircular canal becomes more oval (Fig. 10D) (character 17). As stated above, the semicircular canals (particularly the anterior one) were all rounded in *Eritherium* and *Phosphatherium* (Fig. 10A-C), as well as in *Ocepeia* (Gheerbrant et al. 2014), the fossil hyracoid *Seggeurius* (Benoit et al. 2016), embrithopods (*Arsinoitherium* and *Stylolophus*; Benoit et al. 2013c; Gheerbrant et al. in press), and *Prorastomus* and the sirenian from Chambi (Benoit et al. 2013a). *Moeritherium*, the Deinotheriidae, and more derived proboscideans also differ from more basal "plesielephantiforms" by the flattening of the semicircular canals in cross-section (character 21), the poorly defined ampullae (character 13), the loss of the *lamina secundaria* (character 28), and the fusion of the *aquaeductus cochleae* and the *fenestra cochleae* to form

the perilymphatic canal (character 3). The paedomorphic retention of a single perilymphatic foramen during ontogeny instead of separated *fenestra cochleae* and *aquaeductus cochleae* is a derived feature encountered in extant elephants and sirenians (Fischer 1990). Such a single perilymphatic foramen is present in *Moeritherium* (Court 1994), *Prodeinotherium,* and all elephantimorphs studied here (Figs. 15.8-12), as well as in the embrithopod *Arsinoitherium* and was previously considered a synapomorphy of the clade Tethytheria (Fischer 1990; Court and Jaeger 1991). In contrast, the basal "plesielephantiforms" *Eritherium*, *Phosphatherium,* and *Numidotherium,* the basal sirenians *Prorastomus* and the unidentified specimen from Chambi all display a cochlear fenestra separated from the aqueduct (Court and Jaeger 1991; Benoit et al. 2013a, c; Schmitt and Gheerbrant 2016). As the separated condition is plesiomorphic for placental mammals (Court and Jaeger 1991; Ekdale 2011), the single perilymphatic foramen condition most likely evolved in a convergent manner in derived Proboscidea, Embrithopoda and Sirenia (Court 1990; Court and Jaeger 1991; Benoit et al. 2013a, c). Court and Jaeger (1991) hypothesized that it could be the result of independent adaptations to low-frequency hearing in Proboscidea and Sirenia (see below).

(Insert Tables 15.4 and 15.5)

15.4.3.2 The evolution of low-frequency hearing

Both elephants (Manoussaki et al. 2008) and sirenians (Ketten et al. 1992; Gaspard et al. 2012) exhibit adaptations allowing low-frequency hearing; however, low-frequency hearing might not be primitive for paenungulates as *Ocepeia*, hyracoids, *Prorastomus*, the basal embrithopod *Stylolophus*, and basal proboscideans all possess a secondary bony lamina (or *lamina secundaria*) that narrows and stiffens the basilar membrane at the base of the cochlear canal, making it more sensitive to high frequencies (West 1985; Court 1992; Ketten 1992; Meng et al. 1997; Benoit et al. 2013a, 2016; Gheerbrant et al. 2014; Schmitt and Gheerbrant 2016; Ekdale 2016). *Numidotherium* differs from other "plesielephantiforms" by

its lower number of cochlear turns. Most proboscideans display a cochlear canal making a least two full turns (Table 15.4) but those of the two specimens of *Numidotherium* examined here only complete 1.5 and 1.62 turns. The cochlear canal of the specimen described by Court (1992) also completes 1.5 turns (Fig. 15.6a). Thus, although this feature appears extremely variable in modern elephants, it seems stable in *Numidotherium*. As the basilar membrane becomes wider in the apical turns of the cochlea, it becomes more sensitive to low-frequency sounds (West 1985; Ketten et al. 1992). The low number of turns of the cochlear canal in *Numidotherium* might then reflect poorly developed low-frequency hearing. This is supported by the presence of a secondary bony lamina in *Numidotherium* (Court 1992). The secondary bony lamina is present in the cochlear canal of most mammals (Ekdale 2013, 2016), but it is absent in all the proboscideans studied herein except *Eritherium*, *Phosphatherium*, and *Numidotherium* (Figs. 15.10, 15.11). In *Phosphatherium*, it is extremely shallow and in *Numidotherium* it has only been observed in the specimen described by Court (1992); its absence in the specimens studied here may be explained by the resolution of the CT scan, preservation, or a genuine intraspecific variability. Its absence in proboscideans more derived than *Numidotherium* (Node E), modern sirenians (Ketten et al. 1992; Benoit et al. 2013a; Ekdale 2013) and *Arsinoitherium* is interpreted as a secondary loss due to adaptation to low-frequency hearing (Benoit et al. 2013c). This is supported by our measurements of the radii ratio in proboscideans, which indicates that even though *Moeritherium* had lost the secondary bony lamina, its radii ratio remains quite low, which is indicative of poorly developed, or non-specialized, low-frequency hearing according to Manoussaki et al. (2008). A relatively small radii ratio is likely plesiomorphic for the Proboscidea as it is also present in *Ocepeia* (Table 15.4) and most hyracoids (Benoit et al. 2016). A radii ratio within the range of variation observed in modern elephants is only seen in deinotheriids and elephantimorphs (Table 15.4), suggesting a lag between the loss of the secondary bony lamina and the change in cochlear

geometry, and possibly a gradual adaptation to more specialized low-frequency hearing across the Eocene and Oligocene. A more recent evolution of the capacity for low-frequency hearing in proboscideans is consistent with the works by Shoshani (1998) and Meng et al. (1997) who studied the middle ear, hyoid apparatus and interaural distance in *Mammut*, *Gomphotherium*, *Stegodon*, *Palaeoloxodon,* and *Mammuthus*, and concluded that the ability to hear and produce infrasonic calls likely evolved in the last common ancestor of Elephantimorpha.

(Insert Figs 15.8, 15.9, 15.10, 15.11, 15.12)

15.4.3.3 Deinotheriidae and Elephantimorpha

The bony labyrinth and ear region become essentially elephant-like in the last common ancestor of the Deinotheriidae and Elephantimorpha (Node F, Fig. 15.7), concurrent with the presence of most of the defining features of modern elephants. This is reflected distinctly in the vestibular morphology, as the studied proboscideans belonging to this clade have lost the secondary common crus (character 24) and exhibit a short and stocky common crus (character 15). A short lateral semicircular canal (character 23) and thickened semicircular canals (character 22) may also have evolved in this clade or the next one (node G) as these characters appear to be present in the *Deinotherium giganteum* specimen figured by Claudius (1865) (Fig. 15.6d) but not in *Prodeinotherium* (Figs. 15.8-12e). The more elephant-like aspect of the vestibular morphology of Claudius's *Deinotherium* compared to *Prodeinotherium* (if not due to an artistic license or misidentification) may be due to the difference in body mass between these two taxa (up to ten tons according to Larramendi (2015)). The presence of thickened semicircular canals, a stocky common crus, and a shortened lateral semicircular canal is commonly encountered in many large tetrapods such as *Arsinoitherium* (Benoit et al. 2013c), *Hippopotamus* (Hyrtl 1845), the giant subfossil lemur *Megaladapis* (Walker et al. 2008), the giant wombat *Diprotodon* (Alloing-Séguier et al. 2013), and many sauropod dinosaurs (Witmer et al. 2008; Knoll et al. 2012). The exact allometric relationship and possible

functional significance of the more robust aspect of the vestibule in these taxa have not yet been investigated. If not synapomorphic, characters 22 and 23 may thus be the result of a convergent evolution toward a more robust morphology of the vestibular apparatus due to an increase in body mass.

Clade F is also marked by a change in the position of the internal auditory meatus, which becomes more anteriorly oriented, whereas it was dorsally positioned in basal proboscideans (character 2). This reorientation affects the bony labyrinth as it results in a more obtuse angle between the basal turn of the cochlear canal and the vestibule in *Prodeinotherium* and more derived species (Table 15.4). As such, the basal turn of the cochlear canal is aligned with the ampullary limb of the anterior semicircular canal in anterior view, whereas it is not in more basal proboscideans (Fig. 15.10). The vestibulocochlear angle increases even further in node L (character 31), which includes *Anancus* and the Elephantidae (Table 15.4).

The Deinotheriidae nevertheless retain some noticeable plesiomorphies, such as the absence of a dorsal extension of the anterior canal (character 19). The apices of these two vertical semicircular canals reach the same height in *Phosphatherium, Numidotherium, Moeritherium,* and *Prodeinotherium* (the condition could not be evaluated from Claudius's figures of *Deinotherium*) (Fig. 15.1C). In contrast, the anterior canal apex always extends higher than the posterior one in more derived proboscidean taxa, except for *Stegomastodon* (Fig. 15.8). The relative dorsal extension is variable, from slightly higher (as in *Anancus*, Fig. 15.10n-q) to much higher (as in e.g. *Mammuthus columbi*, Fig. 15.8w, x).

The bony labyrinth morphology remains quite conservative among the Elephantimorpha (node G) as the differences observed between taxa do not depart significantly from the intraspecific variability observed in modern species (Tables 15.2-5). *Gomphotherium* stands out in this respect, as its *crus commune* is extremely large at its base

and progressively tapers dorsally, forming a conical shape in lateral view (Fig. 15.8h, i, j). In *Prodeinotherium*, *Anancus, Cuvieronius, Gomphotherium, Mammuthus,* and *Stegodon* the lateral canal is completely separated from the posterior canal and ampulla (character 20) and enters the vestibule in a higher position than in the Elephantidae *Loxodonta*, *Elephas*, *Mammuthus* and *Palaeoloxodon* (Figs. 15.8-12), in which the point of insertion of the lateral canal into the vestibule migrates back toward the posterior ampulla (node M). This character may constitute a synapomorphy of the Elephantidae (Fig. 15.7).

15.5 FINAL CONSIDERATIONS

The ear region is a key anatomical complex useful for anatomical, evolutionary, and functional studies. Its peculiar but poorly known morphology in proboscideans deserves further investigation. The petrosal of extant elephants is solidly fused to the skull and therefore difficult to access. While this region has already been described in the past, many previous studies failed to provide most of the anatomical details taken into account in recent studies of the petrosal and bony labyrinth of extant and extinct mammals. This study is the first comprehensive attempt to document the morphological diversity of the ear region and bony labyrinth of extant and extinct proboscideans using CT scanning. We found no feature that could discriminate between the bony labyrinths of the three extant elephant species. The bony labyrinth is described in sixteen extinct genera, covering most major proboscidean groups. We show that the modern morphotype evolved gradually in “plesielephantiforms” to become essentially elephant-like during the Oligocene, in the clade that includes deinotheriids and elephantiforms.

Although more data on the bony labyrinth of *Palaeomastodon* and the endocranial cast of deinotheriids would be necessary to confirm this trend, it is noteworthy that both the bony labyrinth and braincase morphology underwent an evolutionary limp toward an essentially

elephant-like condition simultaneously around the late Eocene - Early Oligocene. This suggests that the brain and inner ear coevolved in the common ancestors of elephantiforms and deinotheriids (Fig. 15.13). Examples of brain-ear region coevolution are not uncommon in mammals (e.g. Rowe 1996; Sánchez-Villagra 2002). It has been proposed that complex social interactions may result in brain size increase in paenungulates, artiodactyls, and perissodactyls (Pérez-Barbería and Gordon 2005; Shultz and Dunbar 2006). Such social bonds are supported by long-term memory of chemical scents and sounds of relatives in elephants (Payne et al. 1986; Poole et al. 1988, 2005; O'Connell-Rodwell et al. 2001, 2007; Günther et al. 2004; O'Connell-Rodwell 2007b; Hart et al. 2008). As the overall African climate became dryer in the Oligocene, droughts became more frequent and pockets of more humid environments (e.g., in Egypt and equatorial Africa) became more isolated (Boureau et al. 1983; Zachos et al. 2001; Kappelman et al. 2003; Bobe 2006; Seiffert 2007b; Feakins and Demenocal 2010; Mudelsee et al. 2014; Jacobs et al. 2016b; de Vries et al., 2021). We here speculate that the necessity to locate and remember the location of widely spaced sources of water and maintain social communication despite this distance using infrasonic vocalizations and foot drumming might have fuelled the coevolution of brain and inner ear morphology (Poole et al. 1988, 2005; Langbauer 2000; O'Connell-Rodwell et al. 2001, 2007; Günther et al. 2004; O'Connell-Rodwell 2007b; Hart et al. 2008). Low-frequency sounds propagate long distances as seismic waves (O'Connell-Rodwell 2007b), and modern elephants use these seismic waves as alarms, to locate mates and to maintain intra- and intergroup cohesion (Poole et al. 1988; Langbauer 2000; Günther et al. 2004; O'Connell-Rodwell et al. 2007). Elephants may even be able to locate places where rain falls and underground water reservoirs using infrasounds (Arnason et al. 2002; Garstang et al. 2014). A tight correlation between the onset of low-frequency hearing and the increase in drought frequency is supported by studies of the hyoid apparatus (Shoshani 1998; Shoshani et al. 2001; Meng et al. 1997), which show

that the ability to store water in a pharyngeal pouch and that of producing infrasonic calls are correlated and were already present in the last common ancestor of the Elephantimorpha. The possible evolutionary origin of the trunk in elephantiforms, an organ essential to infrasound vocalizations and filling up the pharyngeal pouch (Shoshani 1998; Shoshani et al. 2001; Meng et al. 1997), concurrently involved an increase in the size of the cerebellum to coordinate its movements (Maseko et al. 2012). The presence of a trunk also aided drinking and smelling at ground level as proboscideans evolved a larger body size, taller shoulder height and a shorter neck in the Oligocene (Larramendi 2015). As explained earlier in this chapter, a larger body mass is correlated to changes in the encephalization quotient (Manger et al. 2013) and the morphology of the bony labyrinth (thickening of the semicircular canals and common crus, reduced lateral canal). Low-frequency sound production and hearing are also more likely to evolve in larger species (e.g. rhinos and hippos) as large absolute body size increases the size of vocal organs and interaural distance (von Muggenthaler and Reinhart 2003; Barklow 2004a, b; Policht et al. 2008; Benoit et al. 2013c; Mourlam and Orliac 2017; Shoshani et al. 2001). It is noteworthy that low-frequency hearing may also be an adaptation to underwater hearing (Barklow 2004a, b; Mourlam and Orliac 2017), while the earliest proboscidean for which the loss of the *lamina secundaria* is documented coincidently is *Moeritherium*, a species that has long been reconstructed as semiaquatic (Osborn 1936; Clementz et al. 2008; Liu et al. 2008). Finally, herbivores living in open habitats have more chance to be grazers, and thus to display higher body mass, as a large body consumes less energy per unit of mass than a small one, and can accommodate a larger gut that improves digestion of coarse, comparatively nutrient deficient, grass (Peters 1983; Christiansen 2004; Franzen, 2010; Sander et al. 2011). Incidentally, living in an open habitat also increases the probability to live in large social and hierarchized groups, which in turn correlates with an increase in encephalization (Pérez-Barbería and Gordon 2005). As such, it is possible that a dryer climate

in Africa during the Oligocene had long-term cascading and self-reinforcing effects on body mass, encephalization, and bony-labyrinth morphology (Fig. 15.13). This hypothesis will have to be tested when more data become available, particularly from key late Eocene and Oligocene taxa such as early Elephantiformes, Deinotheriidae and other "Plesielephantiformes" for which reasonably small, yet highly relevant material could be CT scanned, such as specimen AMNH 13468 of the basal elephantiform *Phiomia serridens* and specimen Dt1008-1 of the "plesielephantiform" *Barytherium grave* (Andrews 1906; Sanders et al. 2010; Jaeger et al. 2012).

(Insert Fig. 15.13)

Acknowledgments

The authors would like to thank the financial support of La Fondation des Treilles, créée par Anne Gruner Schlumberger, a notamment pour vocation d'ouvrir et de nourrir le dialogue entre les sciences et les arts afin de faire progresser la création et la recherche contemporaines. Elle accueille également des chercheurs et des écrivains dans le domaine des Treilles (Var, France). www.les treilles.com. T.O. thanks Dr. Ştefan Vasile, University of Bucharest for access to the mammoth endocast from Naslavcea. A.S. thanks Emmanuel Gheerbrant and Pascal Tassy (MNHN, Paris, France) for supervising him during his PhD, and Erik Seiffert (Keck School of Medicine of USC, Los Angeles), Marcelo Sánchez (Paläontologisches Institut und Museum, Zürich), Pierre-Olivier Antoine (Université de Montpellier 2), and Guillaume Billet (MNHN, Paris) for taking part of his defense jury and improvement of his work. A.S. and J.B. thank Christine Argot, Joséphine Lesur, Aurélie Verguin, Marc Herbin, Eric Pellé and Jacques Cuisin (MNHN, Paris), Pip Brewer, Dan Sykes, and Farah Ahmed (Natural History Museum, London), Reinhard Ziegler (State Museum of Natural History, Stuttgart), Judith Galkin, Henry Tobin, Alana Gishlick, Ruth O'Leary,

Morgan Hill and Meng Jin (AMNH) for providing access to the specimens studied here. A.S. also thanks the Department of Human Evolution of the Max Planck for Evolutionary Anthropology (Leipzig, Germany) for welcoming him twice and allowing him to scan some specimens described in this study - in particular, Fred Spoor for providing some dataset and Romain David for his support. G.L. thanks Carolina di Patti (MGG), Pip Brewer (NHM-UK), Judith Galkin and Meng Jin (AMNH) for providing access to specimens studied here and Bartholomeus van der Geer for digitizing the endocasts. The authors finally thank Thomas E. Macrini and another anonymous reviewer for their comments on the manuscript.

References

Accordi FS, Palombo MR (1971) Morfologia endocranica degli elefanti nani pleistocenici di Spinagallo (Siracusa) e comparazione con l'endocranio di *Elephas antiquus*. Rendiconti della Accademia Nazionale Lincei, serie VIII 51:111–124

Alloing-Séguier L, Sánchez-Villagra MR, Lee MSY et al (2013) The bony labyrinth in Diprotodontian marsupial mammals: Diversity in extant and extinct forms and relationships with size and phylogeny. J Mammal Evol 20:191–198 https://doi.org/10.1007/s10914-013-9228-3

Andrews, CW (1921) Note on the skull of *Dinotherium giganteum* in the British Museum. Proc Zool Soc London 91:525–534 https://doi.org/10.1111/j.1096-3642.1921.tb03278.x

Andrews CW (1906) A descriptive catalogue of the Tertiary Vertebrata of the Fayum, Egypt. order of the Trustees of the British museum, London

Andrews CW (1904) On the evolution of the Proboscidea. Philosophical Transactions of the Royal Society of London Series B, Containing Papers of a Biological Character 196:99–118 https://doi.org/10.1098/rstb.1904.0004

Arnason BT, Hart LA, O'Connell-Rodwell CE (2002) The properties of geophysical fields and their effects on elephants and other animals. J Comp Psychol 116:123–132 https://doi.org/10.1037/0735-7036.116.2.123

Asher RJ (2007) A web-database of mammalian morphology and a reanalysis of placental phylogeny. BMC Evol Biol 7:108 https://doi.org/10.1186/1471-2148-7-108

Barklow WE (2004a) Amphibious communication with sound in hippos, *Hippopotamus amphibius*. Anim Behav 68:1125–1132 https://doi.org/10.1016/j.anbehav.2003.10.034

Barklow WE (2004b) Low-frequency sounds and amphibious communication in *Hippopotamus amphibious*. J Acoust Soc Am 115:2555–2555 https://doi.org/10.1121/1.4783854

Bauchot R, Stephan H (1968) Etude des modifications encéphaliques observées chez les insectivores adaptés à la recherche de nourriture en milieu aquatique. Mammalia 32:228–275 https://doi.org/10.1515/mamm.1968.32.2.228

Beaudet A, Clarke RJ, de Jager EJ et al (2019) The endocast of StW 573 ("Little Foot") and hominin brain evolution. J Hum Evol 126:112–123 https://doi.org/10.1016/j.jhevol.2018.11.009

Benoit J (2015) A new method of estimating brain mass through cranial capacity in extinct proboscideans to account for the non-neural tissues surrounding their brain. J Vertebr Paleontol 35:e991021 https://doi.org/10.1080/02724634.2014.991021

Benoit J, Adnet S, El Mabrouk E et al (2013a) Cranial remain from Tunisia provides new clues for the origin and evolution of Sirenia (Mammalia, Afrotheria) in Africa. PLoS ONE 8:e54307 https://doi.org/10.1371/journal.pone.0054307

Benoit J, Crochet J-Y, Mahboubi M et al (2016) New material of *Seggeurius amourensis* (Paenungulata, Hyracoidea), including a partial skull with intact basicranium. J Vertebr Paleontol 36:e1034358 https://doi.org/10.1080/02724634.2015.1034358

Benoit J, Crumpton N, Mérigeaud S et al (2013b) A memory already like an elephant's? The advanced brain morphology of the last common ancestor of Afrotheria (Mammalia). Brain Behav Evol 81:154–169 https://doi.org/10.1159/000348481

Benoit J, Legendre LJ, Tabuce R et al (2019) Brain evolution in Proboscidea (Mammalia, Afrotheria) across the Cenozoic. Sci Rep 9:1–8 https://doi.org/10.1038/s41598-019-45888-4

Benoit J, Lehmann T, Vatter M et al (2015) Comparative anatomy and three-dimensional geometric-morphometric study of the bony labyrinth of Bibymalagasia (Mammalia, Afrotheria). J Vertebr Paleontol 35:e930043 https://doi.org/10.1080/02724634.2014.930043

Benoit J, Merigeaud S, Tabuce R (2013c) Homoplasy in the ear region of Tethytheria and the systematic position of Embrithopoda (Mammalia, Afrotheria). Geobios 46:357–370 https://doi.org/10.1016/j.geobios.2013.07.002

Bever G, Macrini T, Jass C (2008) A natural endocranial cast of a fossil proboscidean with comments on elephant endocranial evolution and the scientific value of "no data" specimens. Unlocking the unknown: Papers honouring Dr Richard Zakrewski, Fort Hays Studies, Special Issue No 1, Fork Hays State University, Hays, Kansas, pp 11–22

Bianchi S, Bauernfeind AL, Gupta K et al (2011) Neocortical neuron morphology in Afrotheria: comparing the rock hyrax with the African elephant. Ann N Y Acad Sci 1225:37–46 https://doi.org/10.1111/j.1749-6632.2011.05991.x

Bibi F, Kraatz B, Craig N et al (2012) Early evidence for complex social structure in Proboscidea from a late Miocene trackway site in the United Arab Emirates. Biol Lett 8:670–673 https://doi.org/10.1098/rsbl.2011.1185

Blair P (1710a) A continuation of the osteographia elephantina: or, a description of the bones of an elephant, which died near Dundee, April the 27th, 1706. Philos Trans R Soc Lond 27:117–168 https://doi.org/10.1098/rstl.1710.0009

Blair P (1710b) Osteographia Elephantina: A full and exact description of all the bones of an elephant, which died near Dundee, April the 27th, 1706. with their several dimensions. Communicated in a letter to Dr. Hans Sloane, R, S, Secr. By Mr Patrick Blair, Surgeon, & Phil Trans R Soc 27:53–116 https://doi.org/10.1098/rstl.1710.0008

Blair P (1717) A description of the organ of hearing in the elephant, with the figures and situation of the ossicles, labyrinth and cochlea, in the ear of that large animal. Philos Trans R Soc Lond 30:885–899

Boas JEV (1908) The elephant's head: Studies in the comparative anatomy of the organs of the head of the Indian Elephant and other mammals. Fischer in Komm, Copenhagen

Bobe R (2006) The evolution of arid ecosystems in eastern Africa. J Arid Environ 66:564–584 https://doi.org/10.1016/j.jaridenv.2006.01.010

Boule M, Thevenin A (1920) Mammifères fossiles de Tarija. Imprimerie Nationale, Paris

Boureau E, Cheboldaeff-Salard M, Koeniguer J-C et al (1983) Evolution des flores et de la végétation Tertiaires en Afrique, au nord de l'Equateur. Bothalia 14:355–367 https://doi.org/10.4102/abc.v14i3/4.1180

Bruner E, Mantini S, Musso F et al (2011) The evolution of the meningeal vascular system in the human genus: From brain shape to thermoregulation. Am J Hum Biol 23:35–43 https://doi.org/10.1002/ajhb.21123

Buck AH (1888) A contribution to the anatomy of the elephant's ear. Transactions of the American Otological Society 240–253

Buck AH (1890) A revised description of the anatomy of the elephant's ear. Transactions of the American Otological Society 3–15

Byrne RW, Bates LA (2007) Sociality, evolution and cognition. Curr Biol 17:R714–R723 https://doi.org/10.1016/j.cub.2007.05.069

Christiansen P (2004) Body size in proboscideans, with notes on elephant metabolism. Zool J Linn Soc 140:523–549 https://doi.org/10.1111/j.1096-3642.2004.00113.x

Claudius M (1865) Das Gehörlabyrinth von *Dinotherium giganteum* nebst Bemerkungen über den Werth der Labyrinthformen für die Systematik der Säugethiere. Palaeontographica (1846-1933) 65–74

Clementz MT, Holroyd PA, Koch PL (2008) Identifying aquatic habits of herbivorous mammals through stable isotope analysis. Palaios 23:574–585 https://doi.org/10.2110/palo.2007.p07-054r.

Court N (1990) Periotic anatomy of *Arsinoitherium* (Mammalia, Embrithopoda) and its phylogenetic implications. J Vertebr Paleontol 10:170–182 https://doi.org/10.1080/02724634.1990.10011806

Court N (1992) Cochlea anatomy of *Numidotherium koholense*: auditory acuity in the oldest known proboscidean. Lethaia 25:211–215 https://doi.org/10.1111/j.1502-3931.1992.tb01385.x

Court N (1994) The periotic of *Moeritherium* (Mammalia, Proboscidea): homology or homoplasy in the ear region of Tethytheria McKenna, 1975? Zool J Linn Soc Lond 112:13–28 https://doi.org/10.1111/j.1096-3642.1994.tb00310.x

Court N, Jaeger J-J (1991) Anatomy of the periotic bone in the Eocene proboscidean *Numidotherium koholense*: an example of parallel evolution in the inner ear of tethytheres. C R Acad Sci 312:559–565

Cozzi B, Spagnoli S, Bruno L (2001) An overview of the central nervous system of the elephant through a critical appraisal of the literature published in the XIX and XX centuries. Brain Res Bull 54:219–227 https://doi.org/10.1016/S0361-9230(00)00456-1

Crumpton N, Thompson RS (2013) The holes of moles: osteological correlates of the trigeminal nerve in Talpidae. J Mammal Evol 20:213–225 https://doi.org/10.1007/s10914-012-9213-2

DeCasien AR, Thompson NA, Williams SA et al (2018) Encephalization and longevity evolved in a correlated fashion in Euarchontoglires but not in other mammals. Evolution 72:2617–2631 https://doi.org/10.1111/evo.13633

Dechaseaux C (1958) L'encéphale d'*Elephas meridionalis*. Ann Paléontol 64:269–278

Dechaseaux C (1962) Cerveaux d'animaux disparus: essai de paléoneurologie. Masson

Decimo I, Fumagalli G, Berton V et al (2012) Meninges: from protective membrane to stem cell niche. Am J Stem Cells 1:92–105

Delmer C (2005) Les premières phases de différenciation des Proboscidiens (Tethyria, Mammalia): le rôle du Barytherium grave de Lybie. These de doctorat, Paris, Muséum national d'histoire naturelle

de Vries D, Heritage S, Borths MR et al (2021) Widespread loss of mammalian lineage and dietary diversity in the early Oligocene of Afro-Arabia. Commun Biol 4:1172 https://doi.org/10.1038/s42003-021-02707-9

Eales NB (1926) XI.—The Anatomy of the head of a fœtal African elephant, *Elephas africanus* (*Loxodonta africana).* Earth Environ Sci Trans R Soc Edinb 54:491–551 https://doi.org/10.1017/S0080456800016082

Edinger T (1948) Evolution of the horse brain. Geol Soc Am Mem 25:1–177

Edinger T (1960) Anthropocentric misconceptions in paleoneurology. Proc Rudolf Virchow Med Soc City N Y 19:56–107 https://doi.org/10.1159/000405771

Edinger T (1963) Neues aus der Paläoneurologie. Paläont Z 37:49–55 https://doi.org/10.1007/BF02989599

Edinger T (1964) Midbrain exposure and overlap in mammals. Am Zool 4:5–19

Edinger T (1975) Paleoneurology 1804-1966: an annotated bibliography. Adv Anat Embryol Cell Biol 49:3–258

Eisenberg JF (1981) The mammalian radiations: an analysis of trends in evolution, adaptation, and behaviour. University of Chicago Press. 610 pp

Ekdale EG (2011) Morphological variation in the ear region of pleistocene elephantimorpha (Mammalia, Proboscidea) from central Texas. J Morphol 272:452–464 https://doi.org/10.1002/jmor.10924

Ekdale EG (2013) Comparative anatomy of the bony labyrinth (inner ear) of placental mammals. PLoS One 8:e66624 https://doi.org/10.1371/journal.pone.0066624

Ekdale EG (2016) Form and function of the mammalian inner ear. J Anat 228:324–337 https://doi.org/10.1111/joa.12308

Elliot Smith G (1902) The brains of the Mammalia. In: Owen R (ed) Descriptive and illustrated catalogue of the physiological series of comparative anatomy contained in the Museum of the Royal College of Surgeons of England. London, pp 138–481

Feakins SJ, Demenocal PB (2010) Global and African regional climate during the Cenozoic. In: Werdelin L (ed) Cenozoic Mammals of Africa. University of California Press, pp 45–56

Fick L (1844) Über das Labyrinth des Elefanten. Archiv für Anatomie, Physiologie und wissenschaftliche Medizin 431–432

Finlay BL, Darlington RB, Nicastro N (2001) Developmental structure in brain evolution. Behav Brain Sci 24:263–278

Fischer MS (1990) Un trait unique de l'oreille des éléphants et des siréniens (Mammalia): un paradoxe phylogénétique. C R Acad Sci, Sér 3, Sci vie 311:157–162

Fischer MS (1992) Hyracoidea. Handbuch der Zoologie: Mammalia 8:1–169

Fisher DC (2018) Paleobiology of Pleistocene proboscideans. Annu Rev Earth Planet Sci 46:229–260 https://doi.org/10.1146/annurev-earth-060115-012437

Fisher DC, Shirley EA, Whalen CD et al (2014) X-ray computed tomography of two mammoth calf mummies. J Paleontol 88:664–675 https://doi.org/10.1666/13-092

Franzen, J. (2010). The rise of horses: 55 million years of evolution. Baltimore, The Johns Hopkins University Press

Friant M (1951) Sur la forme du cerveau, au cours de l'Ontogénie, chez les éléphants (Elephantidae). C R Acad Sci - Sér 3, Sci vie 232: 2137–2138

Friant M (1954) Sur la forme du cerveau de l'éléphant (*Loxodonta africana* Blum.), au cours de la vie prénatale. Comptes Rendus de l'Académie des Sciences - Series III - Sciences de la Vie 238:1534–1535

Friant M (1957) Morphologie et développement du cerveau des mammifères euthériens. III. Série des ongulés. Ann Soc R Zool Belg 88:321–367

Furusawa H (2004) A phylogeny of the North Pacific Sirenia (Dugongidae: Hydrodamalinae) based on a comparative study of endocranial casts. Paleontol Res 8:91–98 https://doi.org/10.2517/prpsj.8.91

Garstang M, Davis RE, Leggett K et al (2014) Response of African elephants (*Loxodonta africana*) to seasonal changes in rainfall. PLOS ONE 9:e108736 https://doi.org/10.1371/journal.pone.0108736

Gaspard JC, Bauer GB, Reep RL et al (2012) Audiogram and auditory critical ratios of two Florida manatees (*Trichechus manatus latirostris*). J Exp Biol 215:1442–1447 https://doi.org/10.1242/jeb.065649

Gervais P (1872) Mémoire sur les formes cérébrales propres à différents groupes de mammifères. Journal de Zoologie, Paris 1:425–469

Gheerbrant E (2009) Paleocene emergence of elephant relatives and the rapid radiation of African ungulates. Proc Natl Acad Sci USA 106:10717–10721 https://doi.org/10.1073/pnas.0900251106

Gheerbrant E, Amaghzaz M, Bouya B et al (2014) *Ocepeia* (Middle Paleocene of Morocco): The oldest skull of an Afrotherian mammal. PLOS ONE 9:e89739 https://doi.org/10.1371/journal.pone.0089739

Gheerbrant E, Bouya B, Amaghzaz M (2012) Dental and cranial anatomy of *Eritherium azzouzorum* from the Paleocene of Morocco, earliest known proboscidean mammal. Palaeontogr Abt A 297:151–183 https://doi.org/10.1127/pala/297/2012/151

Gheerbrant E, Khaldoune F, Schmitt A et al (in press) Earliest embrithopod mammals (Afrotheria, Tethytheria) from the Early Eocene of Morocco: anatomy, systematics and phylogenetic significance. J Mamm Evol https://doi.org/10.1007/s10914-020-09509-6

Gheerbrant E, Sudre J, Tassy P et al (2005) Nouvelles données sur *Phosphatherium escuilliei* (Mammalia, Proboscidea) de l'Eocène inférieur du Maroc, apports à la phylogénie des Proboscidea et des ongulés lophodontes. Geodiversitas 27:239–333

Gheerbrant E, Tassy P (2009) L'origine et l'évolution des éléphants. C R Palevol 8:281–294 https://doi.org/10.1016/j.crpv.2008.08.003

Gleboff J (1846) Recherches microscopiques sur les parties molles du mammouth (Elephas *primigenius* Blumenbach, *Mammonteus* Fischer). Bulletin de la Société impériale des naturalistes de Moscou 19:108–134

González-Lagos C, Sol D, Reader SM (2010) Large-brained mammals live longer. J Evol Biol 23:1064–1074 https://doi.org/10.1111/j.1420-9101.2010.01976.x

Goodman M, Sterner KN, Islam M et al (2009) Phylogenomic analyses reveal convergent patterns of adaptive evolution in elephant and human ancestries. Proc Natl Acad Sci USA 106:20824–20829 https://doi.org/10.1073/pnas.0911239106

Granger W, Gregory WK, William K et al (1936) Further notes on the gigantic extinct rhinoceros, *Baluchitherium*, from the Oligocene of Mongolia. Bull Am Mus Nat Hist 72:1–73

Gravett N, Bhagwandin A, Sutcliffe R et al (2017) Inactivity/sleep in two wild free-roaming African elephant matriarchs – does large body size make elephants the shortest mammalian sleepers? PLOS ONE 12:e0171903 https://doi.org/10.1371/journal.pone.0171903

Günther RH, O'Connell-Rodwell CE, Klemperer SL (2004) Seismic waves from elephant vocalizations: A possible communication mode? Geophys Res Lett 31: L11602 https://doi.org/10.1029/2004GL019671

Hakeem AY, Hof PR, Sherwood CC et al (2005) Brain of the African elephant *(Loxodonta africana*): Neuroanatomy from magnetic resonance images. Anat Rec 287A:1117–1127 https://doi.org/10.1002/ar.a.20255

Hakeem AY, Sherwood CC, Bonar CJ et al (2009) Von Economo Neurons in the Elephant Brain. Anat Rec 292:242–248 https://doi.org/10.1002/ar.20829

Harris JM (1973) *Prodeinotherium* from Gebel Zelten, Libya. Bull Br Mus Nat Hist 23:283–348

Hart BL, Hart LA, Pinter-Wollman N (2008) Large brains and cognition: where do elephants fit in? Neurosci Biobehav Rev 32:86–98 https://doi.org/10.1016/j.neubiorev.2007.05.012

Herculano-Houzel S, Avelino-de-Souza K, Neves K et al (2014) The elephant brain in numbers. Front Neuroanat 8:46 https://doi.org/10.3389/fnana.2014.00046

Herridge VL, Lister AM (2012) Extreme insular dwarfism evolved in a mammoth. Proc Biol Sci 279:3193–3200 https://doi.org/10.1098/rspb.2012.0671

Higashiyama H, Kuratani S (2014) On the maxillary nerve: the maxillary nerve in vertebrates. J Morphol 275:17–38 https://doi.org/10.1002/jmor.20193

Hofman MA (1993) Encephalization and the evolution of longevity in mammals. J Evol Biol 6:209–227 https://doi.org/10.1046/j.1420-9101.1993.6020209.x

Holloway RL (2013) The evolution of the hominid brain. In: Henke W, Tattersall I (eds) Handbook of Paleoanthropology. Springer Berlin Heidelberg, Berlin, Heidelberg, pp 1–23

Hyrtl J (1845) Vergleichend-anatomische untersuchungen über das innere gehörorgan des menschen und der säugethiere. F. Ehrlich

Jacobs B, Lee L, Schall M et al (2016a) Neocortical neuronal morphology in the newborn giraffe (*Giraffa camelopardalis tippelskirchi)* and African elephant (*Loxodonta africana*). J Comp Neurol 524:257–287 https://doi.org/10.1002/cne.23841

Jacobs B, Lubs J, Hannan M et al (2011) Neuronal morphology in the African elephant (*Loxodonta africana*) neocortex. Brain Struct Funct 215:273–298 https://doi.org/10.1007/s00429-010-0288-3

Jacobs LL, Polcyn MJ, Mateus O et al (2016b) Post-Gondwana Africa and the vertebrate history of the Angolan Atlantic coast. Mem Mus Vic 74:343–362 https://doi.org/10.24199/j.mmv.2016.74.24

Jaeger J-J, Salem MJ, Bilal AA et al (2012) Dūr aṭ Ṭalaḥ vertebrate locality revisited: new data on its stratigraphy, age, sedimentology and mammalian fossils. In: Salem MJ, Elbakai MT, Abutarruma Y (eds) Earth Science Society of Libya. Tripoli, pp 241–258

Jebb D, Hiller M (2018) Recurrent loss of HMGCS2 shows that ketogenesis is not essential for the evolution of large mammalian brains. eLife 7:e38906 https://doi.org/10.7554/eLife.38906

Jerison H (1973) Evolution of the brain and intelligence. Elsevier Science, Saint Louis

Johnson EW, Rasmussen L (2002) Morphological characteristics of the vomeronasal organ of the newborn Asian elephant (*Elephas maximus*). Anat Rec 267:252–259 https://doi.org/10.1002/ar.10112

Kappelman J, Rasmussen DT, Sanders WJ et al (2003) Oligocene mammals from Ethiopia and faunal exchange between Afro-Arabia and Eurasia. Nature 426:549–552 https://doi.org/10.1038/nature02102

Ketten DR (1992) The marine mammal ear: specializations for aquatic audition and echolocation. In: Webster DB, Popper AN, Fay RR (eds) The evolutionary biology of hearing. Springer, New York, NY, pp 717–750

Ketten DR, Odell DK, Domning DP (1992) Structure, function, and adaptation of the manatee ear. In: Thomas JA, Kastelein RA, Supin AYa (eds) Marine mammal sensory systems. Springer US, Boston, MA, pp 77–95

Kharlamova A, Saveliev S, Kurtova A et al (2016) Preserved brain of the woolly mammoth (*Mammuthus primigenius* (Blumenbach 1799)) from the Yakutian permafrost. Quat Internat 406:86–93 https://doi.org/10.1016/j.quaint.2014.09.073

Kharlamova AS, Saveliev SV, Protopopov AV et al (2015) The mummified brain of a pleistocene woolly mammoth (*Mammuthus primigenius*) compared with the brain of the extant African elephant (*Loxodonta africana*). J Comp Neurol 523:2326–2343 https://doi.org/10.1002/cne.23817

Kharlamova AS, Pavlov IS, Saveliev SV (2021) Unique 39 thousand cal. BP brain of the "Yuka" mammoth mummified fossils: A history and methods of the examination: paleoneurological perspectives. Paleontol J 55:1260–1269 https://doi.org/10.1134/S0031030121110034

Kielan-Jaworowska Z (1986) Brain evolution in Mesozoic mammals. In: Flanagan KM, Lillegraven JA (eds) Vertebrates, Phylogeny, and Philosophy. University of Wyoming, Laramie, WY, pp 21–34

Klaauw CJ van der (1931) The auditory bulla in some fossil mammals: with a general introduction to this region of the skull. On the auditory bulla in some fossil mammals. Bull Am Mus Nat Hist 62:1–352

Knoll F, Galton PM, López-Antoñanzas R (2006) Paleoneurological evidence against a proboscis in the sauropod dinosaur *Diplodocus*. Geobios 39:215–221 https://doi.org/10.1016/j.geobios.2004.11.005

Knoll F, Witmer LM, Ortega F et al (2012) The braincase of the basal sauropod dinosaur *Spinophorosaurus* and 3D reconstructions of the cranial endocast and inner ear. PLOS ONE 7:e30060 https://doi.org/10.1371/journal.pone.0030060

Kreps EM, Avrova NF, Chebotarëva MA et al (1981) Brain lipids in fossilized mammoths, *Mammuthus primigenius*. Comp Biochem Physiol B: Comparative Biochemistry 68:135–140 https://doi.org/10.1016/0305-0491(81)90192-9

Kreps EM, Chirkovskaia EV, Pomazanskaia LF et al (1979) Brain lipids of a mammoth, *Elephas primigenius*, which died more than 40,000 years ago. Zh Evol Biokhim Fiziol 15:227–238

Kubacska AT (1944) Der natürliche Schädelhöhlenausguss eines Mammuts aus tata. In: Annales Historico-Naturales Musei Nationalis Hungarici. pp 3–40

Kuntner M, May-Collado LJ, Agnarsson I (2011) Phylogeny and conservation priorities of afrotherian mammals (Afrotheria, Mammalia). Zool Scr 40:1–15 https://doi.org/10.1111/j.1463-6409.2010.00452.x

Kupsky WJ, Marchant GH, Cook K et al (2001) Morphologic analysis of the hippocampal formation in *Elephas maximus* and *Loxodonta africana* with comparison to that of human. In: Proceedings of the first international congress of La Terra degli Elefanti, the world of elephants. Consiglio Nazionale delle Ricerche, Rome, pp 643–647

Langbauer WR (2000) Elephant communication. Zoo Biol 19:425–445 https://doi.org/10.1002/1098-2361(2000)19:5<425::AID-ZOO11>3.0.CO;2-A

Larger R (1917) Théorie de la contre-évolution, ou Dégénérescence par l'hérédité pathologique. Félix Alcan, Paris

Larramendi A (2015) Shoulder height, body mass, and shape of proboscideans. Acta Palaeontol Pol 61:537–574 https://doi.org/10.4202/app.00136.2014

Larramendi A, Palombo MR (2015) Body size, biology and encephalization quotient of *Palaeoloxodon* ex gr. *P. falconeri* from Spinagallo Cave (Hyblean plateau, Sicily). Hystrix 26:102–109 https://doi.org/10.4404/hystrix-26.2-11478

Liakopoulou DE, Theodorou GE, van Heteren AH (2021) The inner morphology of the petrosal bone of the endemic elephant of Tilos Island, Greece. Palaeontol Elec 24:a23 https://doi.org/10.26879/1034

Limacher-Burrell A, Bhagwandin A, Maseko BC et al (2018) Nuclear organization of the African elephant (*Loxodonta africana*) amygdaloid complex: an unusual mammalian amygdala. Brain Struct Funct 223:1191–1216 https://doi.org/10.1007/s00429-017-1555-3

Lister AM (2013) The role of behaviour in adaptive morphological evolution of African proboscideans. Nature 500:331–334 https://doi.org/10.1038/nature12275

Liu AGSC, Seiffert ER, Simons EL (2008) Stable isotope evidence for an amphibious phase in early proboscidean evolution. Proc Natl Acad Sci USA 105:5786–5791 https://doi.org/10.1073/pnas.0800884105

Lomolino MV, Sax DF, Palombo MR et al (2012) Of mice and mammoths: evaluations of causal explanations for body size evolution in insular mammals. J Biogeogr 39:842–854 https://doi.org/10.1111/j.1365-2699.2011.02656.x

Lomolino MV, van der Geer AA, Lyras GA et al (2013) Of mice and mammoths: generality and antiquity of the island rule. J Biogeogr 40:1427–1439

Lyras GA (2018) Brain changes during phyletic dwarfing in elephants and hippos. Brain Behav Evol 92:167–181 https://doi.org/10.1159/000497268

Maccagno AM (1962) Gli elefanti di Riano (Roma). Geologica Romana 1:33–131

Mahboubi M, Ameur R, Crochett JY et al (1984) Earliest known proboscidean from early Eocene of north-west Africa. Nature 308:543–544 https://doi.org/10.1038/308543a0

Manger PR (2006) An examination of cetacean brain structure with a novel hypothesis correlating thermogenesis to the evolution of a big brain. Biol Rev 81:293 https://doi.org/10.1017/S1464793106007019

Manger PR, Hemingway J, Haagensen M et al (2010) Cross-sectional area of the elephant corpus callosum: comparison to other eutherian mammals. Neuroscience 167:815–824 https://doi.org/10.1016/j.neuroscience.2010.02.066

Manger PR, Pillay P, Maseko BC et al (2009) Acquisition of brains from the African elephant (*Loxodonta africana):* perfusion-fixation and dissection. J Neurosci Methods 179:16–21 https://doi.org/10.1016/j.jneumeth.2009.01.001

Manger PR, Prowse M, Haagensen M et al (2012) Quantitative analysis of neocortical gyrencephaly in African elephants (*Loxodonta africana*) and six species of cetaceans: Comparison with other mammals. J Comp Neurol 520:2430–2439 https://doi.org/10.1002/cne.23046

Manger PR, Spocter MA, Patzke N (2013) The evolutions of large brain size in mammals: The 'Over-700-Gram Club Quartet' Brain Behav Evol 82:68–78 https://doi.org/10.1159/000352056

Manoussaki D, Chadwick RS, Ketten DR et al (2008) The influence of cochlear shape on low-frequency hearing. Proc Natl Acad Sci USA 6162–6166 https://doi.org/10.1073/pnas.0710037105

Markov G, Spassov N (2001) A reconstruction of the facial morphology and feeding behaviour of the deinotheres. In: Proceedings of the 1st International Congress. Roma, pp 652–655

Marsh OC (1873) On the gigantic fossil mammals of the order Dinocerata. Am J of Sci s3-5:117–122 https://doi.org/10.2475/ajs.s3-5.26.117

Martin RD (1981) Relative brain size and basal metabolic rate in terrestrial vertebrates. Nature 293:57–60 https://doi.org/10.1038/293057a0

Maschenko EN, Boeskorov GG, Baranov VA (2013) Morphology of a mammoth calf (*Mammuthus primigenius*) from Ol'chan (Oimiakon, Yakutia). Paleontol J 47:425–438 https://doi.org/10.1134/S0031030113040096

Maseko BC, Spocter MA, Haagensen M et al (2011) Volumetric analysis of the African elephant ventricular system. Anat Rec 294:1412-1417 https://doi.org/10.1002/ar.21431

Maseko BC, Jacobs B, Spocter MA et al (2013a) Qualitative and quantitative aspects of the microanatomy of the African elephant cerebellar cortex. Brain Behav Evol 81:40–55 https://doi.org/10.1159/000345565

Maseko BC, Patzke N, Fuxe K et al (2013b) Architectural organization of the African Elephant diencephalon and brainstem. Brain Behav Evol 82:83–128 https://doi.org/10.1159/000352004

Maseko BC, Spocter MA, Haagensen M et al (2012) Elephants have relatively the largest cerebellum size of mammals. Anat Rec 295:661–672 https://doi.org/10.1002/ar.22425

Matsumoto H, Andrews CW (1923) A contribution to the knowledge of *Moeritherium*. Bull Am Mus Nat Hist 48(article 4): 97–140

Meng J, Shoshani J, Ketten D (1997) Evolutionary evidence for infrasonic sound and hearing in proboscideans. J Vertebr Paleontol 17:64-65A https://doi.org/10.1080/02724634.1997.10011028

Milne-Edwards H (1868) Observations sur le stéréocère de Gall. Annales des Sciences Naturelles, Paris 10:203–221

Mirceta S, Signore AV, Burns JM et al (2013) Evolution of mammalian diving capacity traced by myoglobin net surface charge. Science 340 (6138): 1234192 https://doi.org/10.1126/science.1234192

Mothé D, Ferretti MP, Avilla LS (2016) The dance of tusks: rediscovery of lower incisors in the Pan-American proboscidean *Cuvieronius hyodon* revises incisor evolution in Elephantimorpha. PLoS One 11:e0147009 https://doi.org/10.1371/journal.pone.0147009

Mourlam MJ, Orliac MJ (2017) Infrasonic and ultrasonic hearing evolved after the emergence of modern whales. Curr Biol 27:1776-1781.e9 https://doi.org/10.1016/j.cub.2017.04.061

Muchlinski MN (2008) The relationship between the infraorbital foramen, infraorbital nerve, and maxillary mechanoreception: implications for interpreting the paleoecology of fossil mammals based on infraorbital foramen size. Anat Rec 291:1221–1226 https://doi.org/10.1002/ar.20742

Muchlinski MN (2010) Ecological correlates of infraorbital foramen area in primates. Am J Phys Anthropol 141:131–141 https://doi.org/10.1002/ajpa.21137

Mudelsee M, Bickert T, Lear CH et al (2014) Cenozoic climate changes: a review based on time series analysis of marine benthic δ18O records. Rev Geophys 52:333–374 https://doi.org/10.1002/2013RG000440

Nabavizadeh A (2015) Proboscidean jaw mechanics and the evolution of the proboscis and feeding apparatus in extant elephants. FASEB J 29:867.10 https://doi.org/10.1096/fasebj.29.1_supplement.867.10

Nabavizadeh A, Reidenberg JS (2019) Anatomy of the proboscideal nerve in the proboscis of the African elephant (*Loxodonta africana*). FASEB J 33:lb148–lb148 https://doi.org/10.1096/fasebj.2019.33.1_supplement.lb148

Nair S, Balakrishnan R, Seelamantula CS et al (2009) Vocalizations of wild Asian elephants (*Elephas maximus*): structural classification and social context. J Acoust Soc Am 126:2768–2778 https://doi.org/10.1121/1.3224717

Ngwenya A, Patzke N, Ihunwo AO et al (2011) Organisation and chemical neuroanatomy of the African elephant (*Loxodonta africana*) olfactory bulb. Brain Struct Funct 216:403–416 https://doi.org/10.1007/s00429-011-0316-y

Niimura Y, Matsui A, Touhara K (2014) Extreme expansion of the olfactory receptor gene repertoire in African elephants and evolutionary dynamics of orthologous gene groups in 13 placental mammals. Genome Res 24:1485–1496 https://doi.org/10.1101/gr.169532.113

Noubhani A, Hautier L, Jaeger J-J et al (2008) Variabilité dentaire et crânienne de *Numidotherium koholense* (Mammalia, Proboscidea) de l'Éocène d'El Kohol, Algérie. Geobios 41:515–531 https://doi.org/10.1016/j.geobios.2007.09.002

Novacek MJ, Wyss AR (1987) Selected features of the desmostylian skeleton and their phylogenetic implications. Desmostylian skeleton. Am Mus Novit 2870: 7–8

Novacek MJ, Wyss AR (1986) Higher-level relationships of the recent Eutherian orders: Morphological evidence. Cladistics 2:257–287 https://doi.org/10.1111/j.1096-0031.1986.tb00463.x

O'Connell-Rodwell CE (2007a) Keeping an "ear" to the ground: seismic communication in elephants. Physiology 22:287–294. https://doi.org/10.1152/physiol.00008.2007

O'Connell-Rodwell CE (2007b) Keeping an "ear" to the ground: seismic communication in elephants. Physiology 22:287–294 https://doi.org/10.1152/physiol.00008.2007

O'Connell-Rodwell CE, Hart LA, Arnason BT (2001) Exploring the potential use of seismic waves as a communication channel by elephants and other large mammals. Integr Comp Biol 41:1157–1170. https://doi.org/10.1093/icb/41.5.1157

O'Connell-Rodwell CE, Wood JD, Kinzley C et al (2007) Wild African elephants (*Loxodonta africana*) discriminate between familiar and unfamiliar conspecific seismic alarm calls. J Acoust Soc Am 122:823–830 https://doi.org/10.1121/1.2747161

Orihuela J, López LWV, Macrini TE (2019) First cranial endocasts of early Miocene sirenians (Dugongidae) from the West Indies. J Vertebr Paleontol 39:e1584565 https://doi.org/10.1080/02724634.2019.1584565

Osborn HF (1931) *Palaeoloxodon antiquus italicus* sp. nov., final stage in the '*Elephas antiquus*' phylum. Am Mus Nov 460: 1–24

Osborn HF (1936) Proboscidea: a monograph of the discovery, evolution, migration and extinction of the mastodonts and elephants of the world. Vol. 1. New York: Published on the J. Pierpont Morgan Fund by the trustees of the American Museum of Natural History: American Museum Press

Osborn HF (1942) Proboscidea: a monograph of the discovery, evolution, migration and extinction of the mastodonts and elephants of the world. Vol. 2 New York: Published on the J. Pierpont Morgan Fund by the trustees of the American Museum of Natural History: American Museum Press

O'Shea TJ, Reep RL (1990) Encephalization Quotients and Life-History Traits in the Sirenia. J Mammal 71:534–543 https://doi.org/10.2307/1381792

Palkopoulou E, Lipson M, Mallick S et al (2018) A comprehensive genomic history of extinct and living elephants. Proc Natl Acad Sci USA 115:E2566–E2574 https://doi.org/10.1073/pnas.1720554115

Palombo MR, Giovinazzo C (2005) *Elephas falconeri* from Spinagallo Cave (south-eastern Sicily, Hyblean Plateau, Siracusa): a preliminary report on brain to body weight comparison. In: Proceedings of the International Symposium" Insular Vertebrate Evolution: the Palaeontological Approach": September, 16-19 Mallorca. Societat d'Història Natural de les Balears, pp 255–264

Patzke N, Olaleye O, Haagensen M et al (2014) Organization and chemical neuroanatomy of the African elephant (*Loxodonta africana*) hippocampus. Brain Struct Funct 219:1587–1601 https://doi.org/10.1007/s00429-013-0587-6

Patzke N, Spocter MA, Karlsson KÆ et al (2015) In contrast to many other mammals, cetaceans have relatively small hippocampi that appear to lack adult neurogenesis. Brain Struct Funct 220:361–383 https://doi.org/10.1007/s00429-013-0660-1

Payne KB, Langbauer WR, Thomas EM (1986) Infrasonic calls of the Asian elephant (*Elephas maximus*). Behav Ecol Sociobiol 18:297–301 https://doi.org/10.1007/BF00300007

Pérez-Barbería FJ, Gordon IJ (2005) Gregariousness increases brain size in ungulates. Oecologia 145:41–52 https://doi.org/10.1007/s00442-005-0067-7

Peters RH (1983) The Ecological Implications of Body Size. Cambridge University Press, Cambridge

Pettigrew JD, Bhagwandin A, Haagensen M et al (2010) Visual acuity and heterogeneities of retinal ganglion cell densities and the tapetum lucidum of the African elephant (*Loxodonta africana*). Brain Behav Evol 75:251–261 https://doi.org/10.1159/000314898

Pirlot P, Kamiya T (1985) Qualitative and quantitative brain morphology in the sirenian *Dugong dugong*. J Zool Syst Evol Res 23:147–155 https://doi.org/10.1111/j.1439-0469.1985.tb00577.x

Policht R, Tomášová K, Holečková D et al (2008) The vocal repertoire in Northern White Rhinoceros *Cerathotherium simum cottoni* as recorded in the last surviving herd. Bioacoustics 18:69–96 https://doi.org/10.1080/09524622.2008.9753591

Poole JH, Payne K, Langbauer WR et al (1988) The social contexts of some very low frequency calls of African elephants. Behav Ecol Sociobiol 22:385–392 https://doi.org/10.1007/BF00294975

Poole JH, Tyack PL, Stoeger-Horwath AS et al (2005) Elephants are capable of vocal learning. Nature 434:455–456 https://doi.org/10.1038/434455a

Poulakakis N, Stamatakis A (2010) Recapitulating the evolution of Afrotheria: 57 genes and rare genomic changes (RGCs) consolidate their history. System Biodivers 8:395–408 https://doi.org/10.1080/14772000.2010.484436

Provatidis CG, Theodorou EG, Theodorou GE (2011) Computed tomography and CAD/CAE methods for the study of the osseus inner ear bone of Greek quaternary endemic mammals. Mediterranean Archaeology and Archaeometry 11:121–127

Radinsky L (1973) Evolution of the canid brain; pp. 169–185. Brain Behav Evol 7:169–185 https://doi.org/10.1159/000124409

Radinsky L (1977) Early primate brains: facts and fiction. J Hum Evol 6:79–86 https://doi.org/10.1016/S0047-2484(77)80043-2

Richards H (1890) A further report on the anatomy of the elephant's ear. Transactions of the American Otological Society 4:587–604 https://doi.org/10.5962/bhl.title.101959

Roca AL, O'Brien SJ (2005) Genomic inferences from Afrotheria and the evolution of elephants. Curr Opin Genet Dev 15:652–659 https://doi.org/10.1016/j.gde.2005.09.014

Rodella LF, Buffoli B, Labanca M et al (2012) A review of the mandibular and maxillary nerve supplies and their clinical relevance. Arch Oral Biol 57:323–334 https://doi.org/10.1016/j.archoralbio.2011.09.007

Rohland N, Malaspinas A-S, Pollack JL et al (2007) Proboscidean Mitogenomics: Chronology and Mode of Elephant Evolution Using Mastodon as Outgroup. PLOS Biology 5:e207 https://doi.org/10.1371/journal.pbio.0050207

Rohrs M, Ebinger P (2001) How is cranial capacity related to brain volume in mammals? Mamm Biol 66:102–110

Romano M, Manucci F, Palombo MR (2019) The smallest of the largest: new volumetric body mass estimate and in-vivo restoration of the dwarf elephant *Palaeoloxodon* ex gr. *P. falconeri* from Spinagallo Cave (Sicily). Hist Biol 33:340–353 https://doi.org/10.1080/08912963.2019.1617289

Ronald K, Selley LJ, Amoroso EC (1978) Biological synopsis of the manatee. International Development Research Centre, Ottawa, ON, CA

Roth VL (1990) Insular dwarf elephants: a case study in body mass estimation and ecological inference. Body size in mammalian paleobiology: estimation and biological implications Cambridge University Press, New York 151–179

Rowe T (1996) Coevolution of the mammalian middle ear and neocortex. Science 273:651–654 https://doi.org/10.1126/science.273.5275.651

Salensky W (1904) Über die Hauptresultate der Erforschung des im Jahre 1901 am Ufer der Beresowka entdeckten männlichen Mammutkadavers. Compte-rendu des séances du sixième Congrès international de zoologie 6:67–86

Sánchez-Villagra MR (2002) The cerebellar paraflocculus and the subarcuate fossa in *Monodelphis domestica* and other marsupial mammals — ontogeny and phylogeny of a brain-skull interaction. Acta Theriol 47:1–14 https://doi.org/10.1007/BF03193561

Sander PM, Christian A, Clauss M et al (2011) Biology of the sauropod dinosaurs: the evolution of gigantism. Biol Rev 86:117–155 https://doi.org/10.1111/j.1469-185X.2010.00137.x

Sanders W, Gheerbrant E, Harris J et al (2010) Proboscidea. Cenozoic Mammals of Africa, eds Werdelin L, Sanders WJ. Univ Calif Press, Berkeley, CA

Scheele WE (1955) The first mammals. World Pub. Co., New York, NY

Schlesinger G (1922) Die Mastodonten der Budapester Sammlungen. Geologica Hungarica 2:1–284

Schmitt A (2016) La région de l'oreille osseuse chez les Proboscidea (Afrotheria, Mammalia): anatomie, fonction, évolution. These de doctorat, Paris, Muséum national d'histoire naturelle

Schmitt A, Gheerbrant E (2016) The ear region of earliest known elephant relatives: new light on the ancestral morphotype of proboscideans and afrotherians. J Anat 228:137–152 https://doi.org/10.1111/joa.12396

Seiferle E (1966) On the topography of the brain on long and short skulls in dog breeds. Acta Anat 63:346–362

Seiffert ER (2007a) A new estimate of afrotherian phylogeny based on simultaneous analysis of genomic, morphological, and fossil evidence. BMC Evol Biol 7:224 https://doi.org/10.1186/1471-2148-7-224

Seiffert ER (2007b) Evolution and Extinction of Afro-Arabian Primates Near the Eocene-Oligocene Boundary. Folia Primatol 78:314–327 https://doi.org/10.1159/000105147

Shauer K (2010) Commentary and sources for the evolutionary diagram of the Proboscidea in Africa and Eurasia. In: Meller H (ed) Elefantenreich – Eine Fossilwelt in Europa. Landesamt für Denkmalpflege und Archäologie Sachsen-Anhalt & Landesmuseum Vorgeschichte, pp 631–650

Shoshani J (1998) Understanding proboscidean evolution: a formidable task. Trends Ecol Evol 13:480–487 https://doi.org/10.1016/S0169-5347(98)01491-8

Shoshani J (1982) On the dissection of a female Asian elephant (*Elephas maximus maximus* Linnaeus, 1758) and data from other elephants. Elephant 2:3–93 https://doi.org/10.22237/elephant/1521731887

Shoshani J, Eisenberg JF (1982) *Elephas maximus*. Mamm Species 182:1–8 https://doi.org/10.2307/3504045

Shoshani J, Kupsky WJ, Marchant GH (2006) Elephant brain. Brain Res Bull 70:124–157 https://doi.org/10.1016/j.brainresbull.2006.03.016

Shoshani J, Marchant GH, Cavarretta G (2001) Hyoid apparatus: a little known complex of bones and its "contribution" to proboscidean evolution. In: La terra degli elefanti: atti del 1. Congresso internazionale; Roma, 16-20 ottobre 2001; Proceedings of the 1st International congress. Consiglio nazionale delle ricerche, Roma

Shoshani J, Tassy P (2005) Advances in proboscidean taxonomy & classification, anatomy & physiology, and ecology & behavior. Quat Int 126–128:5–20 https://doi.org/10.1016/j.quaint.2004.04.011

Shoshani J, Tassy P (1996) The Proboscidea: evolution and palaeoecology of elephants and their relatives. Oxford University Press

Shultz S, Dunbar RIM (2006) Both social and ecological factors predict ungulate brain size. Proc Biol Sci 273:207–215 https://doi.org/10.1098/rspb.2005.3283

Simionescu I, Morosan N (1937) Sur le moulage endocrânien d'*Elephas primigenius* de Roumanie. Bulletin de la section scientifique de l'Académie de Roumanie 19:1–7

Stephan H, Bauchot R, Andy OJ (1970) Data on size of the brain and of various brain parts in insectivores and primates. The primate brain Appleton-Century-Crofts, New York 289–297

Stoeger AS, Charlton BD, Kratochvil H et al (2011) Vocal cues indicate level of arousal in infant African elephant roars. J Acoust Soc Am 130:1700–1710 https://doi.org/10.1121/1.3605538

Stoeger AS, Manger P (2014) Vocal learning in elephants: neural bases and adaptive context. Curr Opin Neurobiol 28:101–107 https://doi.org/10.1016/j.conb.2014.07.001

Tassy P (2013) L'anatomie cranio-mandibulaire de *Gomphotherium angustidens* (Cuvier, 1817) (Proboscidea, Mammalia): données issues du gisement d'En Péjouan (Miocène

moyen du Gers, France). Geodiversitas 35:377–445 https://doi.org/10.5252/g2013n2a6

Tassy P (1981) Le crâne de *Moeritherium* (Proboscidea, Mammalia) de l'Eocène de Dor El Talha (Libye) et le problème de la classification phylogénétique du genre dans les Tethytheria McKenna, 1975. Bull Mus Natl Hist Nat, 4 sér, sect C 3:87–147

Tassy P (1994) Gaps, parsimony, and early Miocene elephantoids (Mammalia), with a re-evaluation of *Gomphotherium annectens* (Matsumoto, 1925). Zool J Linn Soc 112:101–117 https://doi.org/10.1111/j.1096-3642.1994.tb00313.x

van der Geer AA, Lyras GA, Mitteroecker P et al (2018) From Jumbo to Dumbo: cranial shape changes in elephants and hippos during phyletic dwarfing. Evol Biol 45:303–317

van der Geer AA, Lyras GA, van den Hoek Ostende LW et al (2014) A dwarf elephant and a rock mouse on Naxos (Cyclades, Greece) with a revision of the palaeozoogeography of the Cycladic Islands (Greece) during the Pleistocene. Palaeogeogr, Palaeoclimatol, Palaeoecol 404:133–144

van der Geer AAE, Bergh GD van den, Lyras GA et al (2016) The effect of area and isolation on insular dwarf proboscideans. J Biogeogr 43:1656–1666 https://doi.org/10.1111/jbi.12743

Van der Made J (2010) The evolution of elephants and their relatives in the context of a changing climate and geography. In: Meller H (ed) Elefantenreich – Eine Fossilwelt in Europa. Landesamt für Denkmalpflege und Archäologie Sachsen-Anhalt & Landesmuseum Vorgeschichte, pp 341–360

van der Merwe NJ, Bezuidenhout AJ, Seegers CD (1995) The skull and mandible of the African elephant (*Loxodonta africana*). Onderstepoort J Vet Res 62:245–260

Van Valen L (1973) Body size and numbers of plants and animals. Evolution 27–35

Vereschagin NK (1981) Morfometricheskoe opisanie mamontenka. In: Vereschagin NK, Mikhelson VM (eds) Magadanskii Mamontenok, Nauka. Leningrad, pp 52–80

Vereschagin NK (1999) Yamal'skiy Mamontenok: Morfometricheskoye OpisaniyeSkeleta. Trudy Zool. Inst. RAS 275, 32e38 (in Russian). Proceedings of the Zoological Institute RAS 275:32–38

von Muggenthaler E, Reinhart P (2003) Songlike vocalizations from a Sumatran rhinoceros calf (*Dicerorhinus sumatrensis*). J Acoust Soc Am 113:2277–2277 https://doi.org/10.1121/1.4780553

Walker A, Ryan TM, Silcox MT et al (2008) The semicircular canal system and locomotion: The case of extinct lemuroids and lorisoids. Evol Anthropol 17:135–145 https://doi.org/10.1002/evan.20165

Wall WP (1980) Cranial evidence for a proboscis in *Cadurcodon* and a review of snout structure in the Family Amynodontidae (Perissodactyla, Rhinocerotoidea). J Paleontol 54:968–977

Warren JC (1855) The *Mastodon giganteus* of North America. Wilson, Boston

Watson M (1874) Contributions to the Anatomy of the Indian Elephant: Part IV. Muscles and Blood-Vessels of the Face and Head. J Anat Physiol 9:118–133

Weber J, Czarnetzki A, Pusch CM (2005) Comment on "The Brain of LB1, *Homo floresiensis.*" Science 310:236b–236b https://doi.org/10.1126/science.1114789

Weisbecker V, Goswami A (2011) Neonatal maturity as the key to understanding brain size evolution in homeothermic vertebrates. BioEssays 33:155–158 https://doi.org/10.1002/bies.201000128

West CD (1985) The relationship of the spiral turns of the cochlea and the length of the basilar membrane to the range of audible frequencies in ground dwelling mammals. J Acoust Soc Am 77:1091–1101 https://doi.org/10.1121/1.392227

Weston EM, Lister AM (2009) Insular dwarfism in hippos and a model for brain size reduction in *Homo floresiensis*. Nature 459:85–88 https://doi.org/10.1038/nature07922

Wible JR (1986) Transformations in the extracranial course of the internal carotid artery in mammalian phylogeny. J Vertebr Paleontol 6:313–325 https://doi.org/10.1080/02724634.1986.10011628

Witmer LM, Ridgely RC, Dufeau DL et al (2008) Using CT to peer into the past: 3D visualization of the brain and ear regions of birds, crocodiles, and nonavian dinosaurs. In: Endo H, Frey R (eds) Anatomical Imaging. Springer Japan, Tokyo, pp 67–87

Witmer LM, Sampson SD, Solounias N (1999) The proboscis of tapirs (Mammalia: Perissodactyla): a case study in novel narial anatomy. J Zool 249:249–267 https://doi.org/10.1111/j.1469-7998.1999.tb00763.x

Zachos J, Pagani M, Sloan L et al (2001) Trends, Rhythms, and Aberrations in Global Climate 65 Ma to Present. Science 292:686–693 https://doi.org/10.1126/science.1059412

Figure captions

Fig. 15.1: Endocranial casts of *Moeritherium lyonsi* (NHM-UK M9116), *Palaeoloxodon falconeri* (MGG RSAL 47), *Mammut americanum* (LACM-M40977), *Zygolophodon* (*Mammut*) *borsoni* (MCFFM-CLB-1), *Stegodon insignis* (MNHN-A952) and *Mammuthus primigenius* (No number, from Naslavcea, Moldova, see Simionescu and Morosan 1937) in dorsal and lateral views. Scale bar is the same size for all proboscideans except *Moeritherium lyonsi*. The endocasts of *Mammut americanum* and *Palaeoloxodon falconeri* are mirrored for comparison.

Fig. 15.2: The evolution of endocast shape in dorsal and lateral views in proboscideans. Redraw after: a, Gheerbrant et al. 2005; b, Andrews 1921; c, Benoit et al. 2019; d, Marsh 1873; e, Jerison 1973; f, Warren 1855; g, Schlesinger 1922; h, Boule and Thevenin 1920; i, Dechaseaux 1958; j, Palombo and Giovinazzo 2005; k, Simionescu and Morosan 1937; l, Kubacska 1944; m, Bever et al. 2008; n, Elliot Smith 1902; o, Osborn 1931; p, Accordi and Palombo 1971. Abbreviations: Cb, cerebellum; EQ, reconstructed ancestral Manger's encephalization quotient after Benoit et al. 2019; Fr, frontal lobe; Ob, olfactory bulb; Ps, pseudosylvia; Sp, spinal cord; Tp, temporal lobe; V, trigeminal nerve. Drawings not to scale.

Fig. 15.3: Endocranial casts of *Palaeoloxodon antiquus* (AMNH 22634), *Palaeoloxodon* aff. *mnaidriensis* (MGG skull), *Palaeoloxodon tiliensis* (adult, AMPG T189/96; juvenile, AMPG T nn), and *Palaeoloxodon falconeri* (MGG RSAL 47). Scale bar = 10cm.

Fig. 15.4: Allometric relationships of the brain and body weight in the genus *Palaeoloxodon* (from Lyras 2018). a Plot of brain weight versus body weight and regressions of intra-specific

scaling in continental Elephantidae (blue line) and "all" mammals excluding Cetacea and Primates (from Manger 2006) (grey line). b, comparison of the skull and endocranial cast of *Palaeoloxodon antiquus*, *Palaeoloxodon* aff. *mnaidriensis*, and *Palaeoloxodon falconeri* to scale (scale bar 30cm).

Fig. 15.5: Reconstruction of the proboscis in a, *Numidotherium koholense*; b, *Palaeomastodon beadnelli*; c, *Deinotherium giganteum*; and d, *Mammuthus primigenius* (after Osborn 1942, 1936; Scheele 1955; Markov and Spassov 2001). Abbreviations: i1, first lower incisor; i2, second lower incisor; I2, second upper incisor; Ioc, infraorbital canal. The white arrow indicates the narial opening.

Fig. 15.6: The bony labyrinth of the Proboscidea. a, natural cast of the cochlear canal of *Numidotherium* studied by Court (1992); b, natural cast of the partial bony labyrinth of *Moeritherium* redrawn after Tassy (1981); c, the bony labyrinth of *Deinotherium* in lateral and anterior views redrawn after Claudius (1865); d, the bony labyrinth of an indeterminate elephantimorph redrawn after Ekdale (2011); e-i, the bony labyrinth of *Elephas maximus* MNHN.ZM.AC.1904-273 in lateral (e), ventral (f), anterior (g), posterior (h), and dorsal (i) views; j, lateral view of the bony labyrinths of MNHN.ZM.AC.2008-71 and CEB130168; k, ventral view of the bony labyrinth of MNHN.ZM.AC.2008-71; l, anterior view of the bony labyrinth of MNHN.ZM.AC.2008-81; m, dorsal view of the bony labyrinths MNHN.ZM.AC.1956-194 and MNHN.ZM.AC.1957-465, illustrating the variability of the bony labyrinth in modern elephants. Abbreviations: a.a., anterior ampulla; a.c., anterior semicircular canal; a.v., *aquaeductus vestibuli*; c.c., crus commune; co, cochlear canal; f.v., fenestra vestibuli; he, helicotrema; l.a., lateral ampulla; l.c., lateral semicircular canal; mo,

modiolus (apical lacuna); p.a., posterior ampulla; p.c., posterior semicircular canal; p.f., perilymphatic foramen. Scale bar = 1cm.

Fig. 15.7: Summary of the principal evolutionary changes of the ear region of the Proboscidea. Only taxa studied in this work are represented. Clades: A) Tethytheria, B) Proboscidea, C,D,E,F) Unnamed clades, G) Elephantimorpha, H) Elephantida, I,J,K,L) Unnamed clades M) Elephantidae, N) Elephantini, O) Unnamed clade, P) *Mammuthus* genus. Phylogeny and time range after Tassy (1994), Shoshani and Tassy (1996), Shoshani (1998), Shauer (2010), and Fisher (2018).

Fig. 15.8: 3D reconstructions of the bony labyrinths of fossil proboscideans in lateral view. a, *Eritherium azzouzorum* (MNHN-PM88); b, *Phosphatherium escuilliei* (MNHN.F PM17); c, *Numidotherium koholense* (UM-UM-UOK5, mirrored); d, *Moeritherium* sp. (68436, mirrored); e, *Prodeinotherium bavaricum* (MNHN 2013.01108E); f, *Mammut americanum* (AMNH-FM14293A, mirrored); g, *Mammut americanum* (AMNH-FM14293B); h, *Gomphotherium angustidens* (MNHN CBar coll. V2, mirrored); i, *Gomphotherium angustidens* (MNHN.F.SEP38, mirrored); j, *Gomphotherium angustidens* (MNHN.F.SEP38); k, *Cuvieronius* sp. (FM103247, mirrored); l, *Stegomastodon* sp. (FM21807, mirrored); m, *Platybelodon grangeri* (MNHN 26564-824+); n, *Anancus arvernensis* (NMNHS.FM2991A); o, *Anancus arvernensis* (NMNHS.FM2991B); p, *Anancus arvernensis* (NMNHS.FM2991C, mirrored); q, *Anancus arvernensis* (NMNHS.FM2991D, mirrored); r, *Anancus arvernensis* (NMNHS.FM2991E, mirrored); s, *Anancus arvernensis* (NMNHS.FM2991F, mirrored); t, *Anancus arvernensis* (NMNHS.FM2991G); u, *Stegodon orientalis* (FM18632); v, *Mammuthus primigenius* (MNHN.F.1904-12); w, *Mammuthus columbi* (FM144658); x, *Mammuthus columbi* (FM144658, mirrored); y, *Palaeoloxodon antiquus* (M82706, mirrored).

Scale bar = 1 cm. Abbreviations: a.a, anterior ampulla; a.c., anterior semicircular canal; a.v., *aquaeductus vestibuli*; aq, *aquaeductus cochleae*; c.c., *crus commune*; c.c.r., crus commune ridge; c.c.s., *crus commune secundaria*; co, cochlear canal; f.c., *fenestra cochleae*; f.v., *fenestra vestibuli*; l.a., lateral ampulla; l.c., lateral semicircular canal; p.a., posterior ampulla; p.c., posterior semicircular canal; p.f., perilymphatic foramen.

Fig. 15.9: 3D reconstructions of the bony labyrinths of fossil proboscideans in ventral view. a, *Eritherium azzouzorum* (MNHN-PM88); b, *Phosphatherium escuilliei* (MNHN.F PM17); c, *Numidotherium koholense* (UM-UOK5, mirrored); d, *Moeritherium* sp. (68436, mirrored); e, *Prodeinotherium bavaricum* (MNHN 2013.01108E); f, *Mammut americanum* (AMNH-FM14293A, mirrored); g, *Gomphotherium angustidens* (MNHN CBar coll. V2, mirrored); h, *Gomphotherium angustidens* (MNHN.F.SEP38, mirrored); i, *Gomphotherium angustidens* (MNHN.F.SEP38); j, *Stegomastodon* sp. (FM21807, mirrored); k, *Platybelodon grangeri* (MNHN 26564-824+); l, *Anancus arvernensis* (NMNHS.FM2991A); m, *Anancus arvernensis* (NMNHS.FM2991C, mirrored); n, *Anancus arvernensis* (NMNHS.FM2991D, mirrored); o, *Anancus arvernensis* (NMNHS.FM2991E, mirrored); p, *Anancus arvernensis* (NMNHS.FM2991F, mirrored); q, *Anancus arvernensis* (NMNHS.FM2991G); r, *Stegodon orientalis* (FM18632); s, *Mammuthus primigenius* (MNHN.F.1904-12). Scale bar = 1 cm. Abbreviations: a.a, anterior ampulla; a.c., anterior semicircular canal; a.v., *aquaeductus vestibuli*; aq, *aquaeductus cochleae*; c.c., *crus commune*; c.c.r., *crus commune* ridge; c.c.s., *crus commune secundaria*; co, cochlear canal; f.c., *fenestra cochleae*; f.v., *fenestra vestibuli*; l.a., lateral ampulla; l.c., lateral semicircular canal; p.a., posterior ampulla; p.c., posterior semicircular canal; p.f., perilymphatic foramen.

Fig. 15.10: 3D reconstructions of the bony labyrinths of fossil proboscideans in anterior view. a, *Eritherium azzouzorum* (MNHN-PM88); b, *Phosphatherium escuilliei* (MNHN.F PM17); c, *Numidotherium koholense* (UM-UOK5, mirrored); d, *Moeritherium* sp. (68436, mirrored); e, *Prodeinotherium bavaricum* (MNHN 2013.01108E); f, *Mammut americanum* (AMNH-FM14293A, mirrored); g, *Mammut americanum* (AMNH-FM14293B); h, *Gomphotherium angustidens* (MNHN CBar coll. V2, mirrored); i, *Gomphotherium angustidens* (MNHN.F.SEP38, mirrored); j, *Gomphotherium angustidens* (MNHN.F.SEP38); k, *Cuvieronius* sp. (FM103247, mirrored); l, *Stegomastodon* sp. (FM21807, mirrored); m, *Platybelodon grangeri* (MNHN 26564-824+); n, *Anancus arvernensis* (NMNHS.FM2991A); o, *Anancus arvernensis* (NMNHS.FM2991B); p, *Anancus arvernensis* (NMNHS.FM2991C, mirrored); q, *Anancus arvernensis* (NMNHS.FM2991D, mirrored); r, *Anancus arvernensis* (NMNHS.FM2991E, mirrored); s, *Anancus arvernensis* (NMNHS.FM2991F, mirrored); t, *Anancus arvernensis* (NMNHS.FM2991G); u, *Stegodon orientalis* (FM18632); v, *Mammuthus primigenius* (MNHN.F.1904-12); w, *Mammuthus columbi* (FM144658); x, *Mammuthus columbi* (FM144658, mirrored); y, *Palaeoloxodon antiquus* (M82706, mirrored). Scale bar = 1 cm. Abbreviations: a.a., anterior ampulla; a.c., anterior semicircular canal; a.c.r., anterior semicircular canal ridge; a.v., *aquaeductus vestibuli*; aq, *aquaeductus cochleae*; c.c., *crus commune*; c.c.s., *crus commune secundaria*; co, cochlear cana; f.c. fenestra cochleae; i.a.v., insertion of the aquaeductus vestibuli; l.a., lateral ampulla; l.c., lateral semicircular canal; l.s., *lamina secundaria*; p.a., posterior ampulla; p.c., posterior semicircular canal; p.f., perilymphatic foramen.

Fig. 15.11: 3D reconstructions of the bony labyrinths of fossil proboscideans in posterior view. A, *Eritherium azzouzorum* (MNHN-PM88); B, *Phosphatherium escuilliei* (MNHN.F PM17); C, *Numidotherium koholense* (UM-UOK5, mirrored); D, *Moeritherium* sp. (68436,

mirrored); E, *Prodeinotherium bavaricum* (MNHN 2013.01108E); F, *Mammut americanum* (AMNH-FM14293A, mirrored); G, *Mammut americanum* (AMNH-FM14293B); H, *Gomphotherium angustidens* (MNHN CBar coll. V2, mirrored); I, *Gomphotherium angustidens* (MNHN.F.SEP38, mirrored); J, *Gomphotherium angustidens* (MNHN.F.SEP38); K, *Cuvieronius* sp. (FM103247, mirrored); L, *Stegomastodon* sp. (FM21807, mirrored); M, *Platybelodon grangeri* (MNHN 26564-824+); N, *Anancus arvernensis* (NMNHS.FM2991A); O, *Anancus arvernensis* (NMNHS.FM2991B); P, *Anancus arvernensis* (NMNHS.FM2991C, mirrored); Q, *Anancus arvernensis* (NMNHS.FM2991D, mirrored); R, *Anancus arvernensis* (NMNHS.FM2991E, mirrored); S, *Anancus arvernensis* (NMNHS.FM2991F, mirrored); T, *Anancus arvernensis* (NMNHS.FM2991G); U, *Stegodon orientalis* (FM18632); V, *Mammuthus primigenius* (MNHN.F.1904-12); W, *Mammuthus columbi* (FM144658); X, *Mammuthus columbi* (FM144658, mirrored); Y, *Palaeoloxodon antiquus* (M82706, mirrored). Scale bar = 1 cm. Abbreviations: a.a., anterior ampulla; a.c., anterior semicircular canal; a.v., *aquaeductus vestibuli*; aq, *aquaeductus cochleae*; c.c., *crus commune*; co, cochlear canal; f.c., fenestra cochleae; i.a.v., insertion of the *aquaeductus vestibuli*; l.a., lateral ampulla; l.c., lateral semicircular canal; l.s., *lamina secundaria*; p.a., posterior ampulla; p.c., posterior semicircular canal; p.c.r., posterior semicircular canal ridge; p.f., perilymphatic foramen.

Fig. 15.12: 3D reconstructions of the bony labyrinths of fossil proboscideans in dorsal view. A, *Eritherium azzouzorum* (MNHN -PM88); B, *Phosphatherium escuilliei* (MNHN.F PM17); C, *Numidotherium koholense* (UM-UOK5, mirrored); D, *Moeritherium* sp. (68436, mirrored); E, *Prodeinotherium bavaricum* (MNHN 2013.01108E); F, *Mammut americanum* (AMNH-FM14293A, mirrored); G, *Mammut americanum* (AMNH-FM14293B); H, *Gomphotherium angustidens* (MNHN CBar coll. V2, mirrored); I, *Gomphotherium angustidens*

(MNHN.F.SEP38, mirrored); J, *Gomphotherium angustidens* (MNHN.F.SEP38); K, *Cuvieronius* sp. (FM103247, mirrored); L, *Stegomastodon* sp. (FM21807, mirrored); M, *Platybelodon grangeri* (MNHN 26564-824+); N, *Anancus arvernensis* (NMNHS.FM2991A); O, *Anancus arvernensis* (NMNHS.FM2991B); P, *Anancus arvernensis* (NMNHS.FM2991C, mirrored); Q, *Anancus arvernensis* (NMNHS.FM2991D, mirrored); R, *Anancus arvernensis* (NMNHS.FM2991E, mirrored); S, *Anancus arvernensis* (NMNHS.FM2991F, mirrored); T, *Anancus arvernensis* (NMNHS.FM2991G); U, *Stegodon orientalis* (FM18632); V, *Mammuthus primigenius* (MNHN.F.1904-12); W, *Mammuthus columbi* (FM144658); X, *Mammuthus columbi* (FM144658, mirrored); Y, *Palaeoloxodon antiquus* (M82706, mirrored). Scale bar = 1 cm. Abbreviations: a.a., anterior ampulla; a.c., anterior semicircular canal; a.v., *aquaeductus vestibuli*; aq, *aquaeductus cochleae*; c.c. *crus commune*; cochlear canal; f.c., *fenestra cochleae*; l.a., lateral ampulla; l.c. lateral semicircular canal, l.s. *lamina secundaria*, p.a. posterior ampulla, p.c. posterior semicircular canal.

Fig. 15.13: Palaeoenvironmental context of proboscidean brain, inner ear and other related characters co-evolution. $\delta^{18}O$ curve and climatic events after Zachos et al. (2001). Abbreviations: EQ: encephalization quotient; ION, infraorbital nerve; SCC: semicircular canals.

Table 15.1: Data on proboscideans cranial capacity, encephalization quotients (EQ) and primary bibliographic references.

[a] Cranial capacity after Osborn (1931, 1942, water displacement?).

[b] Cranial capacity after Maccagno (1962, water displacement).

[c] Cranial capacity after Palombo and Giovinazzo (2005, water displacement?).

[d] Cranial capacity after Lyras (2018, silica balls)(see Fig. 15.3).

[e] Cranial capacity after Bever et al. (2008, water displacement).

[f] Cranial capacity after Kharlamova et al. (2016, CT scan).

[g] Cranial capacity after Fisher et al. (2014, CT scan).

[h] Cranial capacity after Benoit (2015), calculated using double graphic integration including olfactory bulbs on the figures by Simionescu and Morosan (1937)(see Fig. 15.1).

[i] Cranial capacity after Benoit et al. (2013b), calculated using double graphic integration including olfactory bulbs on the figures by Dechaseaux (1958).

[j] Cranial capacity after Benoit et al. (2019), photogrammetry on an artificial endocast made by Gervais (1872)(see Fig. 15.1).

[k] Cranial capacity after Benoit et al. (2013b), calculated using double graphic integration including olfactory bulbs on the figures by Andrews (1906).

[l] Cranial capacity after Jerison (1973, water displacement).

[m] Cranial capacity after Benoit et al. (2019), photogrammetry on an artificial endocast made by the authors)(see Fig. 15.1).

[n] Cranial capacity after Benoit et al. (2019), calculated using double graphic integration on a drawing of the endocast.

[o] Cranial capacity after Benoit et al. (2013b, CT scan).

Taxon	Epoch	Endocranial capacity (cm^3)	Brain mass (g)	Body mass (g)	Jerison's EQ	Manger's EQ	Primary bibliographic references

Elephantoidea	Modern	*Elephas maximus*	5211 (average)	4789	3030982 (average)	1.91	1.69	Benoit et al. 2019; Benoit 2015; Benoit et al. 2013a ; Shoshani et al. 2006
	Modern	*Loxodonta africana*	4927 (average)	4528	3850370 (average)	1.54	1.34	Benoit et al. 2019; Benoit 2015; Benoit et al. 2013a ; Shoshani et al. 2006
	Plio-Quaternary	*Palaeoloxodon antiquus*	6807[a]	6257	3649880	2.20	1.93	Benoit 2015; Osborn 1931, 1942
	Plio-Quaternary	*Palaeoloxodon antiquus*	9000[b]	8274	11000000	1.39	1.14	Lyras 2019; Benoit et al. 2019; Benoit 2015; Weston and Lister 2009; Palombo and Giovinazzo 2005; Accordi and Palombo 1971; Maccagno 1962
	Plio-Quaternary	*Palaeoloxodon falconeri*	1800[c]	1652	189000	4.87	4.42	Lyras 2019; Benoit et al. 2019; Weston and Lister 2009; Palombo and Giovinazzo 2005; Accordi and Palombo 1971
	Plio-Quaternary	*Palaeoloxodon* aff. *mnaidriensis*	4260[d]	3951	1380000	2.63	2.45	Lyras 2019
	Plio-Quaternary	*Palaeoloxodon* aff. *mnaidriensis*	4300[d]	3951	1380000	2.66	2.48	Lyras 2019
	Plio-Quaternary	*Palaeoloxodon tiliensis*	3000[d]	2756	727000	2.84	2.76	Lyras 2019
	Plio-Quaternary	cf. *Mammuthus columbii*	6232[e]	5728	9800000	1.04	0.86	Benoit et al. 2019; Benoit 2015; Bever et al. 2008
	Plio-Quaternary	*Mammuthus primigenius* (juvenile, Yuka)	5025[f]	4618	460000	6.46	6.45	Kharlamova et al. 2015 ; Kharlamova et al. 2016
	Plio-Quaternary	*Mammuthus primigenius* (juvenile, Khroma)	2300[g]	2112	-	-	-	Fisher et al. 2014
	Plio-Quaternary	*Mammuthus primigenius*	4687[h]	4307	6000000	1.09	0.92	Benoit et al. 2019; Benoit 2015; Kubaska 1944 ; Simiunescu and Morosan 1937
	Plio-Quaternary	*Mammuthus meridionalis*	5828[i]	5357	11000000	0.90	0.74	Benoit et al. 2019; Benoit 2015; Benoit et al. 2013a ; Deschaseaux 1958
	Miocene	*Stegodon insignis*	3838[j]	3527	2000000	1.85	1.69	Benoit et al. 2019; Gervais 1872
Mammutida	Plio-Quaternary	*Mammut americanum*	3862[k]	3549	6384056	0.86	0.73	Benoit et al. 2019; Benoit 2015; Benoit et al. 2013a; Andrews 1906
	Plio-Quaternary	*Mammut americanum*	4600[l]	4227	8000000	0.88	0.74	Benoit et al. 2019; Benoit 2015; Shoshani et al. 2006 ; Jerison 1973
	Plio-Quaternary	*Zygolophodon borsoni*	5133[m]	4718	16000000	0.62	0.50	Benoit et al. 2019
	Oligocene	*Palaeomastodon beadnelli*	771[n]	706	2500000	0.32	0.29	Benoit et al. 2019; Andrews, in Larger 1917
	Oligocene	*Moeritherium lyonsi*	240[l]	218	810000	0.21	0.20	Benoit et al. 2019; Benoit 2015; Jerison 1973; Andrews 1906;
Sirenia	Eocene	*Prorastomus sirenoides*	87[o]	90	98156	0.35	0.39	Benoit et al. 2013a
Hyracoidea	Eocene	*Seggerurius amourensis*	5 [o]	5	2932	0.21	0.29	Benoit et al. 2013a

Table 15.2: Measurements of the semicircular canals of extant elephants. Abbreviations: ASC anterior semicircular canal, LSC lateral semicircular canal, PSC posterior semicircular canal, SCC semicircular canals.

	Crus commune length (mm)	Crus commune section radius (mm)	Crus commune thickness ratio	ASC length (mm)	PSC length (mm)	LSC length (mm)	SCC average thickness ratio	Angle ASC-PSC (°)	Angle ASC-LSC (°)	Angle LSC-PSC (°)	ASC radius of curvature	PSC radius of curvature	LSC radius of curvature
Elephas 1904-273	7.11	1.51	21.19	22.45	22.44	20.33	4.64	72.6	75.7	88.8	5.25	5.20	3.16
Elephas 1941-209	5.58	1.20	21.53	22.79	22.49	23.06	4.13	76.5	74.2	83.2	5.19	5.23	3.52
Elephas 2008-81	6.53	1.48	22.62	26.66	24.56	26.07	3.52	76.6	75.0	85.8	5.97	5.60	4.06
Elephas CEB150009	3.07	1.51	49.20	23.47	21.01	24.10	4.86	78.9	67.9	85.7	5.04	4.65	3.65
Loxodonta 1932-523	5.47	1.38	25.26	24.99	23.65	21.26	3.02	70.9	72.4	85.8	5.66	5.37	3.21
Loxodonta 2008-71 (average)	5.63	1.13	20.09	22.49	22.31	22.54	3.90	75.9	59.8	83.5	5.18	5.14	3.56
L. africana 1861-53	5.50	1.82	27.27	27.42	24.36	21.04	3.57	81.1	73.8	82.2	5.86	5.25	3.54
L. africana CEB130168	4.05	1.51	37.23	27.44	25.40	24.07	3.28	84.8	72.7	78.0	5.80	5.55	3.72
L. cyclotis 1950-728	5.89	1.64	27.87	23.85	21.40	21.06	3.69	83.3	72.3	88.5	5.41	4.91	3.35
L. cyclotis 1956-194	5.37	1.57	29.20	31.98	29.92	23.44	2.74	76.7	72.9	93.8	6.87	6.25	4.09
L. cyclotis 1957-465	4.84	1.94	40.15	23.99	21.88	20.50	4.01	74.7	80.0	85.0	5.48	4.98	3.15

L. cyclotis 1961-69	4.46	1.40	31.33	22.30	20.61	21.16	4.77	80.9	68.1	80.6	5.06	4.78	3.37

Table 15.3: Measurements of the cochlear canal of extant elephants.

Specimens	Number of turns	Coiling (°)	Length (mm)	Aspect ratio	Radii ratio (Manoussaki et al. 2008)
Elephas 1904-273	2.375	855	74.13	0.38	7.16
Elephas 1941-209	2.375	855	80.46	0.38	6.18
Elephas 2008-81	2.375	855	80.28	0.43	6.88
Elephas CEB 150009	2.25	810	73.11	0.36	5.95
Loxodonta sp 1932-523	2.25	810	77.13	0.41	6.82
Loxodonta sp 2008-71 (average)	1.81	653	67.92	0.32	6.90
Left ear	2.00	720	73.61	0.34	6.33
Right ear	1.625	585	62.18	0.30	7.47
Loxodonta africana 1861-53	2.375	855	71.54	0.45	7.38
Loxodonta africana CEB130168	2	720	70.84	0.37	6.50
Loxodonta cyclotis 1950-728	2.25	810	69.16	0.40	8.47
Loxodonta cyclotis 1956-194	2.625	945	74.16	0.40	8.85
Loxodonta cyclotis 1957-465	2.625	945	79.03	0.44	5.35
Loxodonta cyclotis 1961-69	2.625	945	81.55	0.44	8.23

Table 15.4: Measurements of the bony labyrinth of fossil proboscideans and outgroups. Abbreviations: ASC anterior semicircular canal, LSC lateral semicircular canal, PSC posterior semicircular canal.

	Volume			Cochlea					Crus commune			Angles			
	Bony labyrinth volume (mm^3)	Cochlea volume(mm^3)	Relative volume of the cochlea (%)	Stapedial ratio	Number of turns of the cochlea	Aspect ratio of the cochlea	Length of the cochlea (mm)	Radii ratio (after Manoussaki et al 2008)	*Crus commune* length (mm)	*Crus commune* average section radius (mm)	*Crus commune* average thickness ratio	Angle between the ASC and the PSC (°)	Angle between the ASC and the LSC (°)	Angle between the LSC and the PSC (°)	Vestibulo-cochlear angle (°)
Ocepeia daouiensis MNHN-PM45	17.5	11.7	66	2.05	2.13	0.72	19.2	3.47	1.75	0.30	17.4	91.6	80.1	87.8	102
Stylolophus MNHN-PM53	?	?	?	?	?	?	?	?	3.92	0.53	13.7	86.0	83.4	98.6	?
Anancus arvernensis NMNHS.FM2991A	934.6	468.3	50	1.7	2.5	0.43	72.3	7.03	5.11	1.06	20.8	90.5	58.2	77.6	150
Anancus arvernensis NMNHS.FM2991B	?	?	?	?	?	?	?	?	6.70	1.34	20.1	81.0	58.9	78.0	?
Anancus arvernensis NMNHS.FM2991C	957.5e	442.2e	46e	1.6	2.5	0.41	?	7.36	3.28	1.32	40.4	79.8	63.8	81.3	166
Anancus arvernensis NMNHS.FM2991D	1151e	539.3e	47e	1.7	2.5	0.37	78e	7.24	4.58	1.64	35.8	92.4	70.4	81.2	154
Anancus arvernensis	1440.5	701.8	49	1.6	2.5	0.37	80.1	7.22	6.39	1.38	21.7	87.5	70.4	87.9	145

NMNHS.FM2991E															
Anancus arvernensis NMNHS.FM2991F	1215e	502.1e	41e	1.8	2.5	0.47	78e	9	7.23	1.33	18.4	88.6	68.9	80.5	150
Anancus arvernensis NMNHS.FM2991G	933.9e	394.1e	42e	1.6	>2.5	0.45	73e	?	6.04	1.23	20.3	78.5	64.6	79.7	147
Cuvieronius sp FM103247	?	?	?	?	?	?	?	?	9.52	1.65	17.4	82.1	77.4	85.5	?
Eritherium azzouzorum MNHN-PM88	11.22	5.91	53	1.57	2	0.35	16.8	3.10	2.33	0.27	11.46	93.8	83.5	91.4	117
Gomphotherium angustidens CBar coll. V2	988.3	497.0	50	1.5	2.63	0.47	90.1	6.65	8.73	1.24	14.2	79.2	67.8	85.3	132
Gomphotherium angustidens SEP38	814.4	400.2	49	1.5	2.38	0.47	69.3	5.72	6.82	1.27	18.7	85.7	72.8	91.1	120
Mammut americanum AMNH-FM14293A	936.3	343.1	37e	?	2.38	0.44	68.0	?	7.74	1.18	15.2	86.5	68.8	81.4	153
Mammut americanum AMNH-FM14293B	?	?	?	?	?	?	?	?	7.21	1.55	21.6	80.5	65.1	80.9	?
Mammuthus columbi FM144658	?	?	?	?	?	?	?	?	5.23	1.41	27	76.6	73.3	87.2	?
Mammuthus primigenius MNHN.F.1904-12	1131	480.1	42	?	2.25	0.46	67.6	8.02	5.57	1.42	25.5	68.6	71.4	88.0	148
Moeritherium 68436	?	?	?	?	1.5e	?	?	?	?	?	?	?	?	?	?
Numidotherium koholense UM-UOK5	84.4	35.1	42	?	1.5	0.48	27.1	2.88	4.50	0.67	14.9	78.0	75.5	96.1	128
Palaeoloxodon antiquus M82706	?	?	?	?	?	?	?	?	6.35	1.41	22.2	77.1	76.2	92.6	?
Phosphatherium escuilliei MNHN.F PM17	32.54	22.38	69	1.62	>1	>0,41	?	?	2.56	0.32	12.45	85.6	77.1	89.7	102

Platybelodon grangeri 26564 (824+)	854.5	373.8	44	?	2	0.41	56.8	?	4.20	1.17	27.9	73.9	67.4	98.8	132
Prodeinotherium bavaricum 2013.01108E	674.4	322.1	48e	?	2.25	0.29	?	6.75	5.91	1.26	21.4	77.2	67.6	90.7	132
Stegodon orientalis FM18632	1117.5	507.8	45	?	2	0.50	68.7	6.74	5.34	1.37	25.7	108	74.9	94.0	122
Stegomastodon sp FM21807	?	530	?	?	2	0.45	65.8	7.04	6.67	1.29	19.4	96.6	?	?	139

Table 15.5: Measurements of the semicircular canals of fossil proboscideans and outgroups. Abbreviations: ASC anterior semicircular canal, LSC lateral semicircular canal, PSC posterior semicircular canal. Average thickness ratio is calculated = average section radius/central streamline length*100.

	Radius of curvature				Central streamline length (mm)			Average section radius (mm)			Average thickness ratio			
	ASC	PSC	LSC	Lateral canal ratio (%)	ASC	PSC	LSC	ASC	PSC	LSC	ASC	PSC	LSC	Global thickness ratio
Ocepeia daouiensis MNHN-PM45	1.64	1.55	1.24	78.5	6.87	7.49	6.79	0.15	0.16	0.14	2.22	2.18	2.04	2.15
Stylolophus MNHN-PM53	3.26	3.13	2.3e	71.7	12.6	13.4	11e	0.22	0.21	0.12	1.72	1.57	1.1e	1.46
Anancus arvernensis NMNHS.FM2991A	5.02	4.79	3.19	65	22.7	20.9	20.3	0.70	0.70	0.74	3.09	3.37	3.63	3.36
Anancus arvernensis NMNHS.FM2991B	5.91	5.63	4.06	70.4	25.4	23.9	24.4	0.58	0.64	0.66	2.29	2.66	2.72	2.56
Anancus arvernensis NMNHS.FM2991C	5.15	4.89	3.39	67.6	23.8	21.5	21.7	0.76	0.74	0.78	3.18	3.43	3.58	3.40
Anancus arvernensis NMNHS.FM2991D	5.24	5.39	3.39	64.5	23.5	24.1	21.7	0.79	0.82	0.84	3.36	3.40	3.86	3.54
Anancus arvernensis NMNHS.FM2991E	5.52	5.37	3.54	65.1	24.3	23.0	21.8	0.91	0.92	1.06	3.75	3.99	4.87	4.20
Anancus arvernensis NMNHS.FM2991F	5.68	5.67	3.92	69 .1	24.6	25	23.6	0.83	0.78	0.83	3.39	3.10	3.50	3.33
Anancus arvernensis NMNHS.FM2991G	5.33	5.67	3.58	66.8	23.2	25.8	22.2	0.79	0.70	0.79	3.39	2.70	3.56	3.21
Cuvieronius sp FM103247	6.18	6.06	3.57	58.5	25.0	25.4	21.4	0.85	0.86	0.89	3.41	3.37	4.18	3.65
Eritherium azzouzorum MNHN-PM88	1.74	1.83	1.78	77.5	6.99	10.8	7.31	0.07	0.05	0.13	0.94	0.49	1.79	1.08
Gomphotherium angustidens CBar coll. V2	5.26	5.56	3.71	66	20.4	23.2	22.2	0.77	0.76	0.78	3.78	3.26	3.50	3.51

Gomphotherium angustidens SEP38	5.45	5.11	3.36	63.7	22.8	21.6	19.1	0.64	0.71	0.78	2.82	3.29	4.09	3.40
Mammut americanum AMNH-FM14293A	6.33	6.09	3.82	61.8	28.8	25.5	24.1	0.95	0.95	0.92	3.30	3.70	3.82	3.61
Mammut americanum AMNH-FM14293B	5.43	5.68	2.96	52.7	23.6	23.8	18.4	1.01	1.04	0.87	4.30	4.33	4.74	4.47
Mammuthus columbi FM144658	5.71	4.84	3.08	60.1	25.9	21.2	21.3	1.10	1.2	0.99	4.24	5.65	4.65	4.85
Mammuthus primigenius MNHN.F.1904-12	5.80	5.53	2.92	51.6	26.8	25.3	19.7	0.88	1.01	0.93	3.28	3.99	4.69	3.99
Numidotherium koholense UM-UOK5	3.52	3.28	2.56	73.3	13.9	14.7	13.9	0.34	0.30	0.28	2.47	2.03	1.99	2.16
Palaeoloxodon antiquus M82706	5.87	5.14	3.93	72.4	26.2	22.2	24.1	0.92	0.93	0.91	3.51	4.18	3.78	3.82
Phosphatherium escuilliei MNHN.F PM17	1.91	1.88	1.9	78.5	7.77	8.77	7.95	0.19	0.17	0.18	2.41	1.99	2.31	2.24
Platybelodon grangeri 26564	5.16	4.89	3.54	69.7	22.0	22.0	22	0.81	0.65	0.68	3.69	2.93	3.11	3.25
Prodeinotherium bavaricum 2013.01108E	5.60	5.01	3.98	75	24.7	22.5	22.7	0.69	0.69	0.59	2.79	3.06	2.62	2.82
Stegodon orientalis FM18632	5.36	7.48	3.27	51	23.7	23.4	15.2	0.83	0.82	0.77	3.51	3.51	5.10	4.04
Stegomastodon sp FM21807	4.91	5.30	?	?	19.4	22.5	?	1.32	1.18	?	6.8	5.24	?	6.02

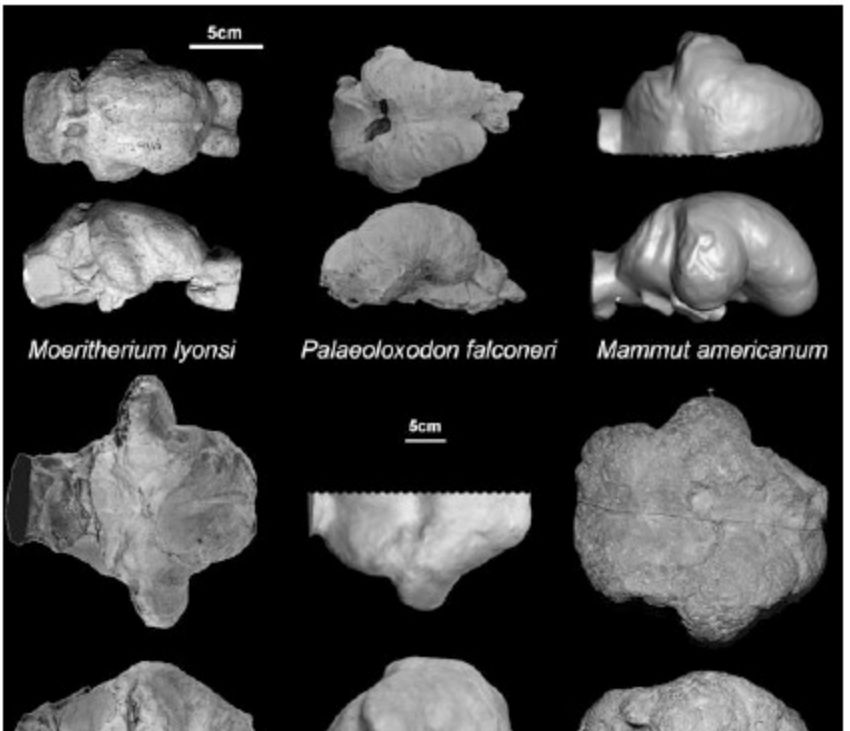

Fig. 15.1 Endocranial casts of *Moeritherium lyonsi* (NHM-UK M9116), *Palaeoloxodon falconeri* (MGG RSAL 47), *Mammut americanum* (LACM-M40977), *Zygolophodon* (*Mammut*) *borsoni* (MCFFM-CLB-1), *Stegodon insignis* (MNHN-A952) and *Mammuthus primigenius* (No number, from Naslavcea, Moldova, see Simionescu and Morosan 1937) in dorsal and lateral views. Scale bar is the same size for all proboscideans except *Moeritherium lyonsi*. The endocasts of *Mammut americanum* and *Palaeoloxodon falconeri* are mirrored for comparison

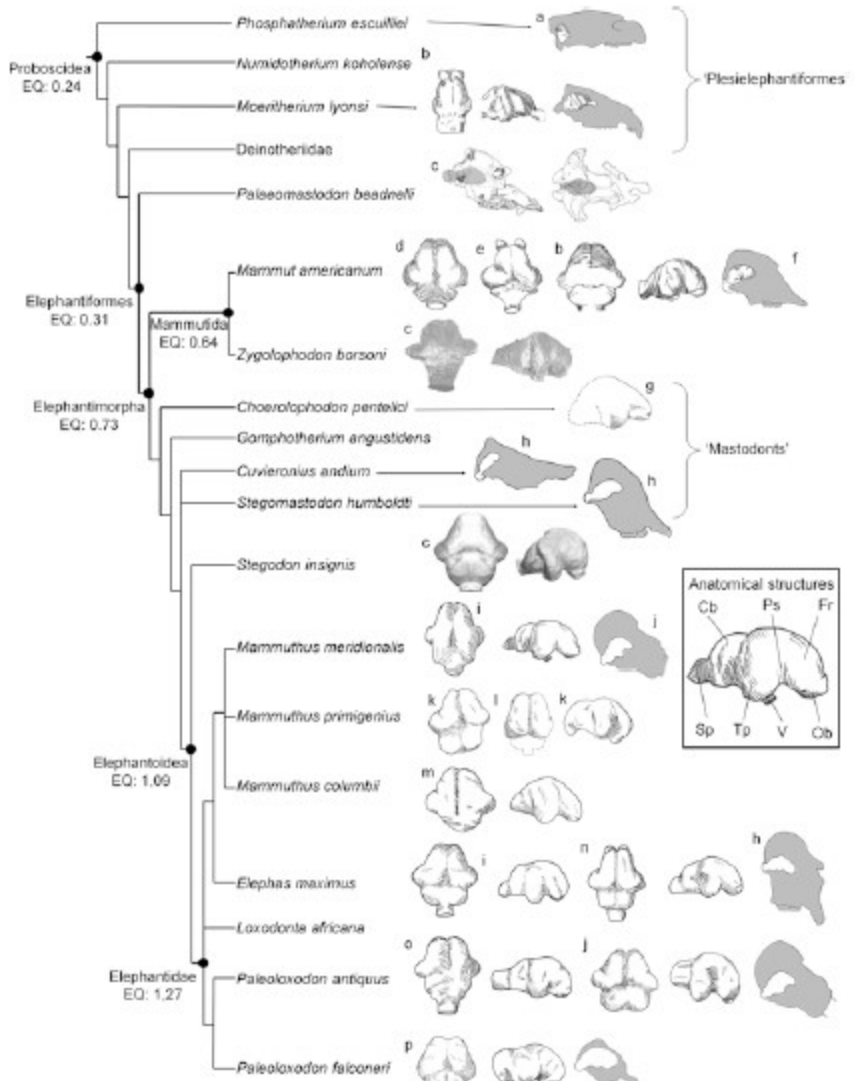

Fig. 15.2 The evolution of endocast shape in dorsal and lateral views in proboscideans. Redraw after: (**a**) Gheerbrant et al. 2005, (**b**) Andrews 1921 (**c**) Benoit et al. 2019, (**d**) Marsh 1873, (**e**) Jerison 1973, (**f**) Warren 1855, (**g**) Schlesinger 1922, (**h**) Boule and Thevenin 1920, (**i**) Dechaseaux 1958, (**j**) Palombo and Giovinazzo 2005, (**k**) Simionescu and Morosan 1937, (**l**) Kubacska 1944, (**m**) Bever et al. 2008, (**n**) Elliot Smith 1902, (**o**) Osborn 1931, (**p**) Accordi and Palombo 1971. Abbreviations: *Cb*, cerebellum; *EQ*, reconstructed ancestral Manger's encephalization quotient after Benoit et al. 2019; *Fr* frontal lobe, *Ob* olfactory bulb, *Ps* pseudosylvia, *Sp* spinal cord, *Tp* temporal lobe, *V* trigeminal nerve. Drawings not to scale

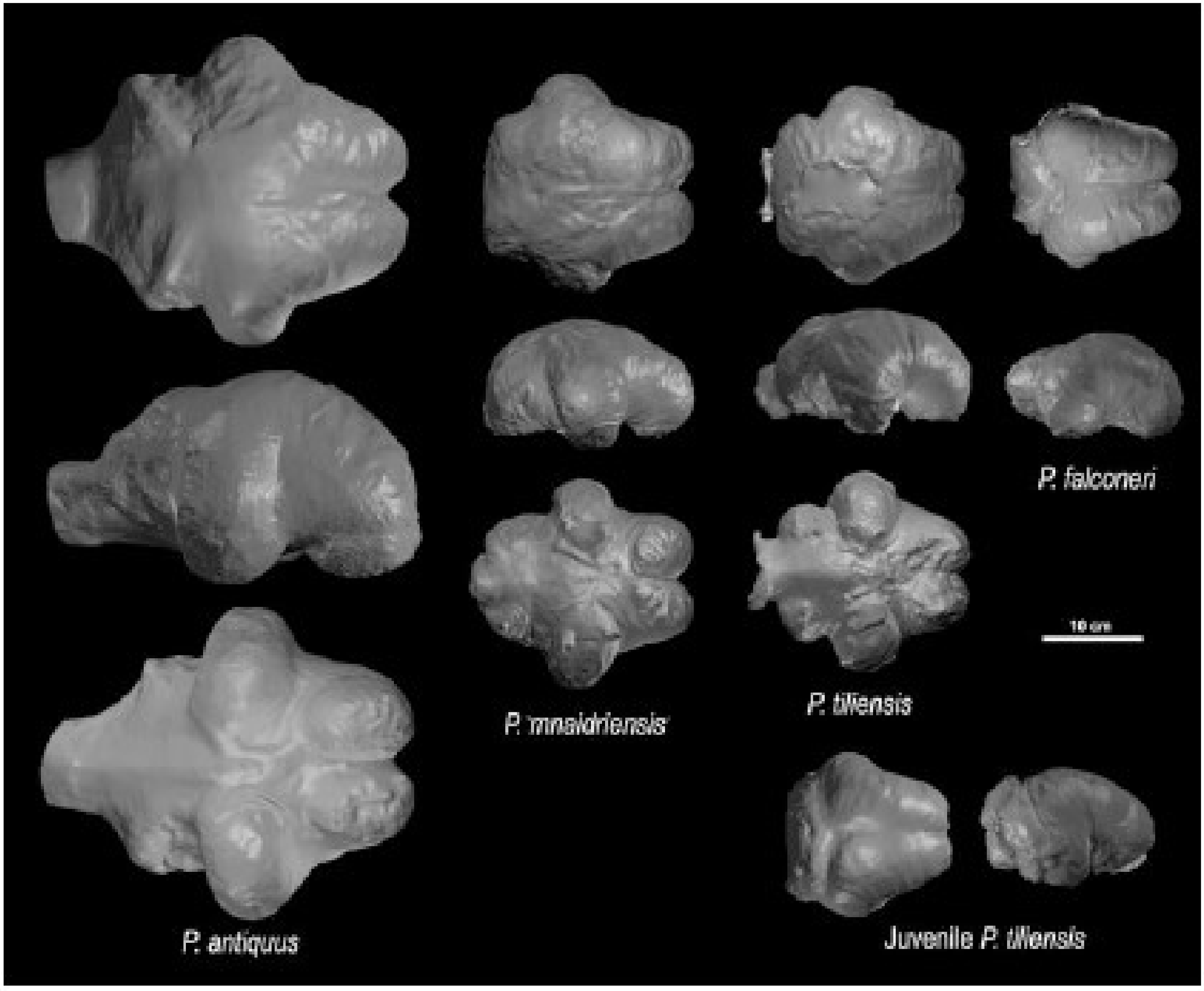

Fig. 15.3 Endocranial casts of *Palaeoloxodon antiquus* (AMNH 22634), *Palaeoloxodon* aff. *mnaidriensis* (MGG skull), *Palaeoloxodon tiliensis* (adult, AMPG T189/96; juvenile, AMPG T nn), and *Palaeoloxodon falconeri* (MGG RSAL 47). Scale bar = 10 cm

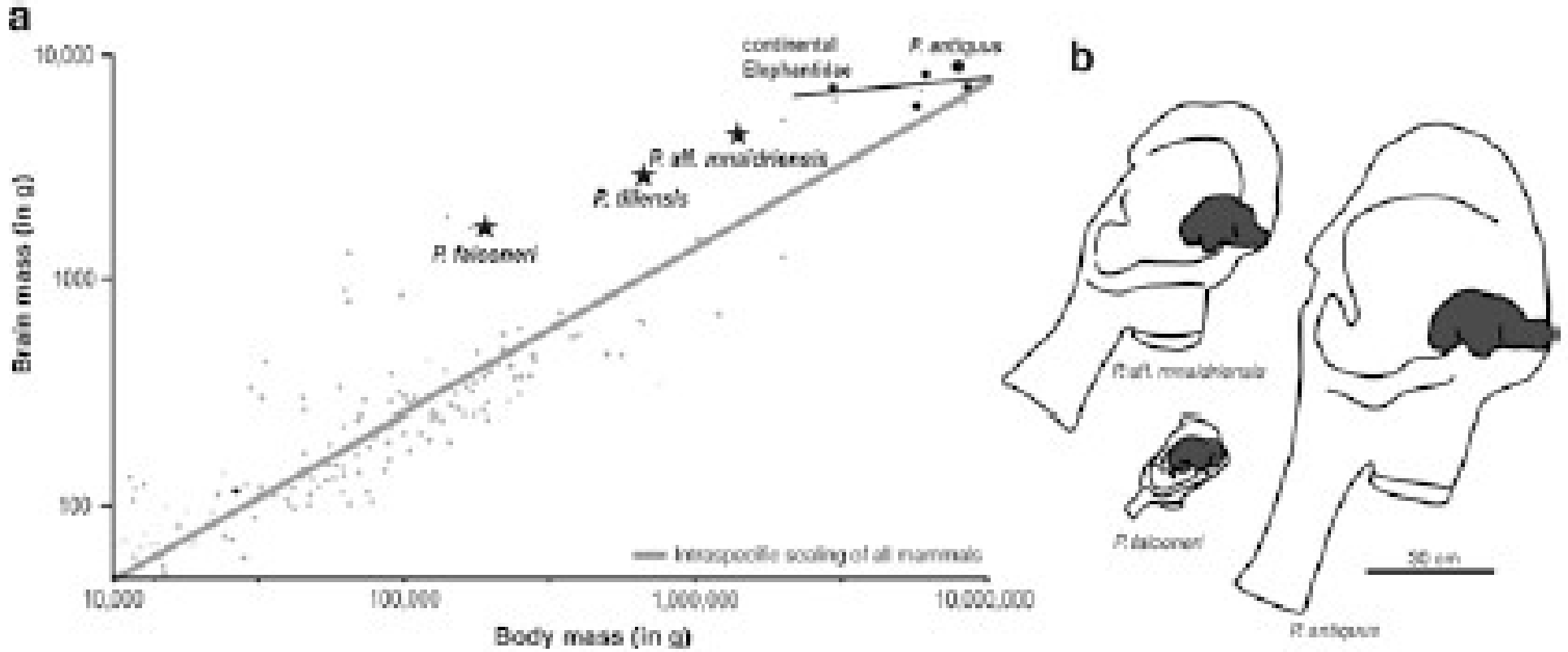

Fig. 15.4 Allometric relationships of the brain and body weight in the genus *Palaeoloxodon* (from Lyras 2018). (**a**) Plot of brain weight versus body weight and regressions of intra-specific scaling in continental Elephantidae (blue line) and "all" mammals excluding Cetacea and Primates (from Manger 2006) (gray line). (**b**) comparison of the skull and endocranial cast of *Palaeoloxodon antiquus*, *Palaeoloxodon* aff. *mnaidriensis*, and *Palaeoloxodon falconeri* to scale (Scale bar = 30 cm)

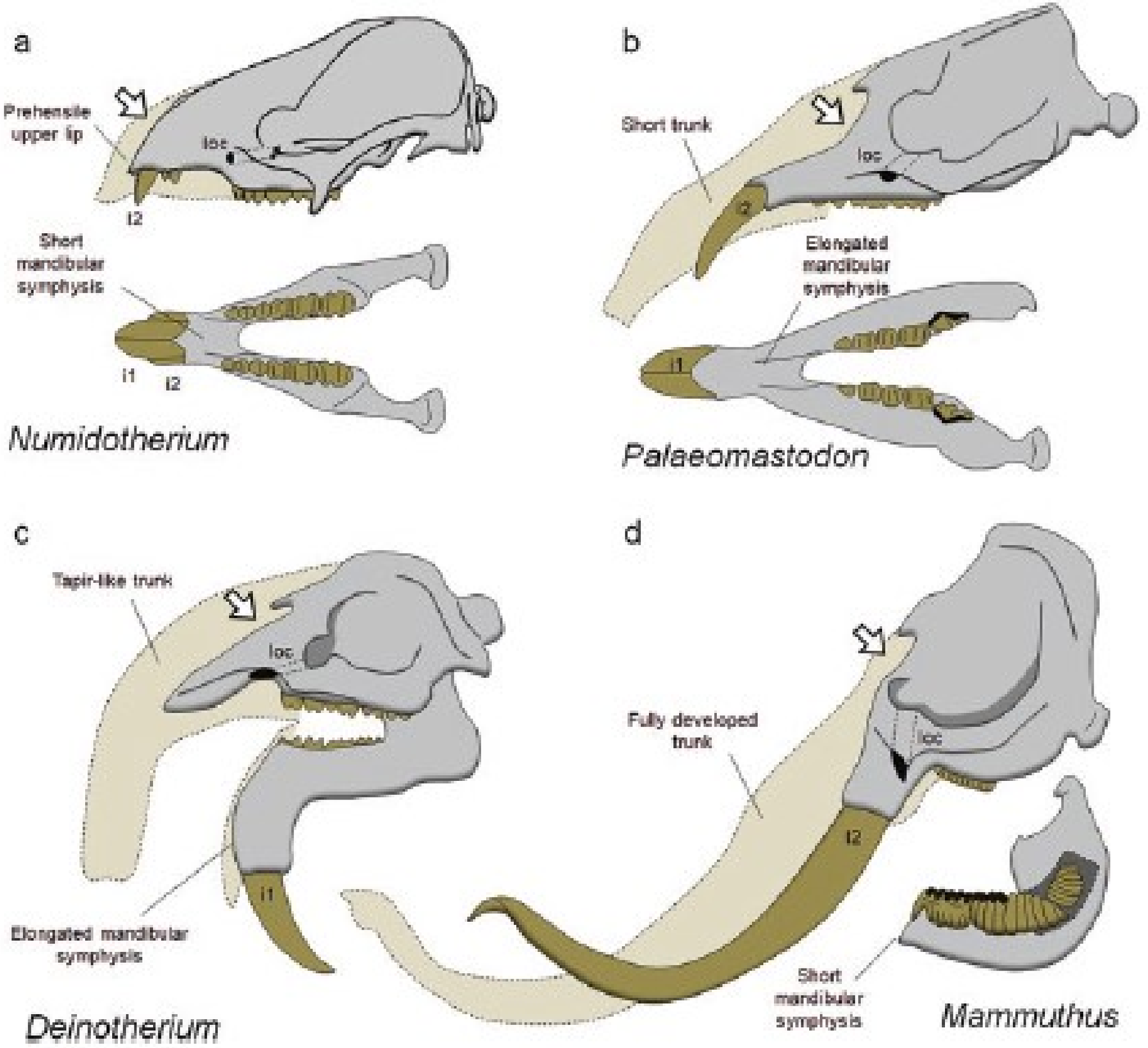

Fig. 15.5 Reconstruction of the proboscis in (**a**) *Numidotherium koholense*, (**b**) *Palaeomastodon beadnelli*, (**c**) *Deinotherium giganteum*, and (**d**) *Mammuthus primigenius* (after Osborn 1936, 1942; Scheele 1955; Markov and Spassov 2001). Abbreviations: *i1* first lower incisor, *i2* second lower incisor, *I2* second upper incisor, *loc* infraorbital canal. The white arrow indicates the narial opening

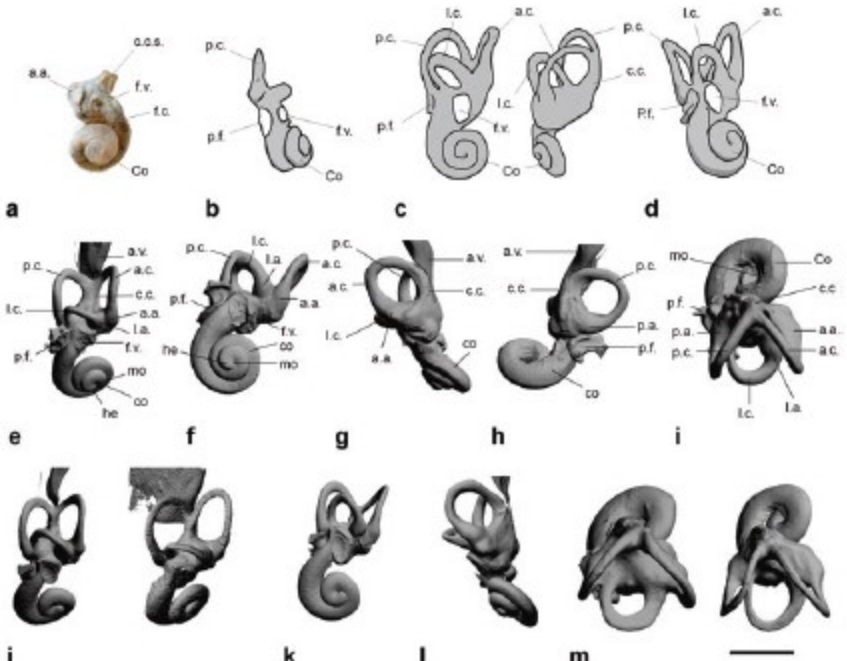

Fig. 15.6 The bony labyrinth of the Proboscidea. (**a**) natural cast of the cochlear canal of *Numidotherium* studied by Court (1992), (**b**) natural cast of the partial bony labyrinth of *Moeritherium* redrawn after Tassy (1981), (**c**) the bony labyrinth of *Deinotherium* in lateral and anterior views redrawn after Claudius (1865), (**d**) the bony labyrinth of an indeterminate elephantimorph redrawn after Ekdale (2011), (**e–i**) the bony labyrinth of *Elephas maximus* MNHN.ZM.AC.1904-273 in lateral (**e**), ventral (**f**), anterior (**g**), posterior (**h**), and dorsal (**i**) views, (**j**) lateral view of the bony labyrinths of MNHN.ZM.AC.2008-71 and CEB130168, (**k**) ventral view of the bony labyrinth of MNHN.ZM.AC.2008-71, (**l**) anterior view of the bony labyrinth of MNHN.ZM.AC.2008-81, (**m**) dorsal view of the bony labyrinths MNHN.ZM.AC.1956-194 and MNHN.ZM.AC.1957-465, illustrating the variability of the bony labyrinth in modern elephants. Abbreviations: *a.a.* anterior ampulla, *a.c.* anterior semicircular canal, *a.v. aquaeductus vestibuli*, *c.c.* crus commune, *co* cochlear canal, *f.v.* fenestra vestibuli, *he* helicotrema, *l.a.* lateral ampulla, *l.c.* lateral semicircular canal, *mo* modiolus (apical lacuna), *p.a.* posterior ampulla, *p.c.* posterior semicircular canal, *p.f.* perilymphatic foramen. Scale bar = 1 cm

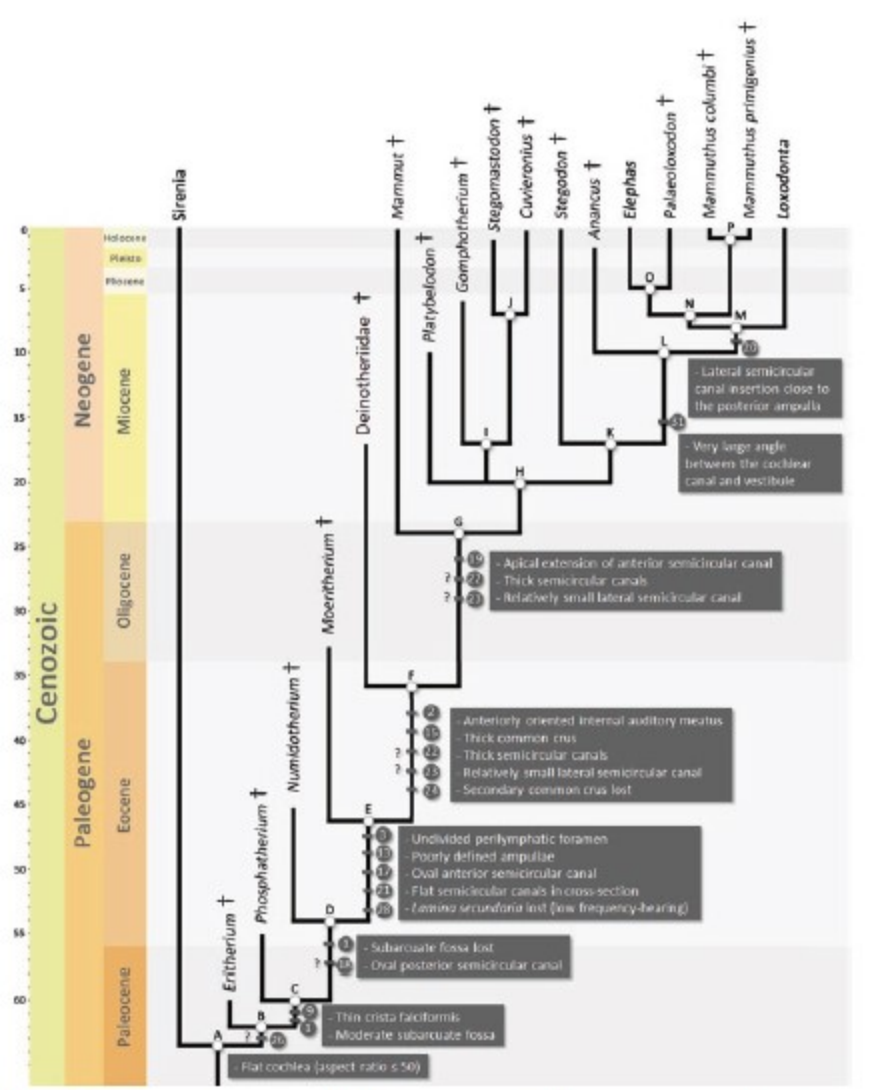

Fig. 15.7 Summary of the principal evolutionary changes of the ear region of the Proboscidea. Only taxa studied in this work are represented. Clades: (A) Tethytheria, (B) Proboscidea, (C, D, E, F) Unnamed clades, (G) Elephantimorpha, (H) Elephantida, (I, J, K, L) Unnamed clades (M) Elephantidae, (N) Elephantini, (O) Unnamed clade, (P) *Mammuthus* genus. Phylogeny and time range after Tassy (1994), Shoshani and Tassy (1996), Shoshani (1998), Shauer (2010), and Fisher (2018)

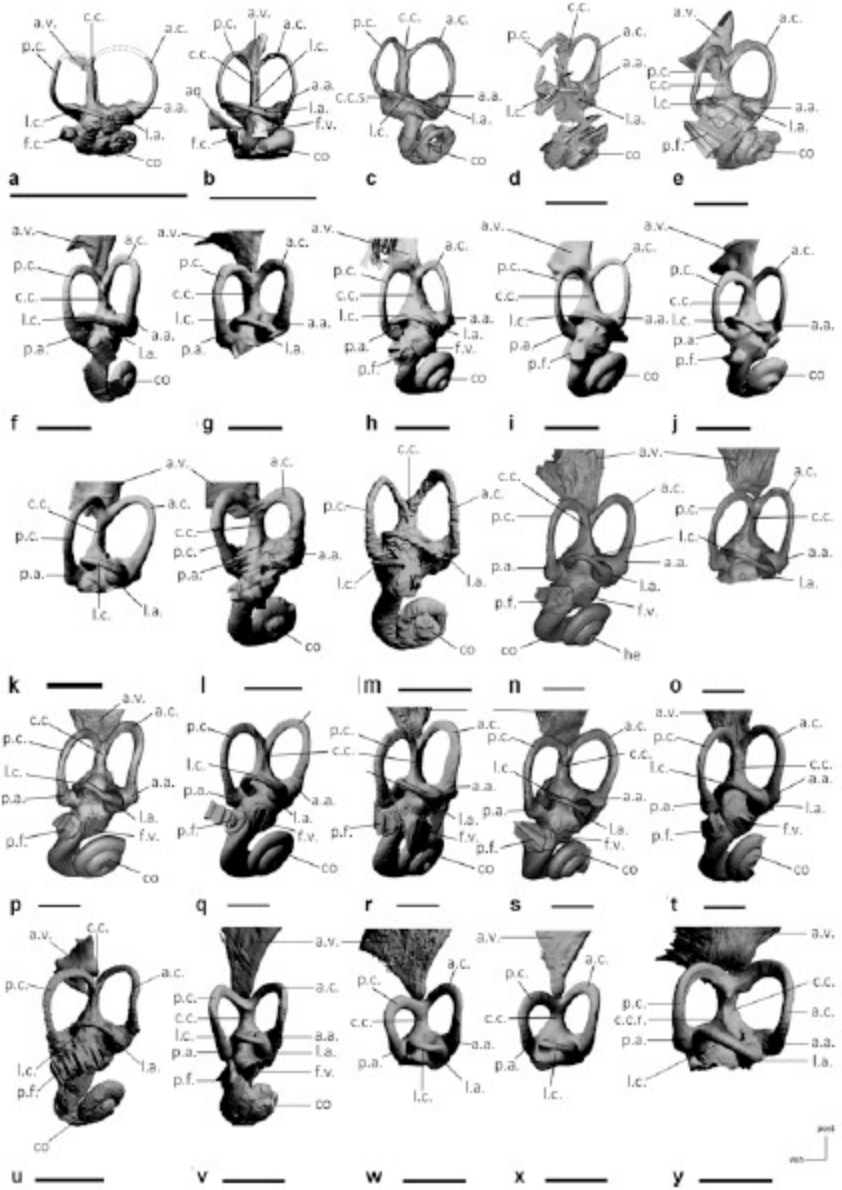

Fig. 15.8 3D reconstructions of the bony labyrinths of fossil proboscideans in lateral view. (**a**) *Eritherium azzouzorum* (MNHN-PM88), (**b**) *Phosphatherium escuilliei* (MNHN.F PM17), (**c**) *Numidotherium koholense* (UM-UM-UOK5, mirrored), (**d**) *Moeritherium* sp. (68436, mirrored), (**e**) *Prodeinotherium bavaricum* (MNHN 2013.01108E), (**f**) *Mammut americanum* (AMNH-FM14293A, mirrored), (**g**) *Mammut americanum* (AMNH-FM14293B), (**h**) *Gomphotherium angustidens* (MNHN CBar coll. V2, mirrored), (**i**) *Gomphotherium angustidens* (MNHN.F.SEP38,

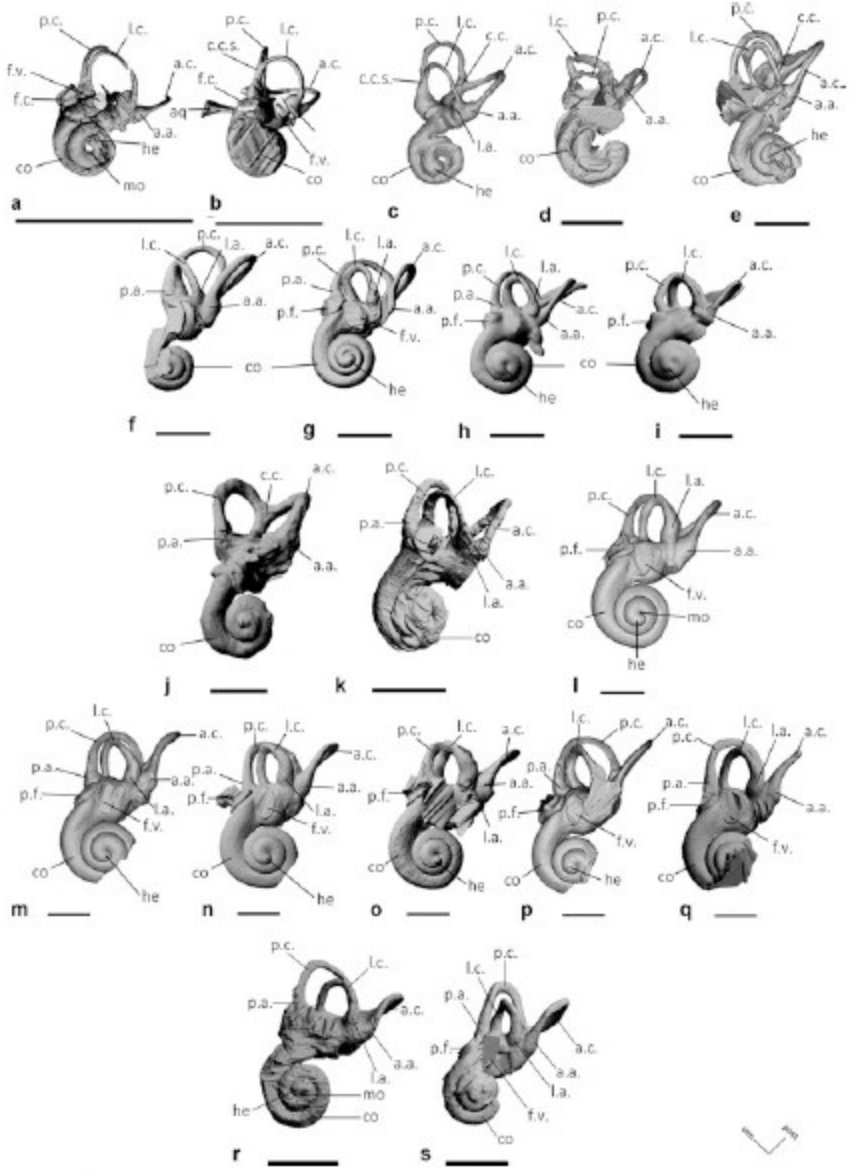

Fig. 15.9 3D reconstructions of the bony labyrinths of fossil proboscideans in ventral view. (**a**) *Eritherium azzouzorum* (MNHN-PM88), (**b**) *Phosphatherium escuilliei* (MNHN.F PM17), (**c**) *Numidotherium koholense* (UM-UOK5, mirrored), (**d**) *Moeritherium* sp. (68436, mirrored), (**e**) *Prodeinotherium bavaricum* (MNHN 2013.01108E), (**f**) *Mammut americanum* (AMNH-FM14293A, mirrored), (**g**) *Gomphotherium angustidens* (MNHN CBar coll. V2, mirrored), (**h**) *Gomphotherium angustidens* (MNHN.F.SEP38, mirrored), (**i**) *Gomphotherium angustidens* (MNHN.F.SEP38), (**j**) *Stegomastodon* sp. (FM21807, mirrored), (**k**) *Platybelodon grangeri*

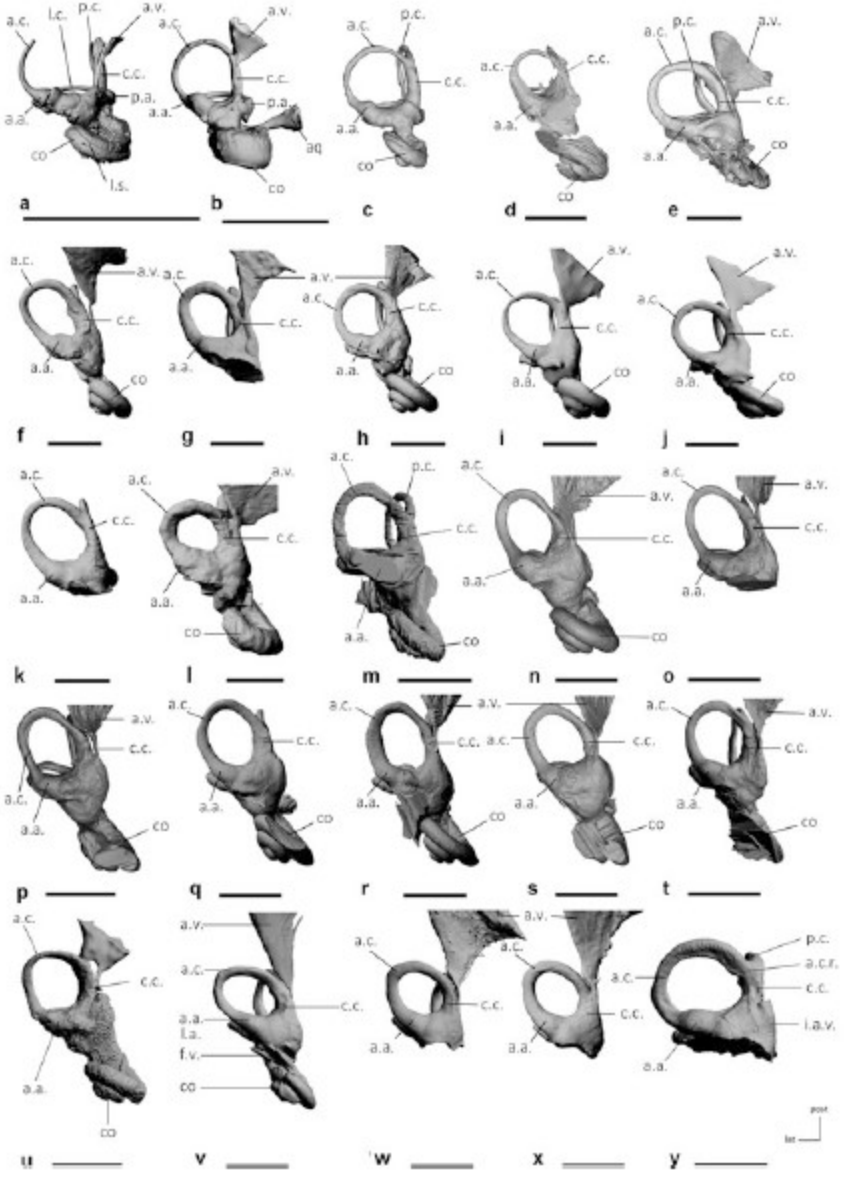

Fig. 15.10 3D reconstructions of the bony labyrinths of fossil proboscideans in anterior view. (**a**) *Eritherium azzouzorum* (MNHN-PM88), (**b**) *Phosphatherium escuilliei* (MNHN.F PM17), (**c**) *Numidotherium koholense* (UM-UOK5, mirrored), (**d**) *Moeritherium* sp. (68436, mirrored), (**e**) *Prodeinotherium bavaricum* (MNHN 2013.01108E), (**f**) *Mammut americanum* (AMNH-FM14293A, mirrored), (**g**) *Mammut americanum* (AMNH-FM14293B), (**h**) *Gomphotherium angustidens* (MNHN CBar coll. V2, mirrored), (**i**) *Gomphotherium angustidens* (MNHN.F.SEP38, mirrored), (**j**) *Gomphotherium angustidens* (MNHN.F.SEP38), (**k**) *Cuvieronius* sp. (FM103247,

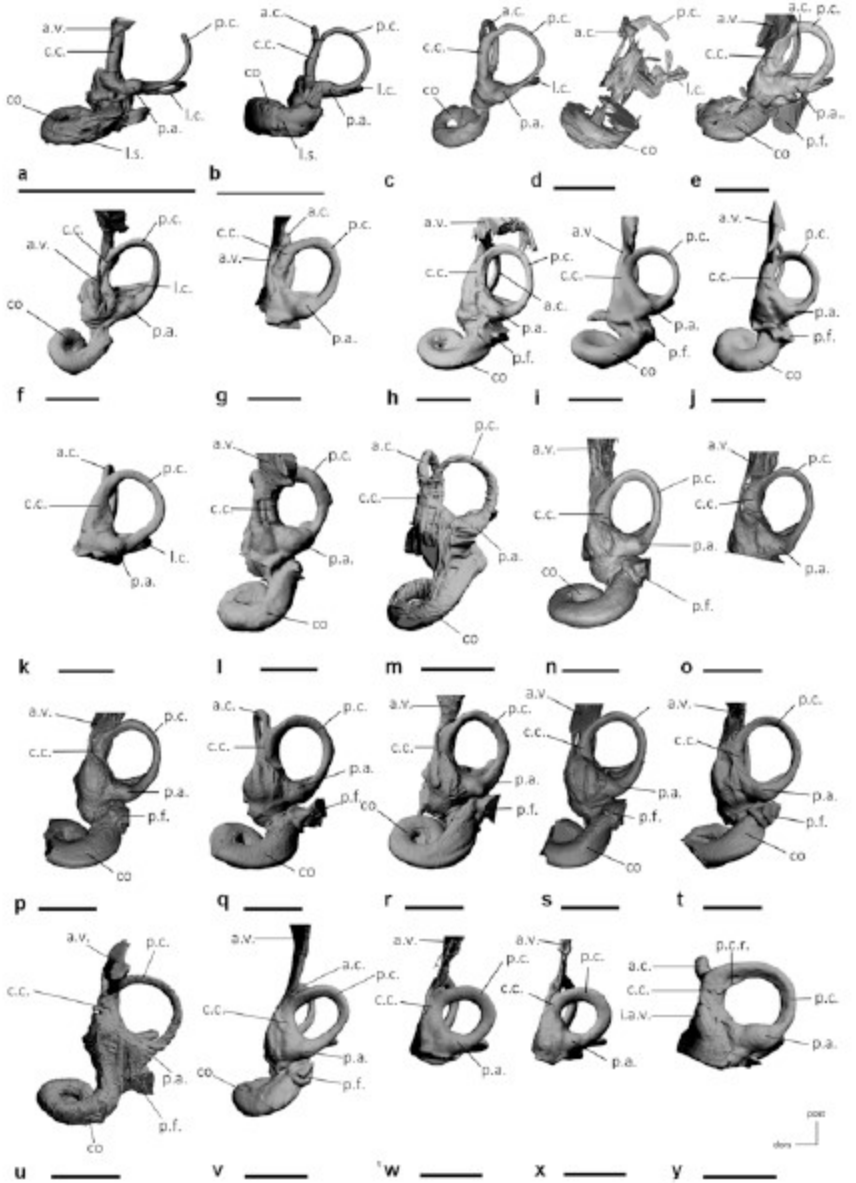

Fig. 15.11 3D reconstructions of the bony labyrinths of fossil proboscideans in posterior view. (**a**) *Eritherium azzouzorum* (MNHN-PM88), (**b**) *Phosphatherium escuilliei* (MNHN.F PM17), (**c**) *Numidotherium koholense* (UM-UOK5, mirrored), (**d**) *Moeritherium* sp. (68436, mirrored), (**e**) *Prodeinotherium bavaricum* (MNHN 2013.01108E), (**f**) *Mammut americanum* (AMNH-FM14293A, mirrored), (**g**) *Mammut americanum* (AMNH-FM14293B), (**h**) *Gomphotherium angustidens* (MNHN CBar coll. V2, mirrored), (**i**) *Gomphotherium angustidens* (MNHN.F.SEP38,

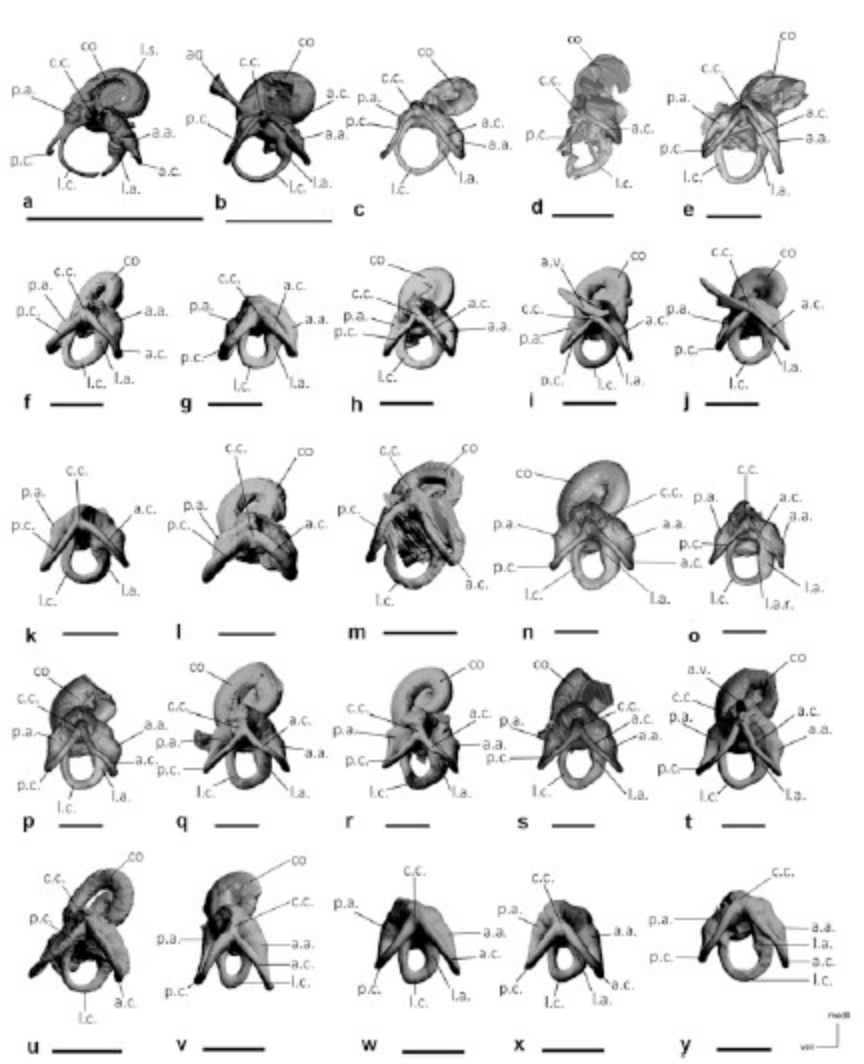

Fig. 15.12 3D reconstructions of the bony labyrinths of fossil proboscideans in dorsal view. (**a**) *Eritherium azzouzorum* (MNHN -PM88), (**b**) *Phosphatherium escuilliei* (MNHN.F PM17), (**c**) *Numidotherium koholense* (UM-UOK5, mirrored), (**d**) *Moeritherium* sp. (68436, mirrored), (**e**) *Prodeinotherium bavaricum* (MNHN 2013.01108E), (**f**) *Mammut americanum* (AMNH-FM14293A, mirrored), (**g**) *Mammut americanum* (AMNH-FM14293B), (**h**) *Gomphotherium angustidens* (MNHN CBar coll. V2, mirrored), (**i**) *Gomphotherium angustidens* (MNHN.F.SEP38, mirrored), (**j**) *Gomphotherium angustidens* (MNHN.F.SEP38), (**k**) *Cuvieronius* sp. (FM103247, mirrored), (**l**) *Stegomastodon* sp. (FM21807, mirrored), (**m**) *Platybelodon grangeri* (MNHN 26564-824+), (**n**) *Anancus arvernensis* (NMNHS.FM2991A), (**o**) *Anancus arvernensis* (NMNHS.FM2991B), (**p**) *Anancus arvernensis* (NMNHS.FM2991C, mirrored), (**q**) *Anancus arvernensis* (NMNHS.FM2991D, mirrored), (**r**) *Anancus arvernensis* (NMNHS.FM2991E, mirrored), (**s**) *Anancus arvernensis* (NMNHS.FM2991F, mirrored), (**t**) *Anancus arvernensis* (NMNHS.

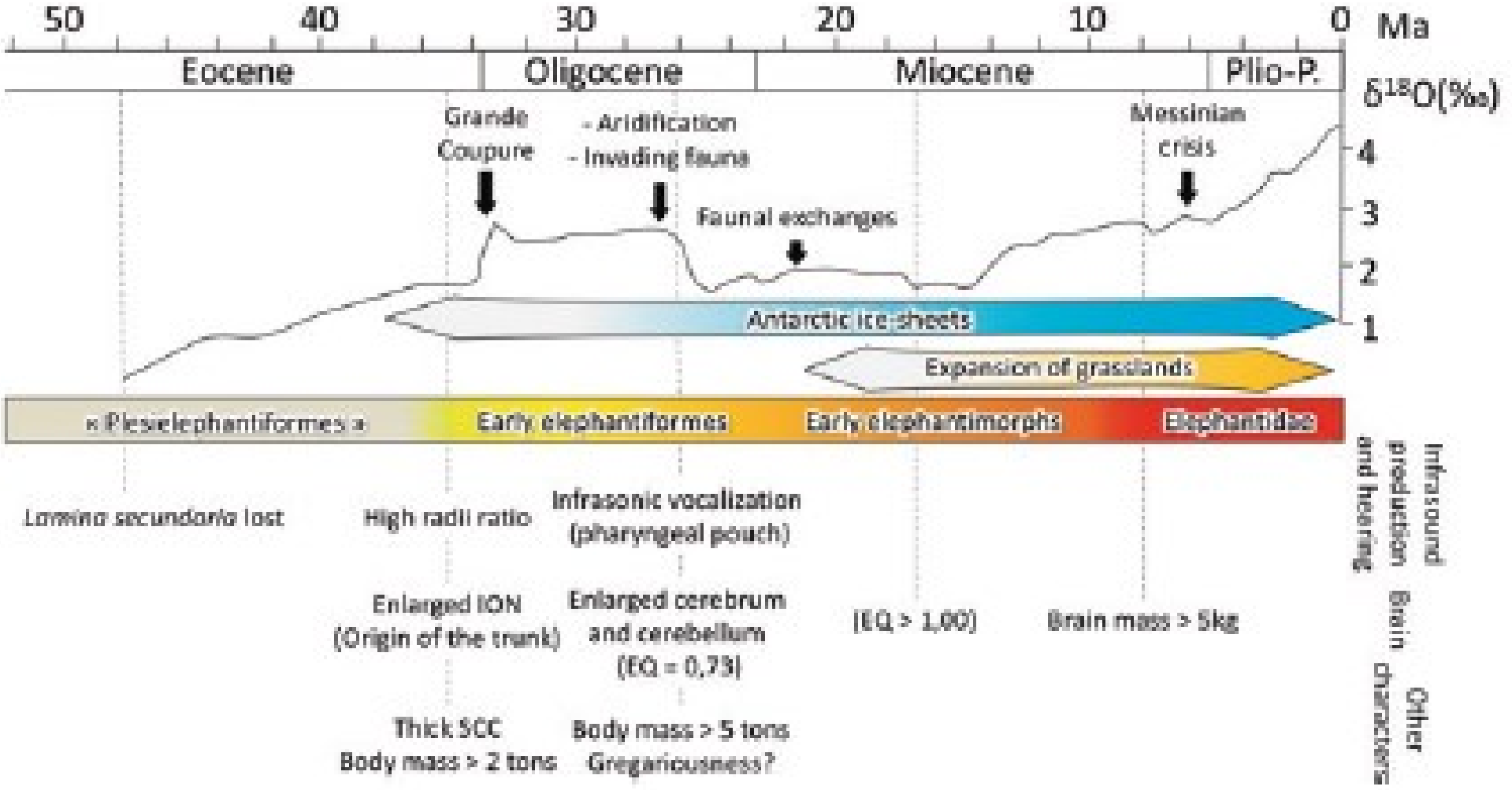

Fig. 15.13 Palaeoenvironmental context of proboscidean brain, inner ear and other related characters co-evolution. $\delta^{18}O$ curve and climatic events after Zachos et al. (2001). Abbreviations: *EQ*: encephalization quotient, *ION* infraorbital nerve, *SCC* semicircular canals